Testing the Standard Model of Elementary Particle Physics I

Eight lecture

Dr. Dominik Duda

14th January 2020

2. Experimental setups

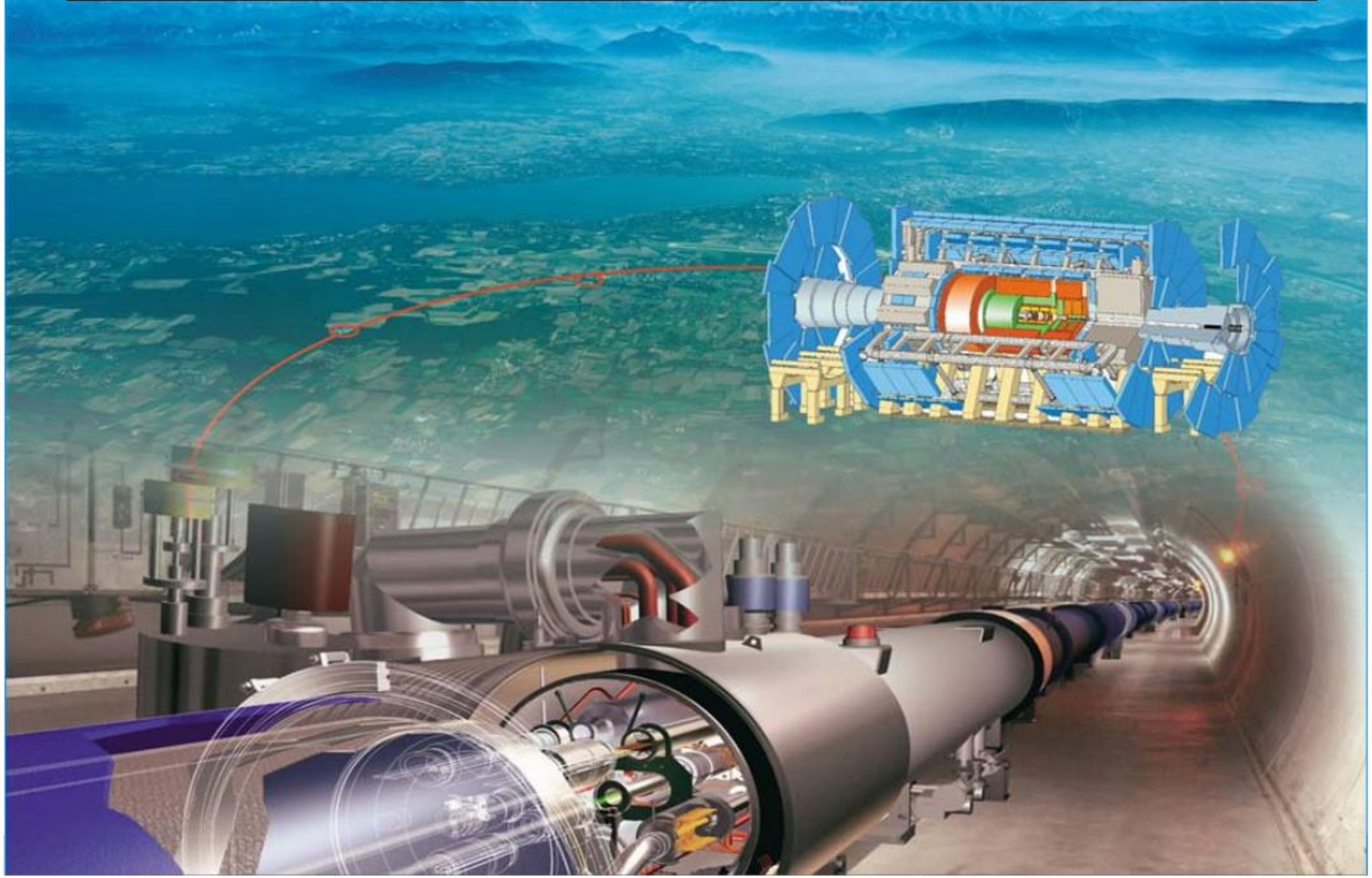

Table of content

2.1 Accelerators

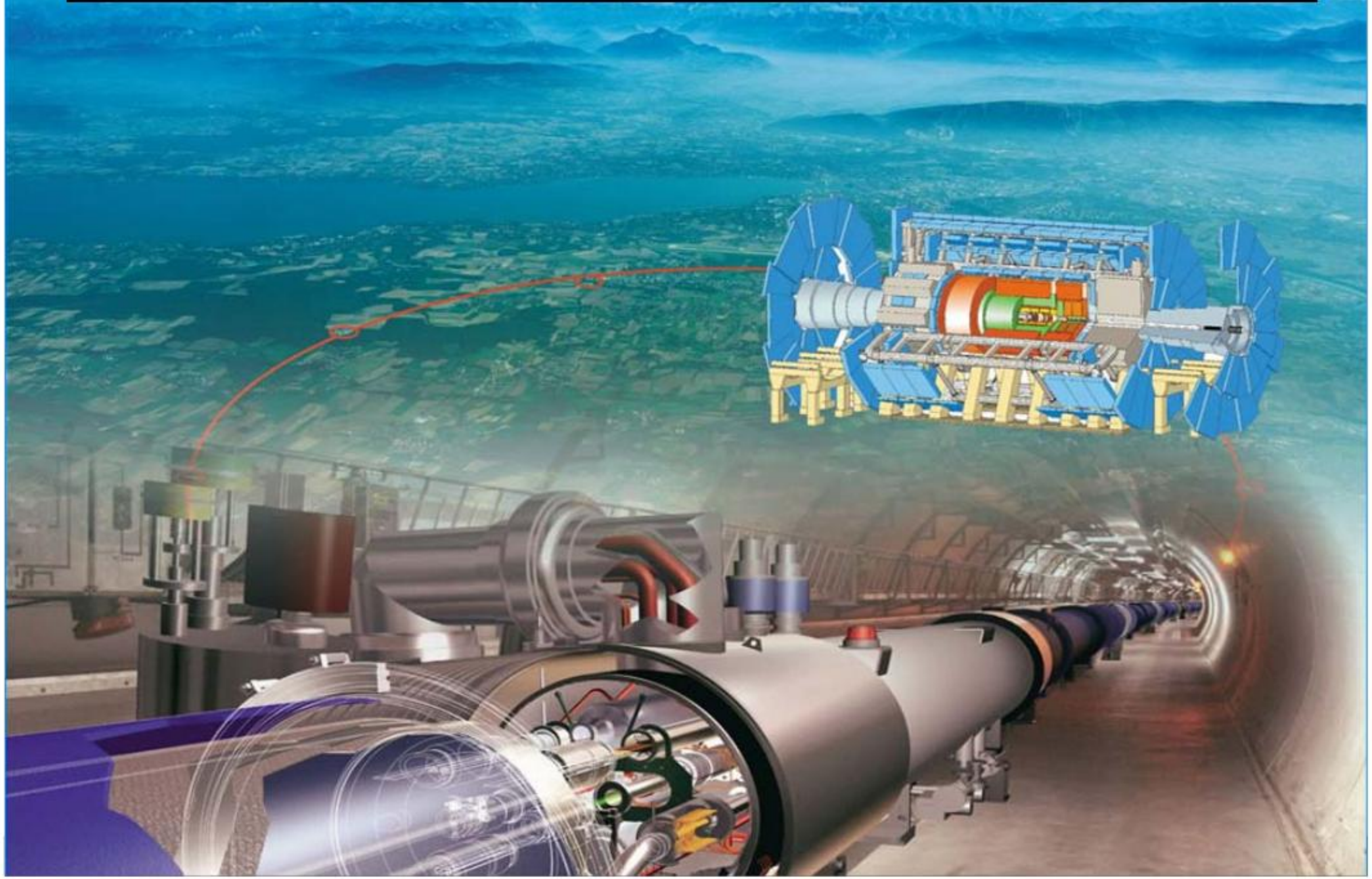

Why are existing accelerators so big ?

- Charged particles lose energy in the form of synchrotron radiation when their trajectory is deflected
  - Depending on the particle energy and bending angle this radiation ranges from visible light to gamma rays
- In a circular storage ring (with bending radius ρ), a particle with charge e and Lorentz factor $\gamma = E/m$ loses an energy of

$$U_0 = \frac{e^2}{3\varepsilon_0}\frac{\gamma^4}{\rho} \sim \frac{1}{\rho}\frac{E^4}{m^4}$$

  per turn.
- At LEP (with a beam energy of 100 GeV) electrons/positrons lost 3% of their energy in a single turn.
- For protons, synchrotron radiation is not a problem
  - Limiting factor on total energy is the magnetic bending field

Energy and luminosity

- **Center-of-mass (CoM) energy:**

$$\sqrt{s} = \sqrt{2E_1 E_2(1 + \cos\theta)}$$

- **Instantaneous luminosity:**

$$\mathcal{L} = fn\frac{N_1 N_2}{A}$$

N_1, N_2 = Number of hadrons per bunch
n = Number of bunches per beam
f = Resolution frequency
A = Beam cross section

For Gaussian-shaped beams with horizontal and vertical r.m.s beam sizes of σ_x and σ_y, the beam cross section is given via: $A = 4\pi\sigma_x\sigma_y$

- The beam sizes are determined by the beam emittance ε and the β function which describes the local focusing properties of the accelerator:

$$\sigma_{x,y} = \sqrt{\beta_{x,y}\epsilon_{x,y}}$$

- **Integrated luminosity:**

$$L = \int \mathcal{L}dt$$

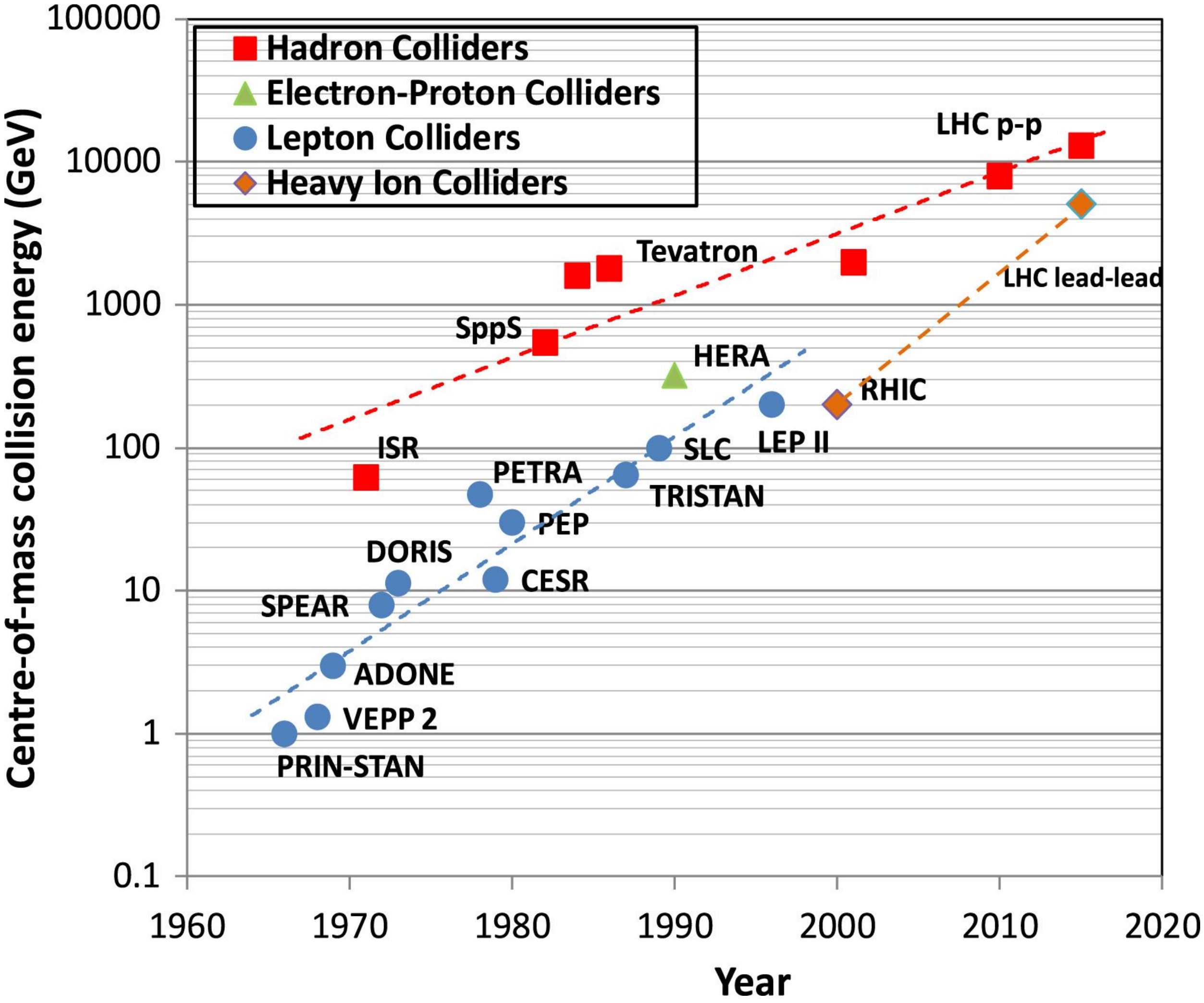

- Lepton collider:
  - High precision measurements
- Proton colliders:
  - “Discovery” machines

- **As a rule of thumb: Hadron machines need a factor six higher energies than lepton machines:**
  - Beam energy is divided between:
    - **Valence quarks**
    - **Sea quarks, gluons**

Event rates/cross sections

$$\frac{dN}{dt} = \mathcal{L} \cdot \sigma$$

Inelastic pp collisions	~10^7 Hz
b-quark production	~10^4 Hz
Jet production E_T> 250 GeV	~1 Hz
W->lv	~1 Hz
top-quark production	~10^{-2}Hz
Higgs bosons	~10^{-4}Hz

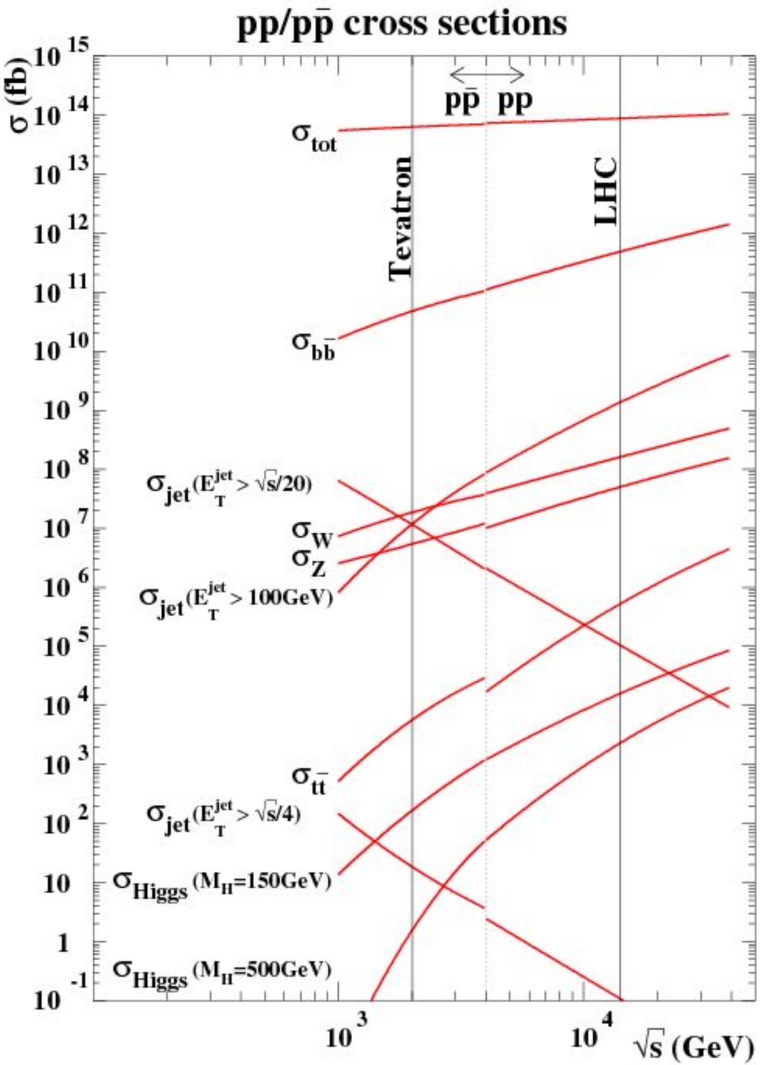

Where do the protons, antiprotons and positrons come from ?

- **Protons:**
  - At the LHC, the proton source is a simple bottle of hydrogen gas. An electric field is used to strip hydrogen atoms of their electrons to yield protons.
- **Antiprotons:**
  - Shoot proton beam on a fixed target
    - Capture and cool resulting antiproton beam (to reduce emittance)
- **Positrons:**
  - To produce positron beams, an electron beams are accelerated and sent into a crystal to produce energetic photons, which hit a second target and produce electron–positron pairs. The positrons are captured and accelerated

Where do the protons, antiprotons and positrons come from ?

Proton source of the LHC

Taken from: http://cdsweb.cern.ch/record/1157734#04

Acceleration

- At the LHC. radiofrequency (RF) cavities are used to accelerate particles:
  - RF cavities are basically resonators tuned to a selected frequency.
  - Charged particles injected into the electromagnetic field of these cavities receive an electrical impulse that accelerates them.
  - To accelerate a proton to 7 TeV, a 7 TV potential must be provided to the beam:
    - In circular accelerators the acceleration is done in small steps, turn after turn.
    - At the LHC the **acceleration** from 450 GeV to 7 TeV lasts ~20 minutes, with **an average energy gain of** ~0.5 MeV on each turn.

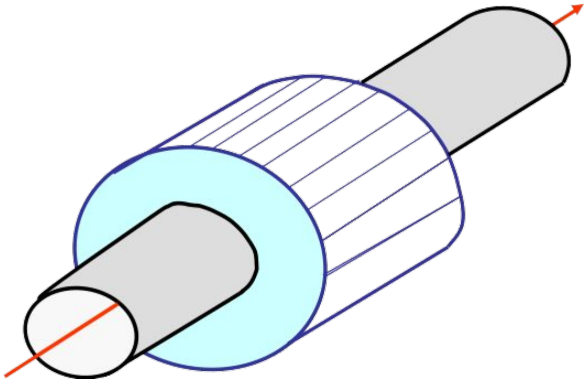

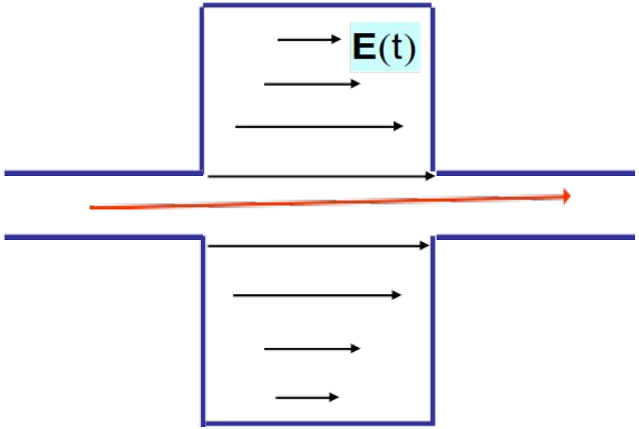

Magnets

- At the LHC **superconducting dipole magnets** are operated at B-field strength of 8.3 T over their full length
  - Forcing the particle beams to follow the circular pipes
- **Quadrupole magnets** are used to focus the beams

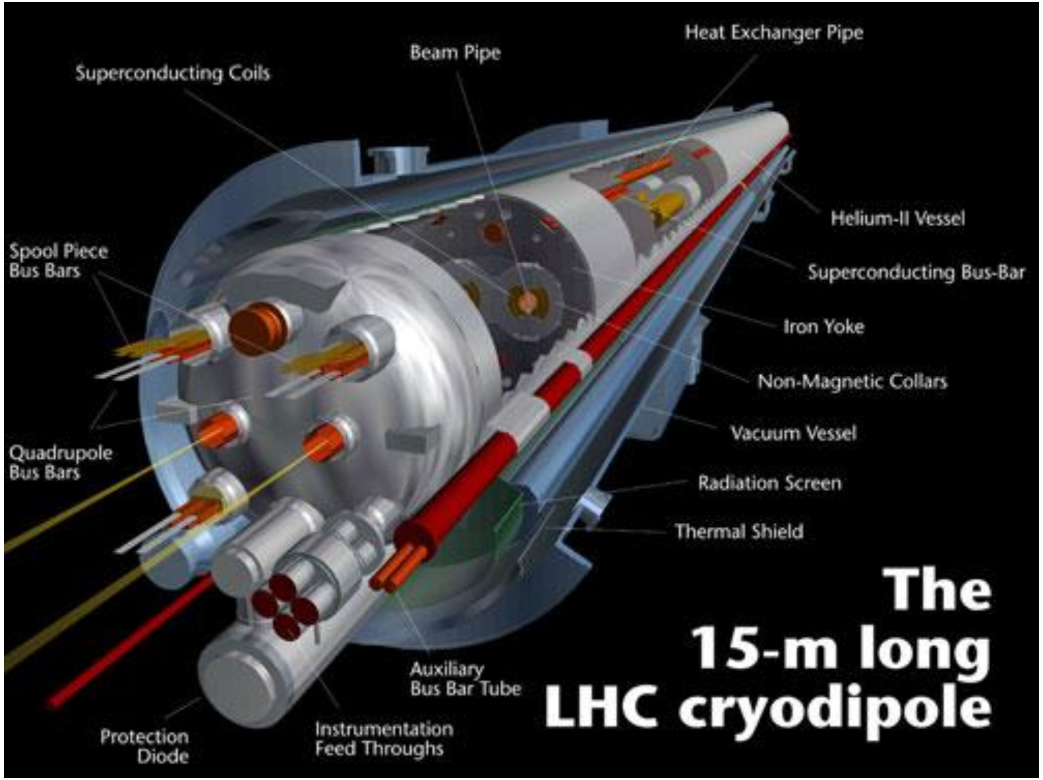

- The LHC magnets are made from niobium-titanium (NbTi) cables.
- LHC is operate at 1.9 K (-271.3°C)

Magnets

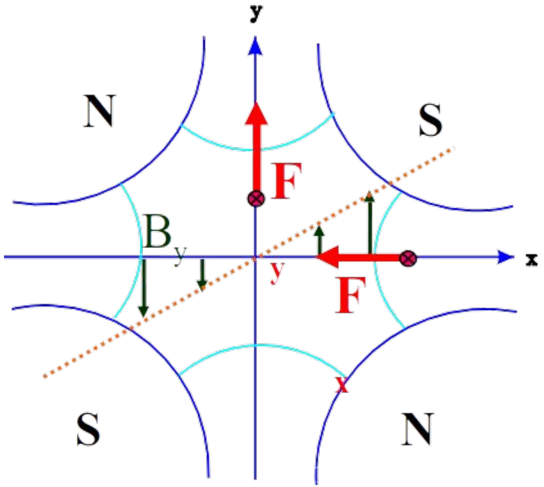

- **Quadrupole magnets** are used to focus the beams (as they act on the beam like an optical lens).
  - Focusing in one plane, de-focusing in the other!

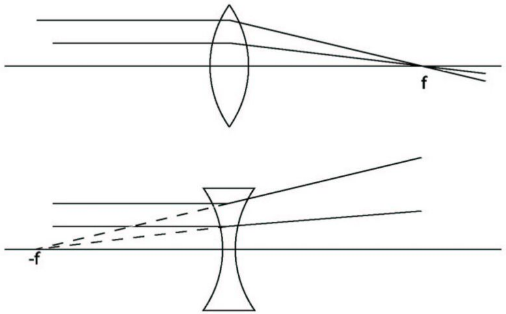

2.1.1 Modern particle accelerators

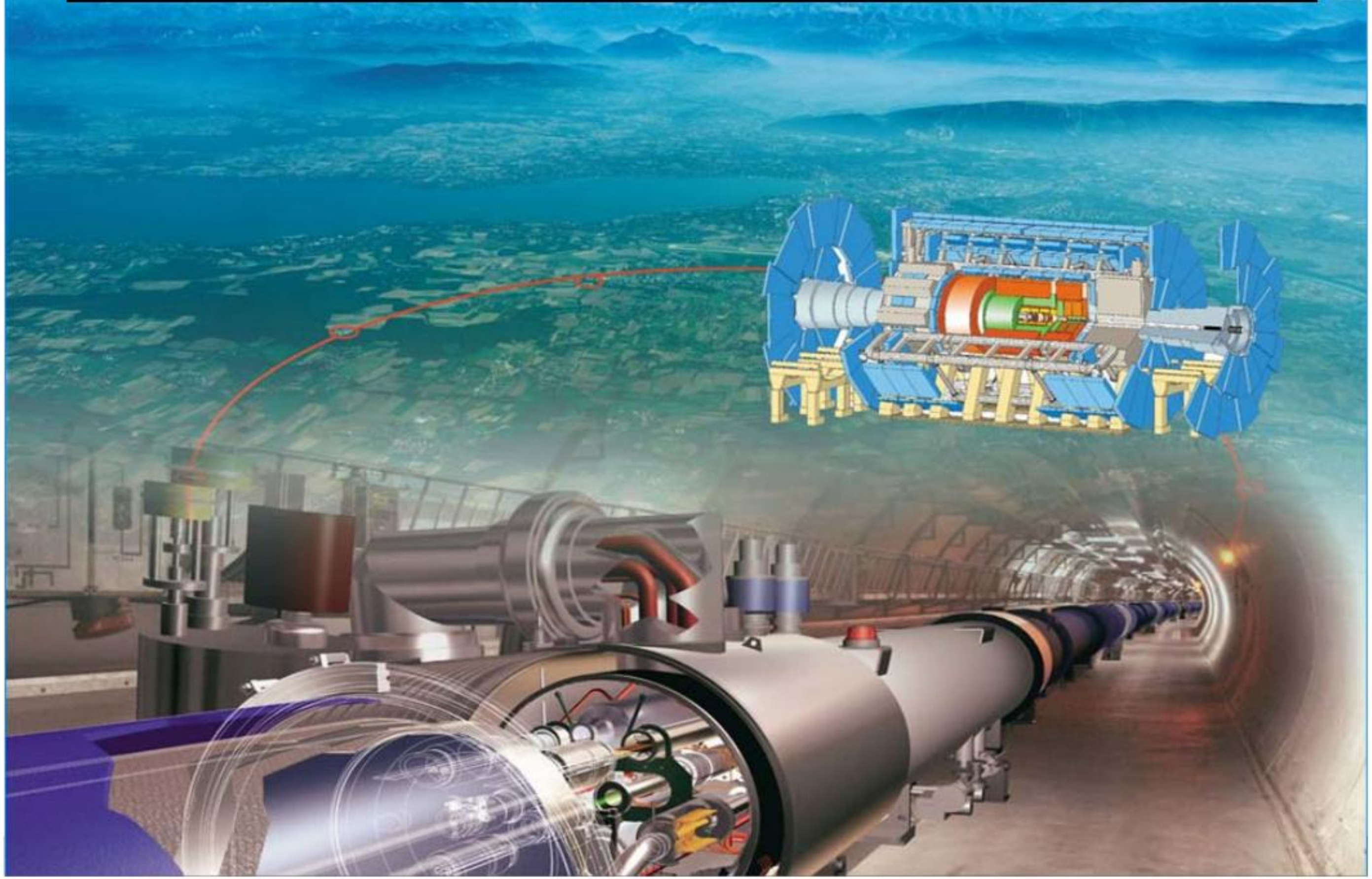

The Large Electron Positron Collider

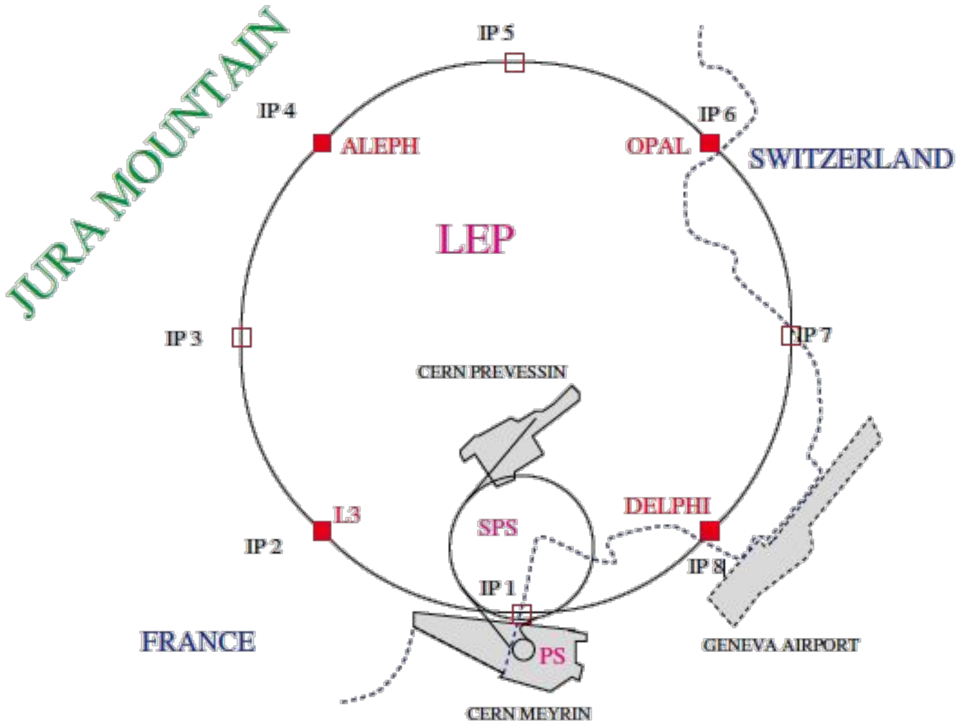

- **Data taking period:** 1989-2000
- **Run summaries:**
  - 1989-1995:
    - Beam energy: 45.6 GeV
    - Collected: 208.44 pb^{-1}
  - 1996:
    - Beam energy: 80.5 - 86 GeV
    - Collected: 24.7 pb^{-1}
  - 1997-2000:
    - Beam energy: 90 - 104 GeV
    - Collected 759,5 pb^{-1}
- **Design luminosity:** $10^{32}\ cm^{-2}\ s^{-1}$
- **Circumference:** 27000 m

Informations are taken from: https://cds.cern.ch/record/549223/files/sl-2002-009.pdf

Hadron Electron Ring Accelerator (HERA)

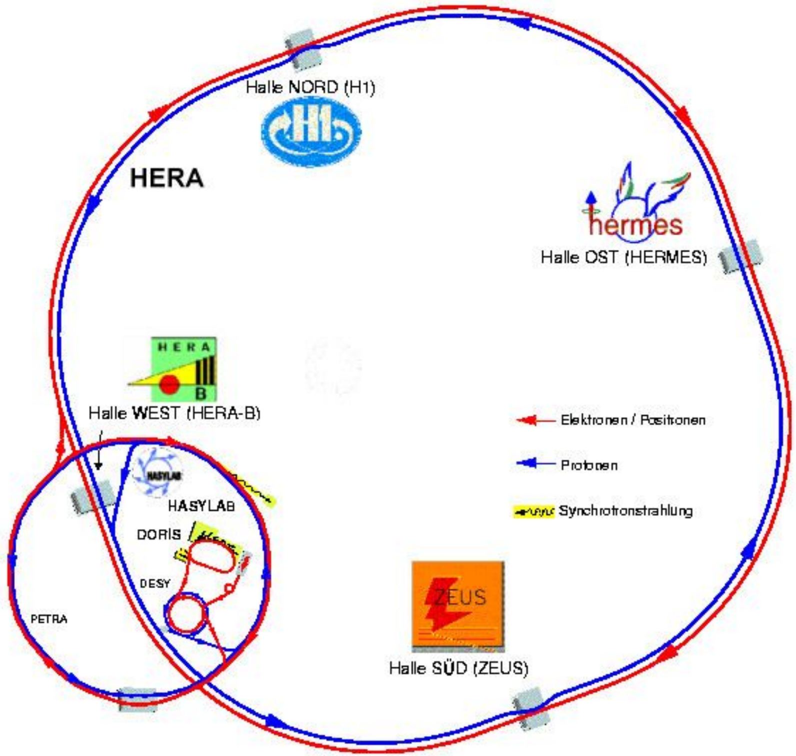

- **Data taking period:** 1992-2007
- **Beam energies:**
  - 30 GeV (electron)
  - 920 GeV (proton)
- **Design luminosity:** $10^{31}\ cm^{-2}\ s^{-1}$
- **Integrated luminosity:** 800 pb^{-1}
- **Circumference:** 6336 m
- So far only electron-proton collider ever build
- **Experiments:**
  - H1
  - ZEUS
  - HERMES
  - HERA

Tevatron Collider

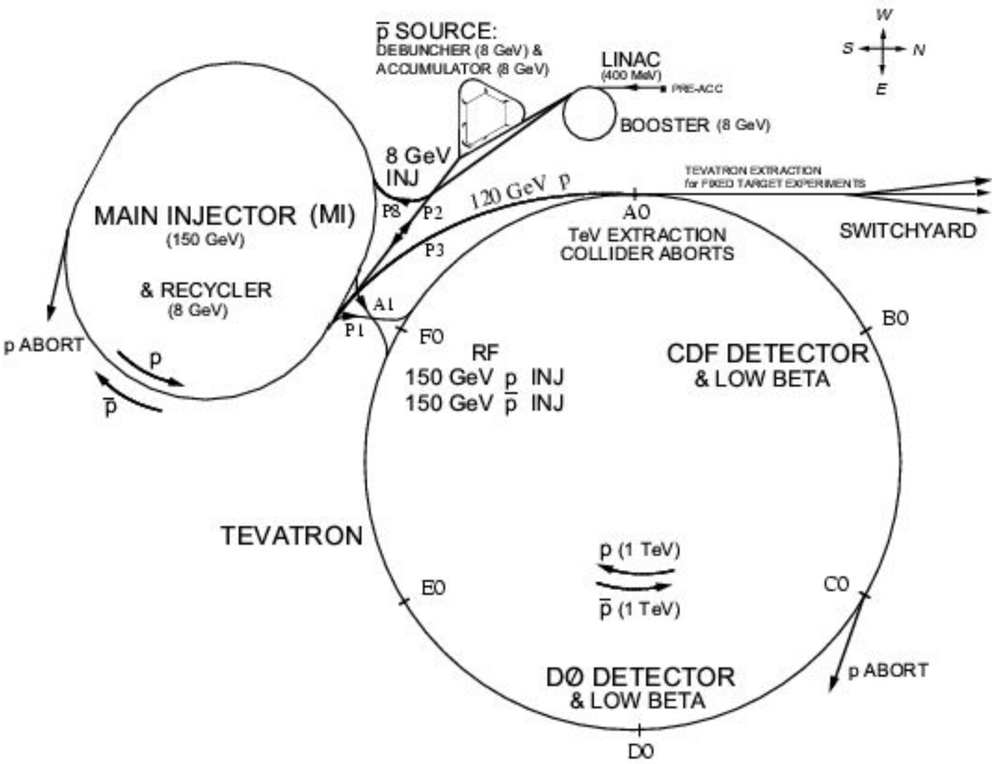

- **Data taking period:** 1983-2011
- **Run summaries:**
  - 1992-1996 (Run 1):
    - CoM energy: 1.8 TeV
    - Collected: 120 pb^{-1}
  - 2001-2007 (Run 2):
    - Beam energy: 1.96 TeV
    - Collected 17 fb^{-1}
- **Design luminosity:** $10^{32}\,cm^{-2}\,s^{-1}$
- **Circumference:** 6280m

Stanford Linear Collider (SLC)

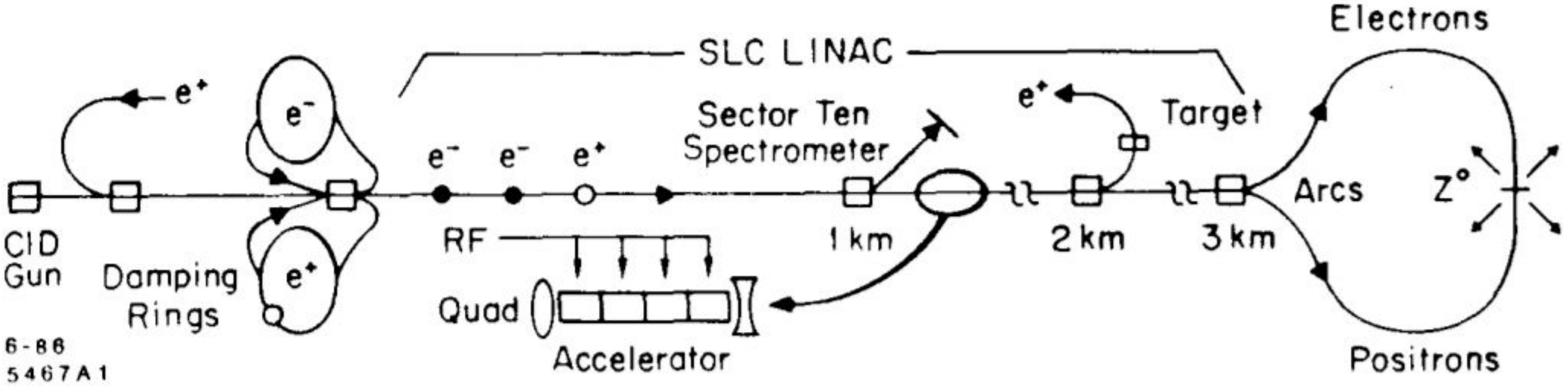

- **Data taking period:** 1989-2000
- **Beam energy:** 50 GeV
- **Design luminosity:** 10^{30} cm^{-2} s^{-1}

KEKB

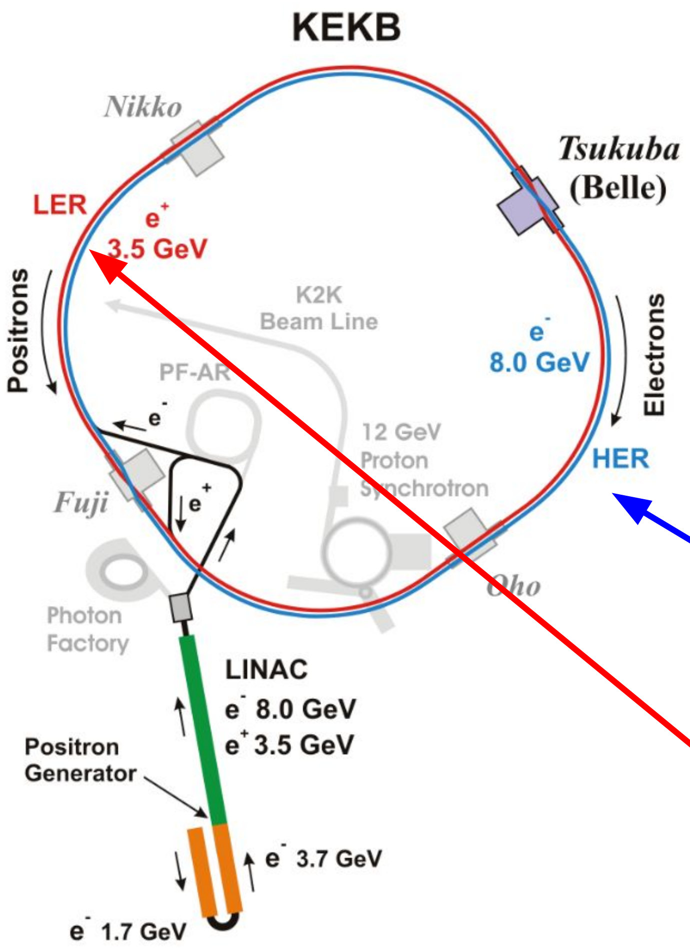

- **B-factory**
- **Data taking period:** 1999-2010
- **Beam energies:**
  - 8.0 GeV electron
  - 3.5 GeV positron
- **Design luminosity:** $10^{34}\ cm^{-2}\ s^{-1}$
- **Data collected:** $711\ fb^{-1}$
  - Corresponds to 772 million B-hadron pairs
- **Circumference:** 3016 m
- CoM energy close to the mass of the Υ(4S) resonance

High energy ring (HER)

Low energy ring (LER)

SuperKEKB

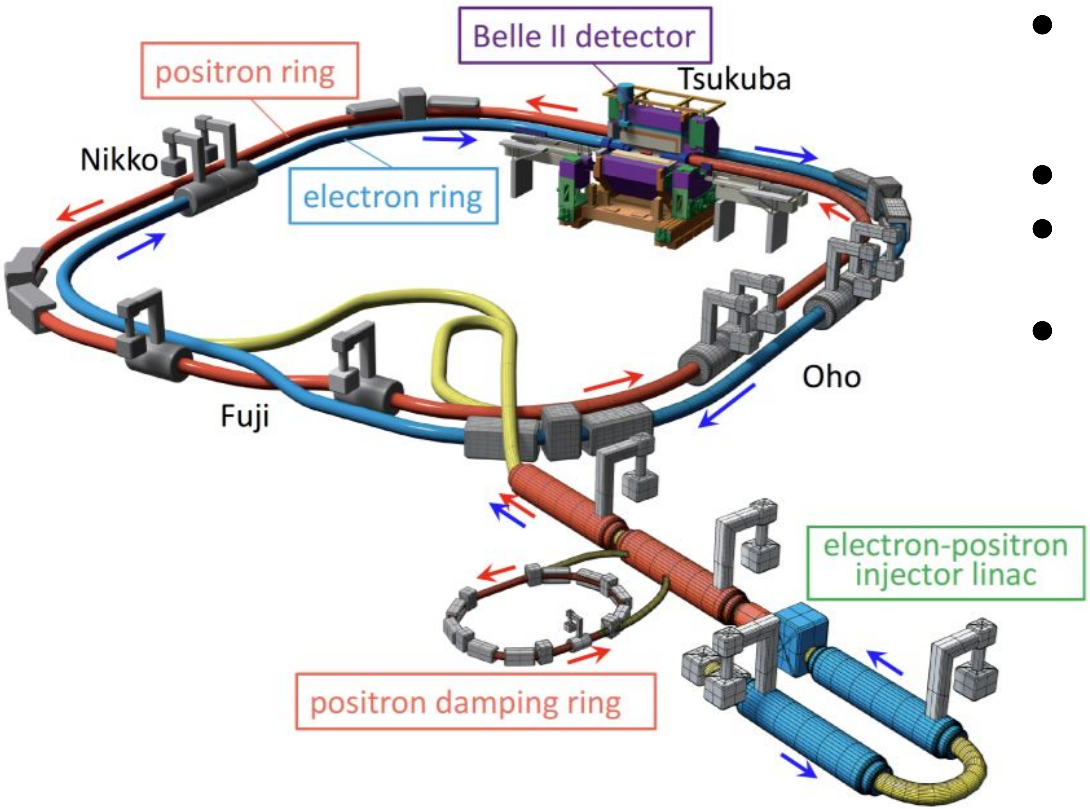

- **Beam energies:**
  - 7 GeV electron
  - 4 GeV positron
- **Data taking since:** 2018
- **Design luminosity:**
  - $8 \times 10^{35} cm^{-2} s^{-1}$
- **Aiming to collect an integrated luminosity of 50 ab^{-1}**

Significant increased instantaneous luminosity due to beam size reductions

The Large Hadron Collider (LHC)

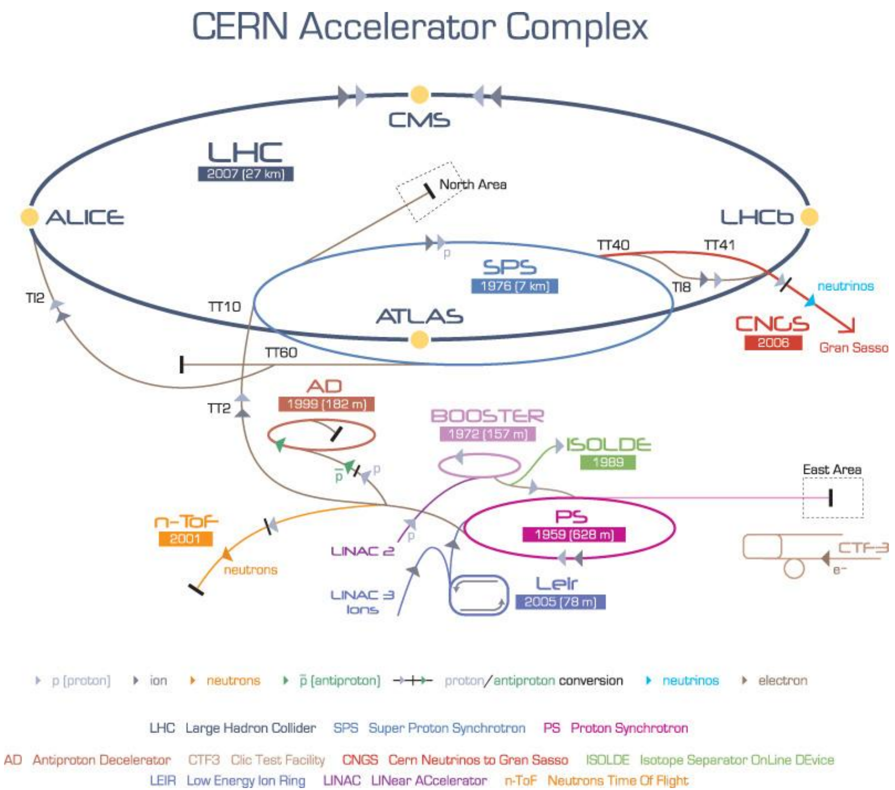

- **Data taking period:** 2010-2040
- **Run summaries:**
  - 2011:
    - Beam energy: 3.5 TeV
    - Collected: 4.8 fb^{-1}
  - 2012:
    - Beam energy: 4 TeV
    - Collected: 20.3 fb^{-1}
  - 2015-2018:
    - Beam energy: 6.5 TeV
    - Collected: 139 fb^{-1}
- **Design luminosity:** $10^{34}\ cm^{-2}\ s^{-1}$
- **Circumference:** 27000 m

Luminosity

- Design goal of LHC:
  - 10^{34} cm^{-2} s^{-1}
    - n = 2835 proton bunches per beam
    - f = 40MHz
    - $N_1/N_2 = 10^{11}$ protons per bunch

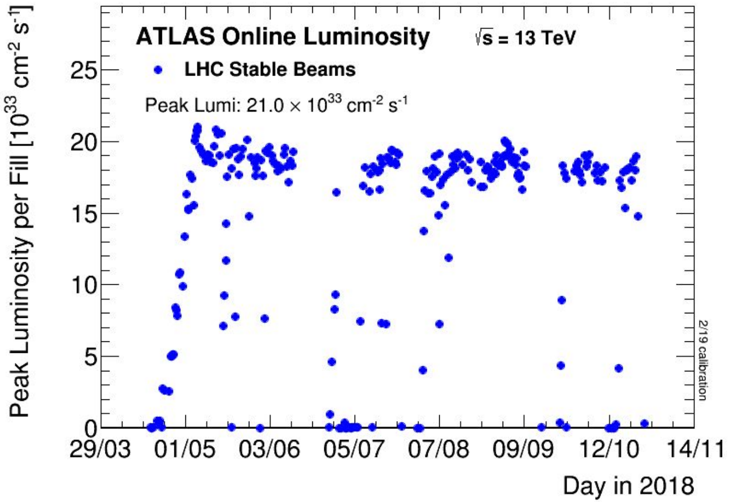

- **Already exceeded in Run-II**

- **Pile-up:**
  - Additional interactions next to the hard process

$$\mathcal{L} = fn\frac{N_1 N_2}{A}$$

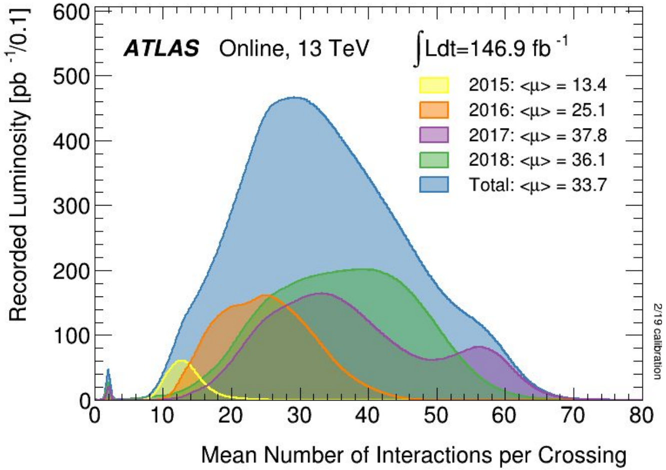

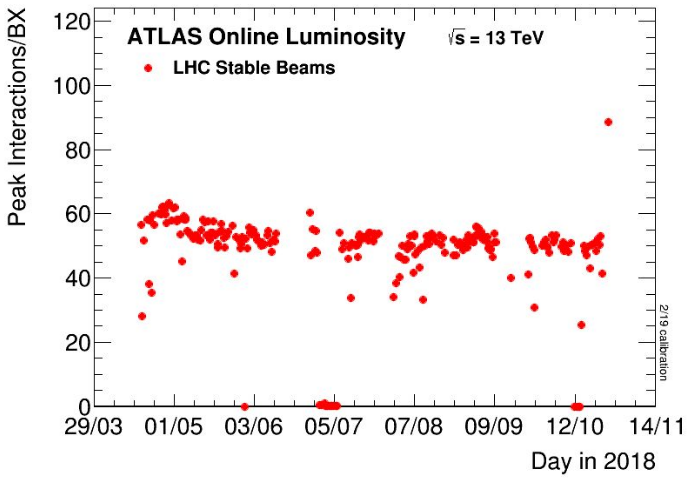

Longer term LHC schedule

LHC design luminosity

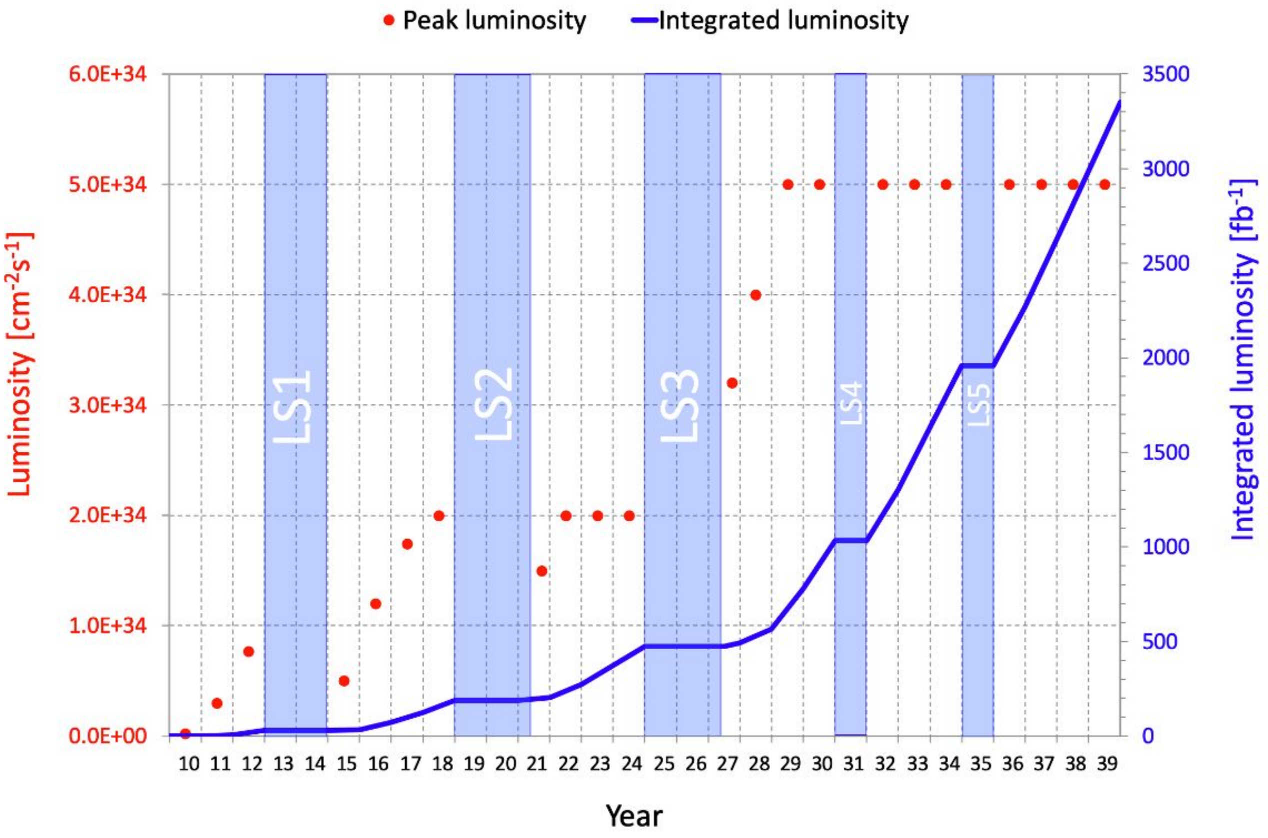

LHC operation

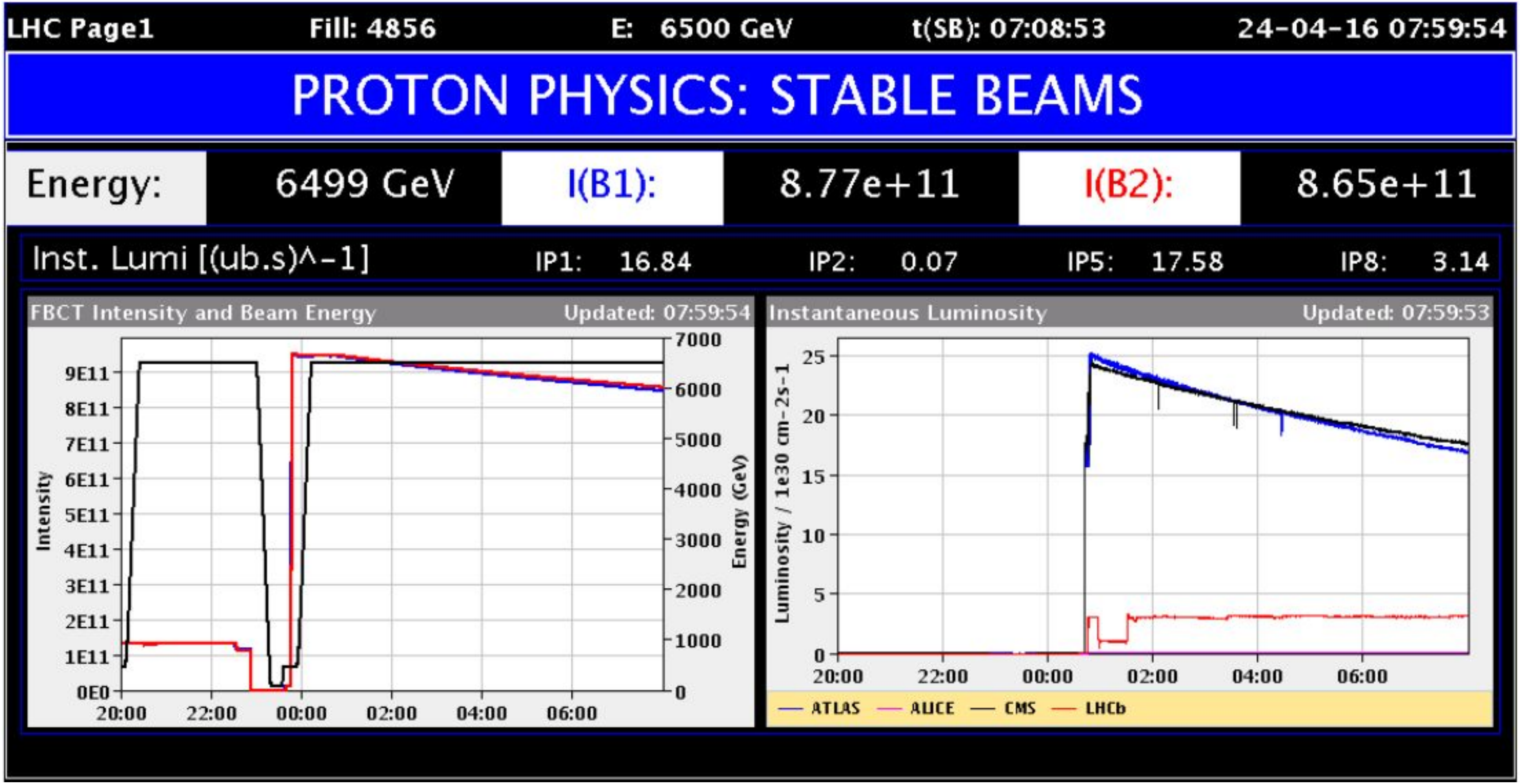

LHC

2.1.2 Proposed future accelerators

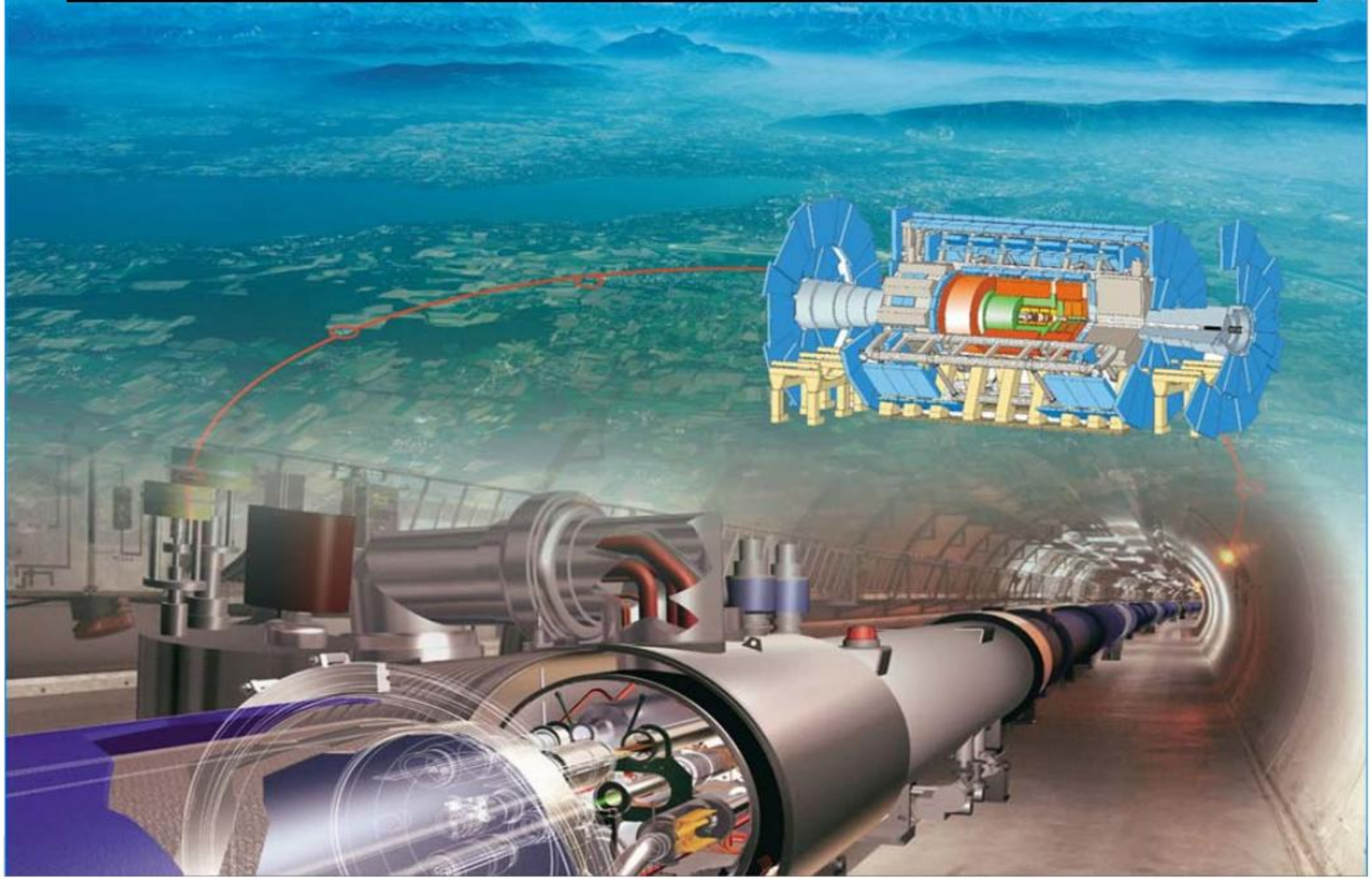

What's next ?

- **Proposed concepts:**
  - **Future Circular Collider (FCC)**
    - pp (e^+e^-) collider
    - Center-of-mass energy up to 100 TeV
  - **International Linear Collider (ILC)**
    - e^+e^- collider
    - Center-of-mass energy up to 1 TeV
  - **Compact Linear Collider (CLIC)**
    - e^+e^- collider
    - Center-of-mass energy up to 3 TeV
  - **Muon collider**

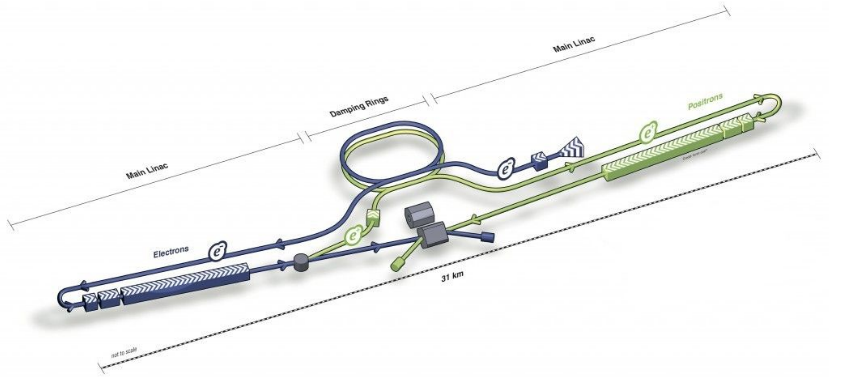

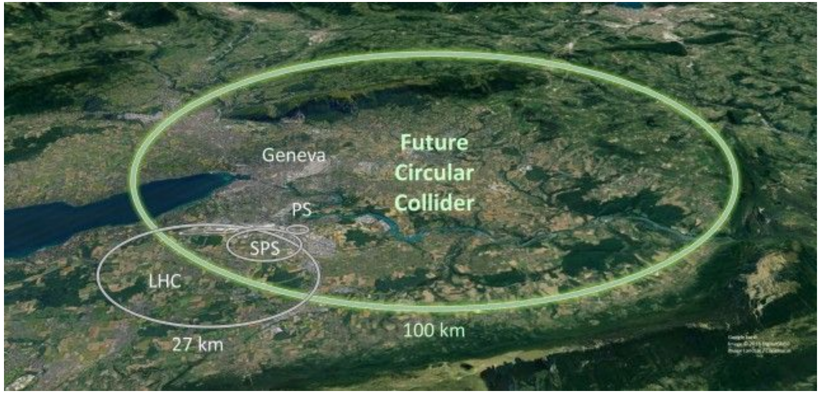

Proposed physics program (ILC)

Energy	Reaction	Physics Goal	Pol.
91 GeV	$e^+e^- \to Z$	ultra-precision electroweak	A
160 GeV	$e^+e^- \to WW$	ultra-precision W mass	H
250 GeV	$e^+e^- \to Zh$	precision Higgs couplings	H
	$e^+e^- \to t\bar{t}$	top quark mass and couplings	A
350–400 GeV	$e^+e^- \to WW$	precision W couplings	H
	$e^+e^- \to \nu\bar{\nu}h$	precision Higgs couplings	L
	$e^+e^- \to f\bar{f}$	precision search for Z'	A
	$e^+e^- \to t\bar{t}h$	Higgs coupling to top	H
500 GeV	$e^+e^- \to Zhh$	Higgs self-coupling	H
	$e^+e^- \to \tilde{\chi}\tilde{\chi}$	search for supersymmetry	B
	$e^+e^- \to AH, H^+H^-$	search for extended Higgs states	B
	$e^+e^- \to \nu\bar{\nu}hh$	Higgs self-coupling	L
	$e^+e^- \to \nu\bar{\nu}VV$	composite Higgs sector	L
700–1000 GeV	$e^+e^- \to \nu\bar{\nu}t\bar{t}$	composite Higgs and top	L
	$e^+e^- \to \tilde{t}\tilde{t}^*$	search for supersymmetry	B

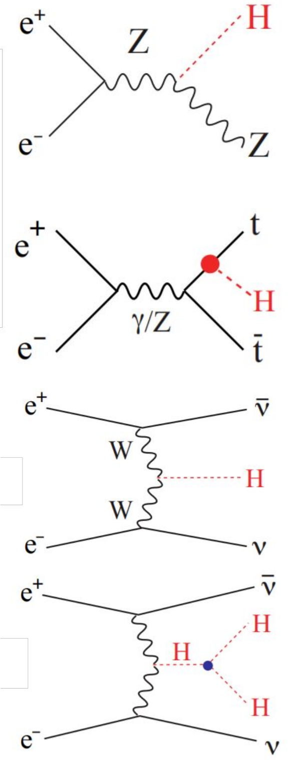

Proposed layout (CLIC)

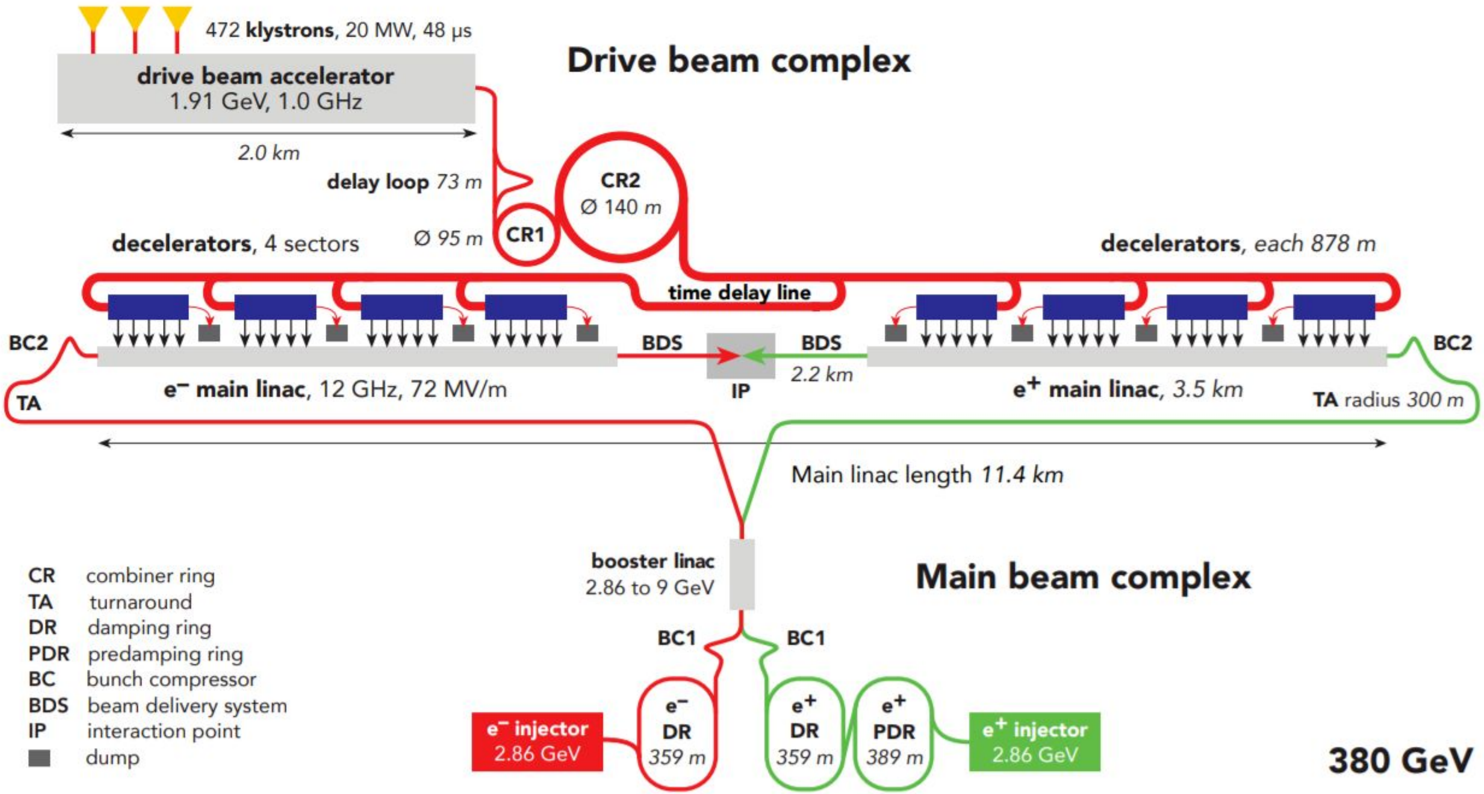

Taken from CLIC summary report: https://arxiv.org/pdf/1812.06018.pdf

Proposed physics program (CLIC)

- 1st stage:
  - SM Higgs physics & top-quark physics
- 2nd & 3rd stage:
  - Double-Higgs production, and rare decays,
  - Sensitivity to many BSM models.
- The energies of the 2nd & 3rd stages are benchmarks, and can be optimised in light of new physics information.
- Each stage would take around 7-8 years

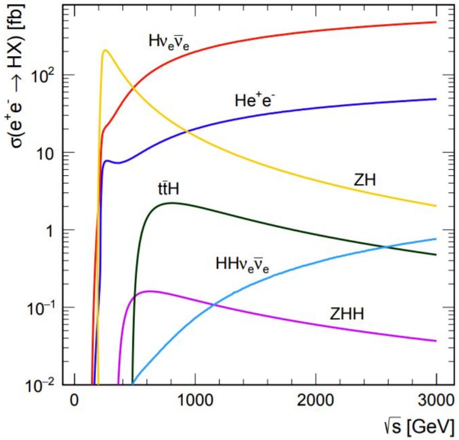

Stage	$\sqrt{s}$ [TeV]	$\mathscr{L}_{int}$ [ab^{-1}]
1	0.38 (and 0.35)	1.0
2	1.5	2.5
3	3.0	5.0

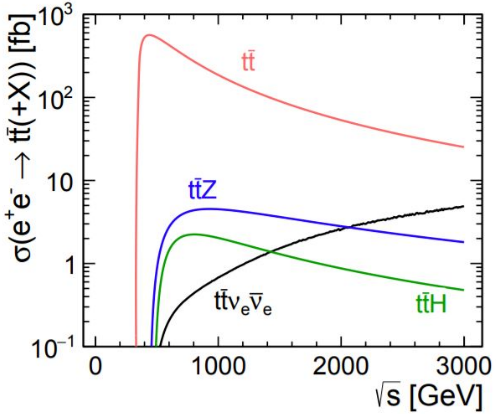

Taken from CLIC summary report: https://arxiv.org/pdf/1812.06018.pdf

Proposed physics program (CLIC)

Process	HL-LHC	CLIC
Heavy Higgs scalar mixing angle $\sin^2\gamma$	$< 4\%$	$< 0.24\%$
Higgs self-coupling $\Delta\lambda$	$\sim 50\%$ at 68% C.L.	$[-7\%, +11\%]$ at 68% C.L.
BR(H $\to$ invisible)		$< 0.69\%$ at 90% C.L.
Higgs compositeness scale m_*	$m_* > 3\,\text{TeV}$ ($> 7\,\text{TeV}$ for $g_* \simeq 8$)	Discovery up to $m_* = 10\,\text{TeV}$ ($40\,\text{TeV}$ for $g_* \simeq 8$)
Top compositeness scale m_*		Discovery up to $m_* = 8\,\text{TeV}$ ($20\,\text{TeV}$ for small coupling g_*)
Higgsino mass (disappearing track search)	$> 250\,\text{GeV}$	$> 1.2\,\text{TeV}$
Slepton mass		Discovery up to $\sim 1.5\,\text{TeV}$
RPV wino mass		$> 1.5\,\text{TeV}$ ($0.03\,\text{m} < c\tau < 30\,\text{m}$)
Z' (SM couplings) mass	Discovery up to 7 TeV	Discovery up to 20 TeV
NMSSM scalar singlet mass	$> 650\,\text{GeV}$ ($\tan\beta = 4$)	$> 1.5\,\text{TeV}$ ($\tan\beta = 4$)
Twin Higgs scalar singlet mass	$m_\sigma = f > 1\,\text{TeV}$	$m_\sigma = f > 4.5\,\text{TeV}$
Relaxion mass	$< 24\,\text{GeV}$	$< 12\,\text{GeV}$ (all for vanishing $\sin\theta$)
Relaxion mixing angle $\sin^2\theta$		$\leq 2.3\%$
Neutrino Type-2 see-saw triplet		$> 1.5\,\text{TeV}$ (for any triplet VEV) $> 10\,\text{TeV}$ (for triplet Yukawa coupling $\simeq 0.1$)
Inverse see-saw RH neutrino		$> 10\,\text{TeV}$ (for Yukawa coupling $\simeq 1$)
Scale $V_{LL}^{-1/2}$ for LFV $(\bar{e}e)(\bar{e}\tau)$		$> 42\,\text{TeV}$

Taken from CLIC summary report: https://arxiv.org/pdf/1812.06018.pdf

Proposed physics program (FCC-ee vs FCC-hh)

- **FCC-ee:**
  - High precision measurements of Higgs boson, W- and Z-boson as well as top quark properties (scans with center-of-mass energies ranging from 90 to 350 GeV)

- **FCC-hh**:
  - Extensive searches for BSM physics with a center-of-mass energy of ~100 TeV

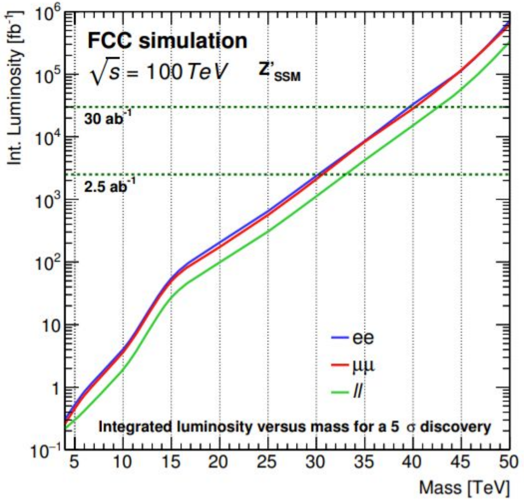

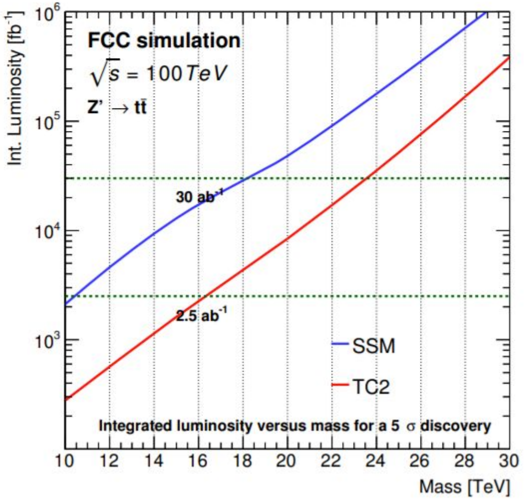

Muon collider

- Main advantages:
  - The large muon mass (207 times that of the electron) suppresses synchrotron radiation by a factor of 10^9 compared with electron beams of the same energy.
    - Thus can use rings for acceleration
  - The physics reach of a muon collider is extended over that of a proton-proton collider of the same energy since all of the beam energy is available for the hard collision, compared to the fraction of the proton-beam energy carried by the colliding partons.
    - A 14 TeV muon collider provides an effective energy reach similar to that of the 100 TeV FCC

- Main challenges:
  - Short muon lifetime
  - The difficulty of producing large numbers of muons in bunches with small emittance
  - The beam background from the decay of the muons

Taken from https://indico.cern.ch/event/867138/attachments/1954116/3245303/Muon_Collider_European_Strategy.pdf

Muon collider

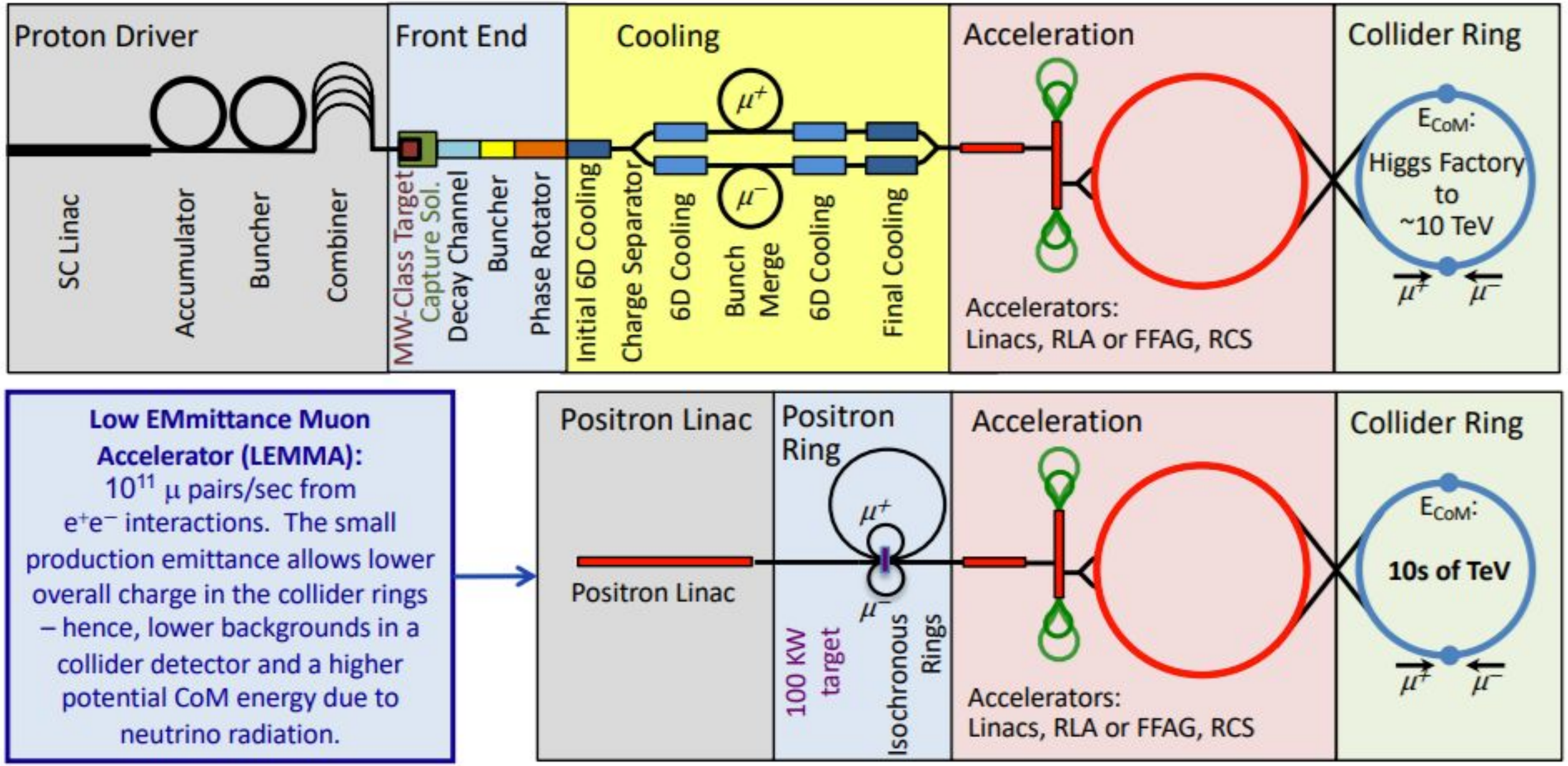

Taken from https://indico.cern.ch/event/867138/attachments/1954116/3245303/Muon_Collider_European_Strategy.pdf

2.2 Particle detection

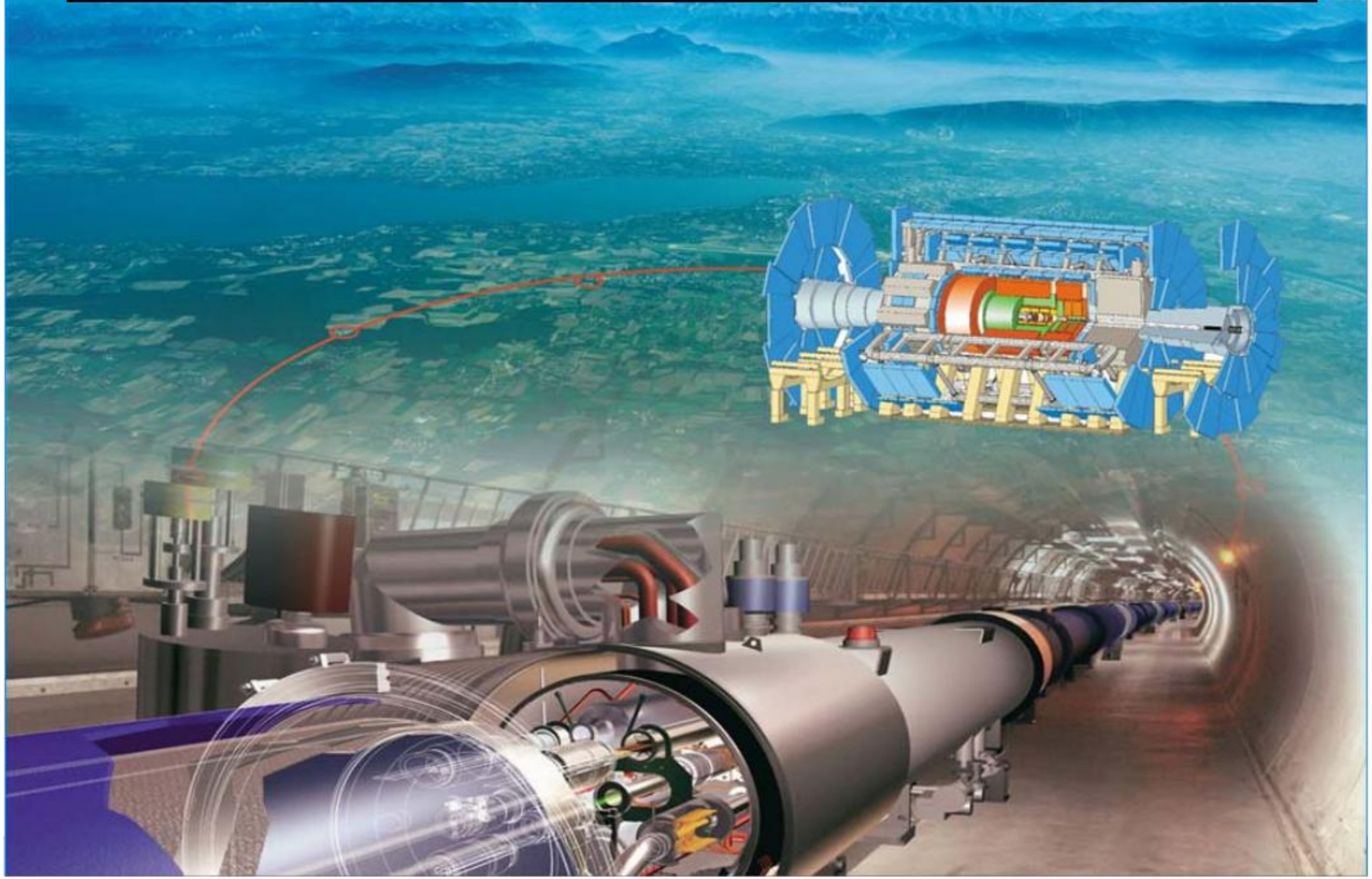

Kinematics

- Detectors determine:
  - Energies
  - Momenta (distinguish between p_T and p_L)
  - Angles (collider experiments usually use cylindrical coordinates)
    - Polar and azimuthal angles: θ and Φ

- Instead of polar angle use:
  - Rapidity:

$$y = \frac{1}{2} \ln \left(\frac{E + p_L}{E - p_L} \right) = \text{arctan} \left(\frac{p_L}{E} \right)$$

  - For high energies (E ≈ p) use pseudorapidity:

$$y \to \eta = - \ln \left(\tan \frac{\theta}{2} \right)$$

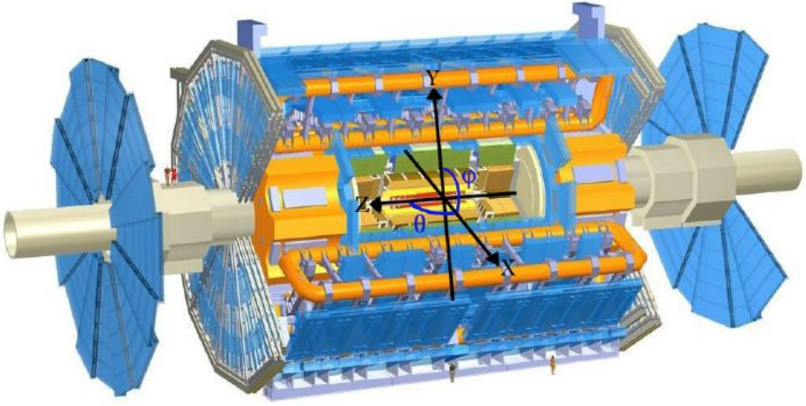

2.2.1 Interaction between particles and matter

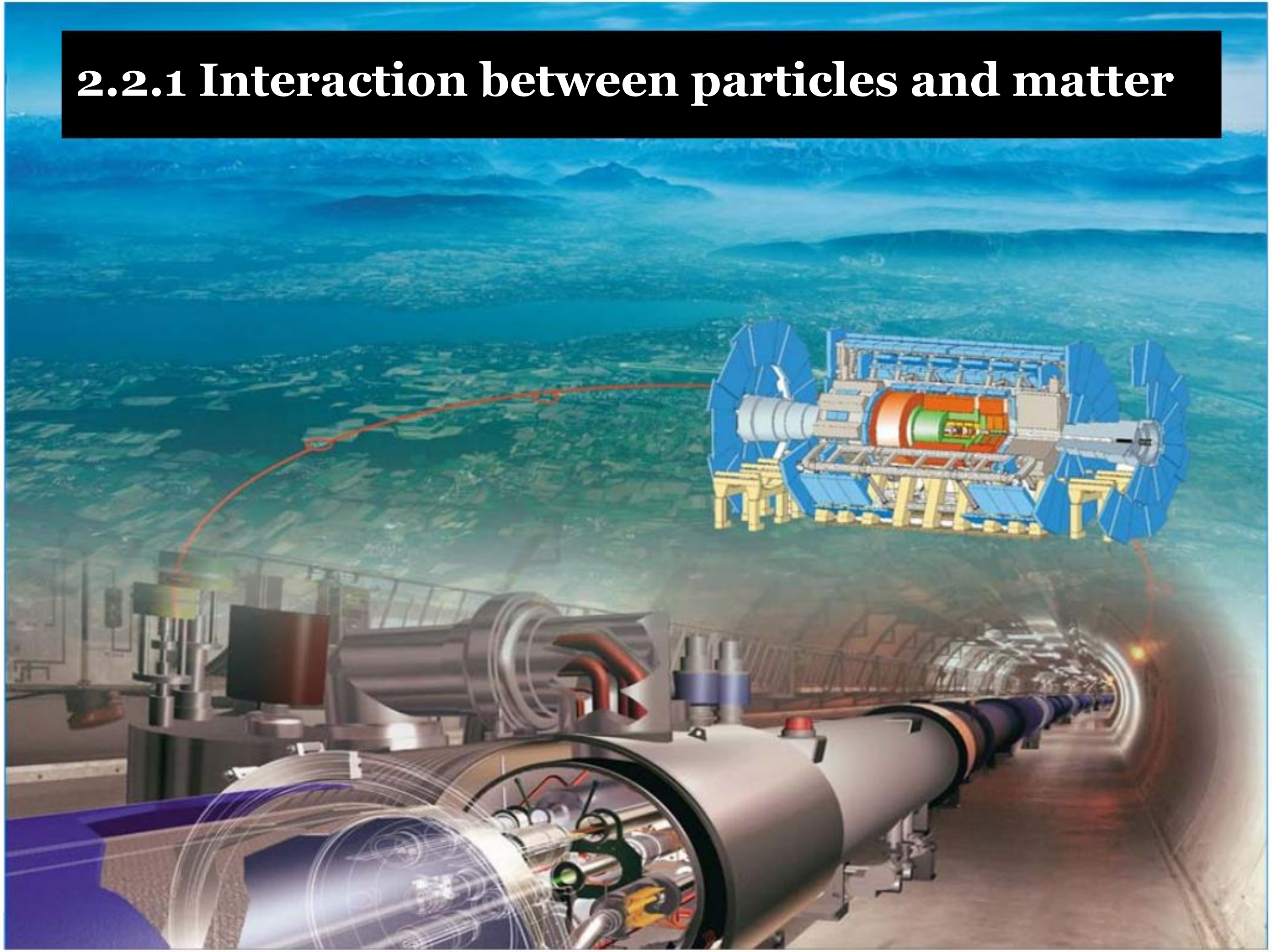

Interaction between particles and matter

- Particles (neutral and charged) can only be noticed via their interaction with matter.
- Modern particle detectors are based on:
  - Ionisation and excitation:
    - Via charged particles passing through matter
  - Bremsstrahlung:
    - Mainly light particles such as electrons or positrons emit photons when traveling through matter
  - Photon scattering and absorption
  - Cherenkov and transition radiation
  - Nuclear interactions:
    - Interaction between the incoming hadrons and atoms of intersected material
  - Weak interaction:
    - Only way to detect neutrinos

Energy loss by electrons

Fractional energy loss per radiation length in lead as a function of electron or positron energy.

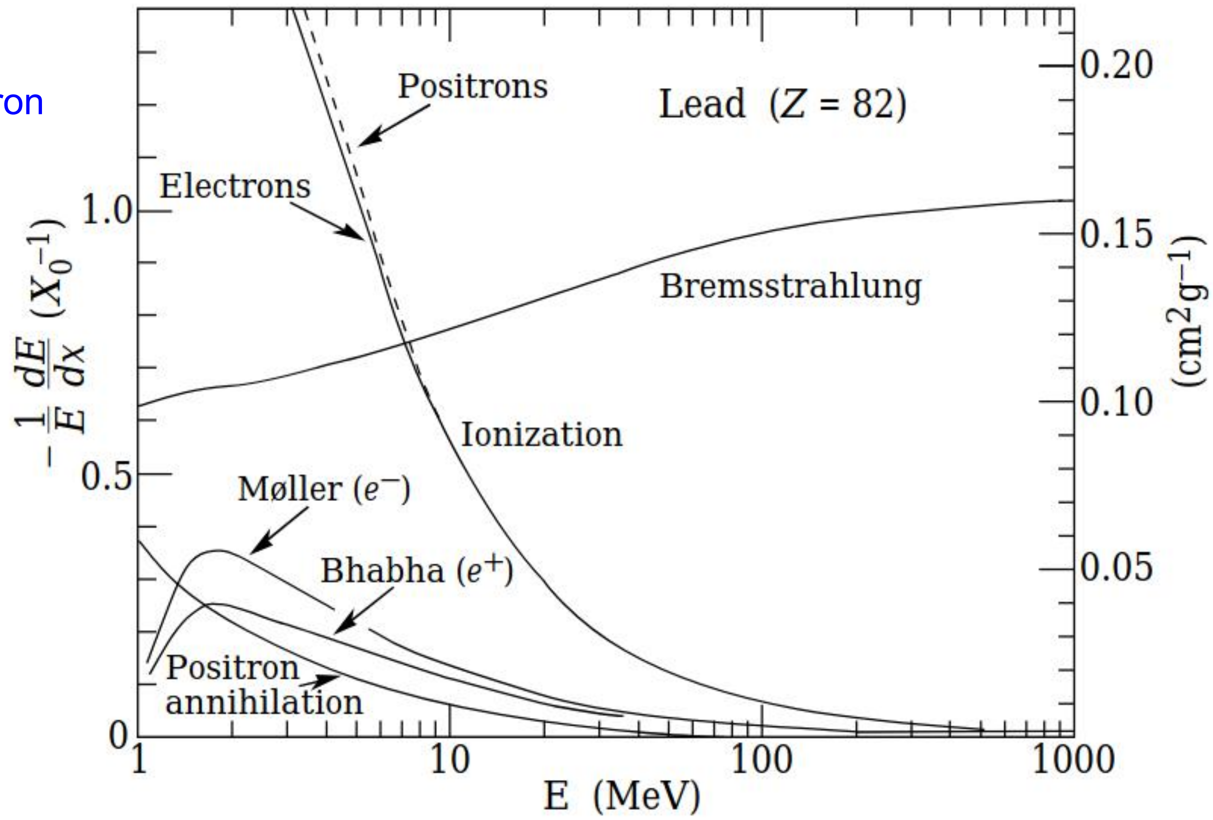

http://pdg.lbl.gov/2009/reviews/rpp2009-rev-passage-particles-matter.pdf

Energy loss by muons

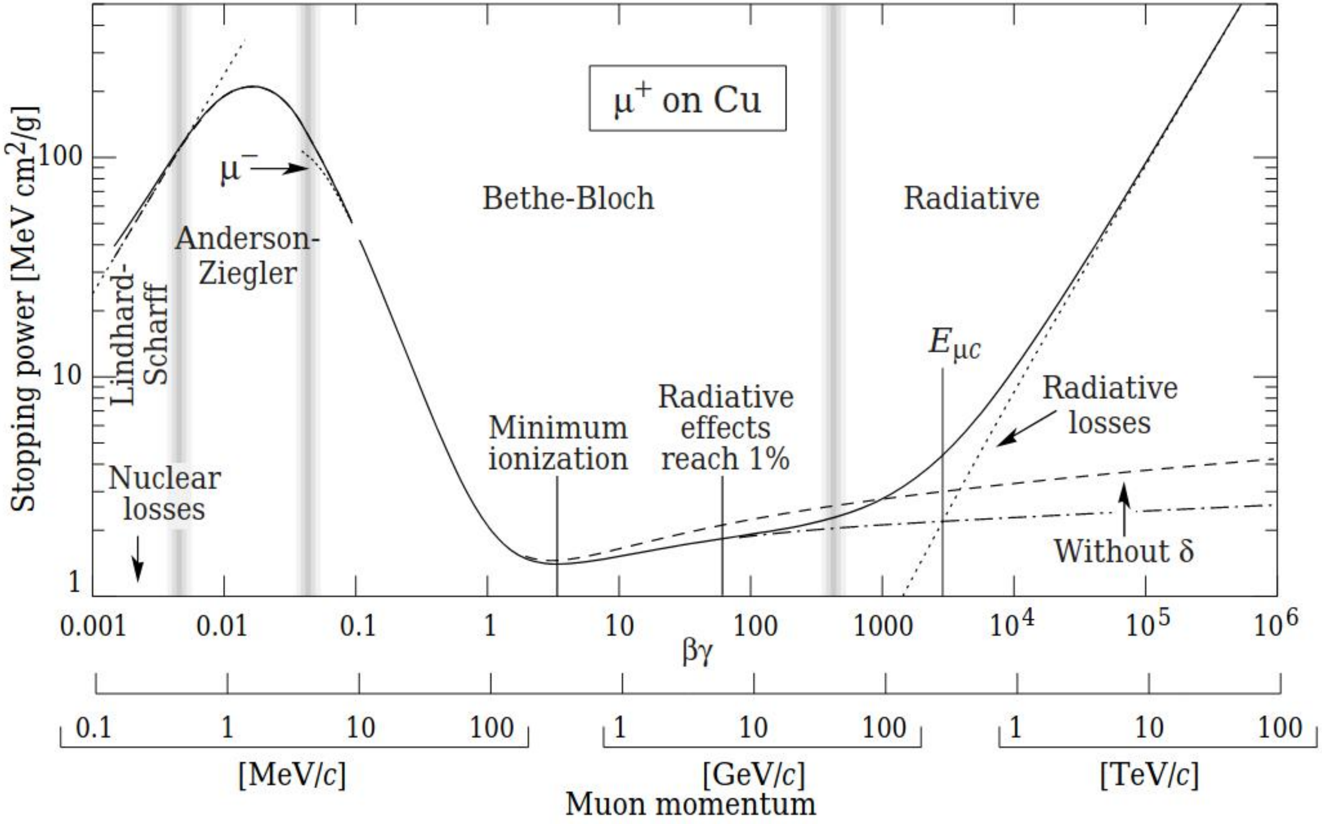

http://pdg.lbl.gov/2009/reviews/rpp2009-rev-passage-particles-matter.pdf

Mean Energy loss

- Mean energy loss rate in:
  - Liquid hydrogen
  - Gaseous helium
  - Carbon
  - Aluminum
  - Iron
  - Tin
  - Lead

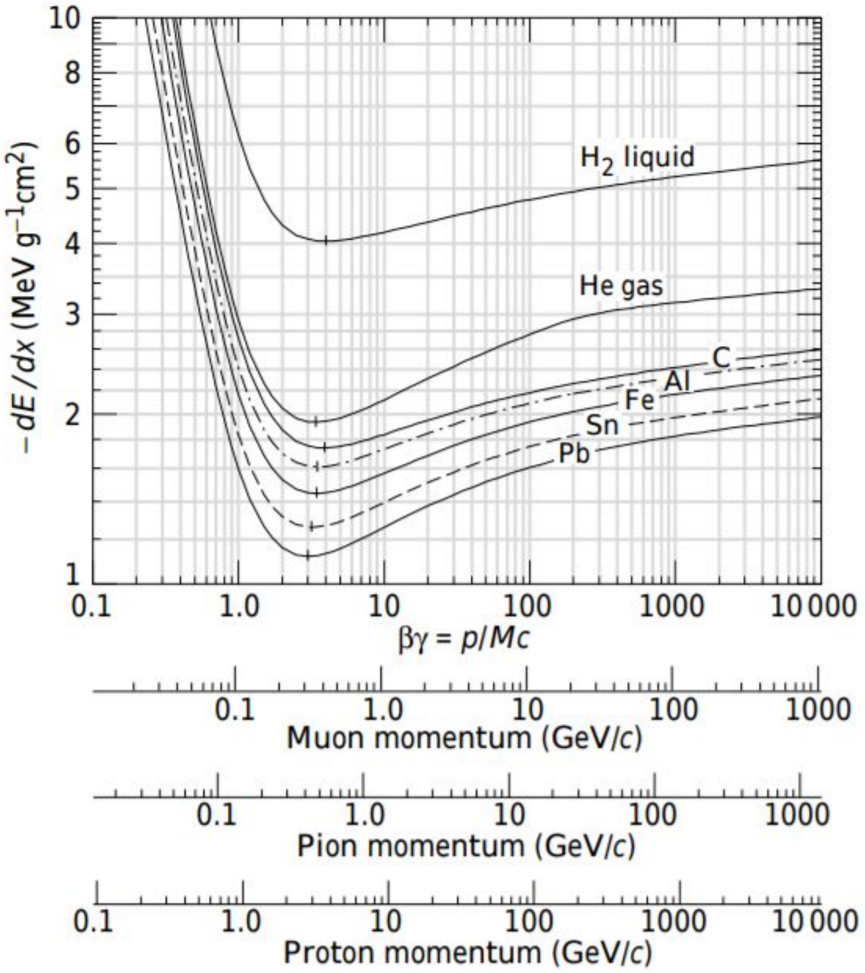

http://pdg.lbl.gov/2009/reviews/rpp2009-rev-passage-particles-matter.pdf

Energy loss of photons

Atomic photoelectric effect (electron ejection, photon absorption)

Rayleigh (coherent) scattering at the atom

Incoherent scattering (Compton scattering off an electron)

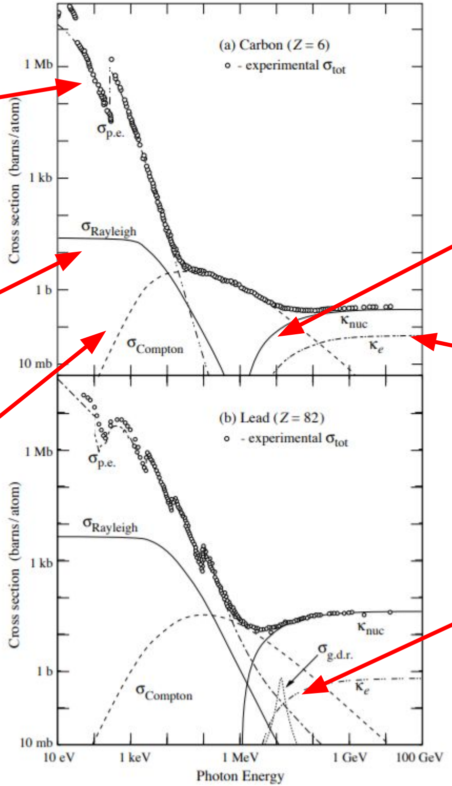

Pair production (nuclear field)

Pair production (electron field)

Photonuclear interactions (target nucleus gets broken up)

http://pdg.lbl.gov/2009/reviews/rpp2009-rev-passage-particles-matter.pdf

Ionisation

- Charged particles passing through a medium lose a fraction of their energy to the electrons of the atoms within the medium (via ionisation and excitation)
  - The average energy loss per unit length is described for (heavy particles i.e. all particles except for electrons and positrons) via the **Bethe-Bloch equation**:

$$-\left\langle \frac{dE}{dx} \right\rangle = K z^2 \frac{Z}{A} \frac{1}{\beta^2} \left[\frac{1}{2} \ln \frac{2 m_e c^2 \beta^2 \gamma^2 T_{\max}}{I^2} - \beta^2 - \frac{\delta(\beta\gamma)}{2} \right]$$

    - It describes the mean rate of energy loss in the region $0.1 < \beta\gamma < 1000$ for intermediate-Z materials with an accuracy of a few %

with:

Z = Atomic number of absorber
A = Atomic mass of absorber
z = Charge number
β = velocity of the incoming particle
I = Mean excitation energy

$K = 4\pi N_A r^2 m_e c^2$
N_A = Avogadro's number
r = Classical electron radius
T_{max} = Maximum kinetic energy which can be imparted to a free electron in a single collision

Bremsstrahlung

- Charged particles lose a fraction of their energy via electromagnetic radiation, while being in the Coulomb field of a atomic nucleus:
  - The mean energy loss per unit length (via Bremsstrahlung) is given via:

$$-\frac{dE}{dx} = \frac{E}{X_0}$$

  - An electron traveling a distance of $x = X_0$ has 1/e of its original energy left, while the fraction 1-1/e = 63% has been radiated off.
    - **The radiation length X_0 is given via:**

$$X_0 = \frac{716.4 \cdot A}{Z(Z+1)\log\left(287/\sqrt{Z}\right)}$$

Z = Atomic number of absorber
A = Atomic mass of absorber
X_0 = Radiation length

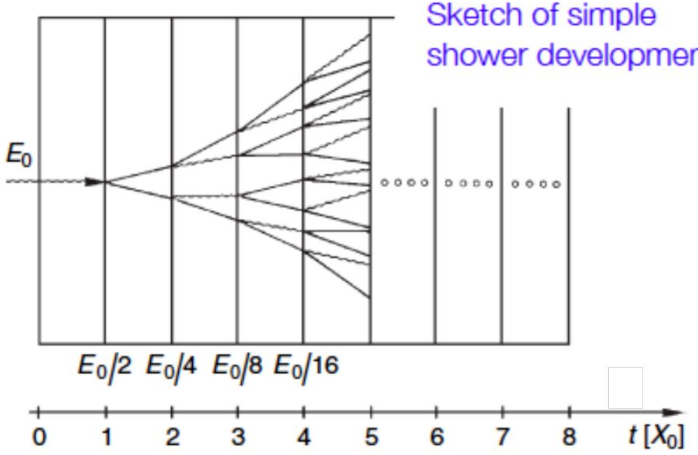

Interaction between Hadrons and matter

- The strong force plays a crucial role for the interaction between Hadrons (p, n, π) and matter
  - **The absorption length** is defined analogously to the radiation length (describing electromagnetic processes)
    - It quantifies the distance λ_a for which the probability that a particle has not been absorbed yet has dropped to 1/e:

$$\lambda_a = \frac{A}{N_A \cdot \rho \cdot \sigma_{\text{Inelastic}}}$$

    - The absorption lengths for hadronic particles are usually significantly larger than the radiation length for electrons and photons.
      - **Thus, hadronic calorimeters are much larger than electromagnetic calorimeter**

Interaction between Hadrons and matter

- Hadronic showers are significantly more complex than EM showers:
  - **Hadronic component:**
    - Inelastic scattering at nucleons
    - Spallation/Fission
    - Evaporation
  - **Electromagnetic component:**
    - Photons from π0 or η decays start EM cascades
  - **Invisible component:**
    - Neutrinos from weak decays

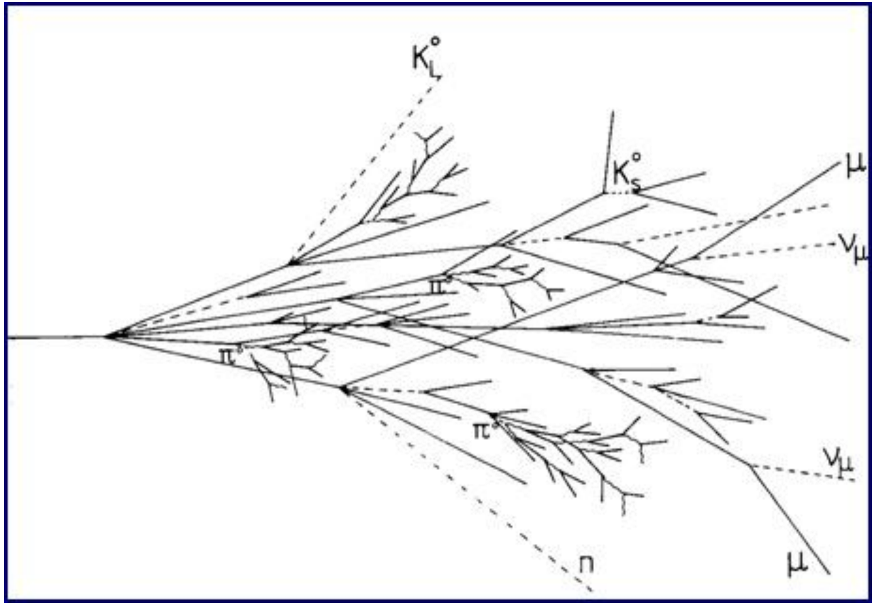

- Worse energy resolution (compared to measurements of electromagnetic cascades) due to large fluctuations in shower developments

Cherenkov and transition radiation

- **Cherenkov radiation:**
  - A charged particle (with velocity v) passing through a medium (with a refraction index n) emits electromagnetic radiation, if v is larger than the phase velocity of light c_0 in that medium
    - The emission angle is:

$$\cos\Theta_C = \frac{c_0}{v \cdot n(\omega)} = \frac{1}{\beta \cdot n(\omega)}$$

    - Energy emitted via Cherenkov radiation per unit length x and per frequency:

$$\frac{d^2E}{d\omega dx} = \frac{z^2e^2}{4\pi\epsilon_0 c^2}\omega \sin^2\Theta_C(\omega)$$

  - Used for e.g. particle identification:
    - After independent momentum measurement

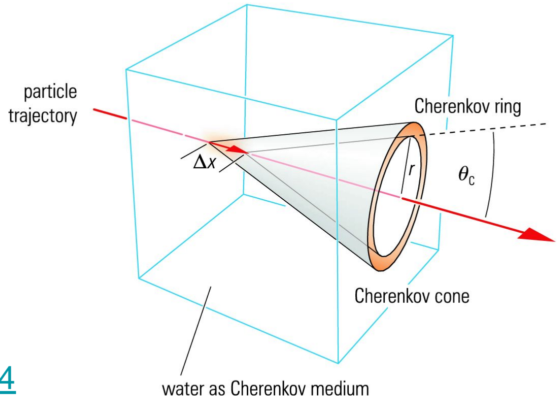

Taken from: https://doi.org/10.1007/978-3-030-27339-2_4

Cherenkov and transition radiation

- **Transition radiation:**
  - A charged particle emits electromagnetic radiation if it passes the boundary between two different media (with different refractive indices n_1 and n_2)
    - Intensity of transition radiation depends on the Lorentz- factor γ of that particle
    - Still suited for particle identification with γ >> 100
      - Cherenkov angle variations $\Delta\Theta_C$ are very small in this phase space

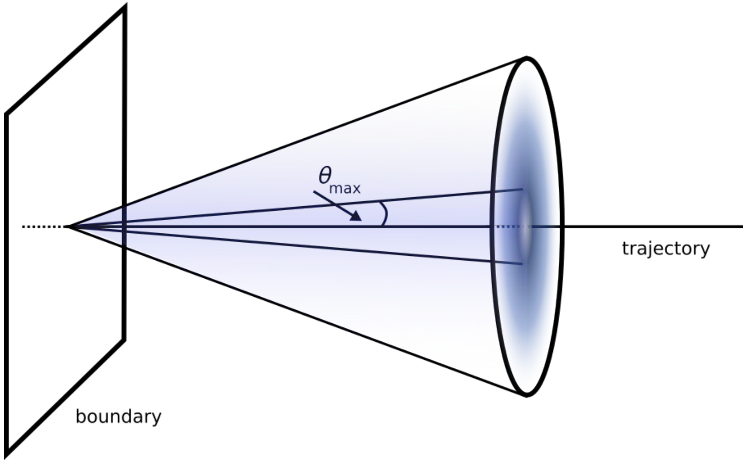

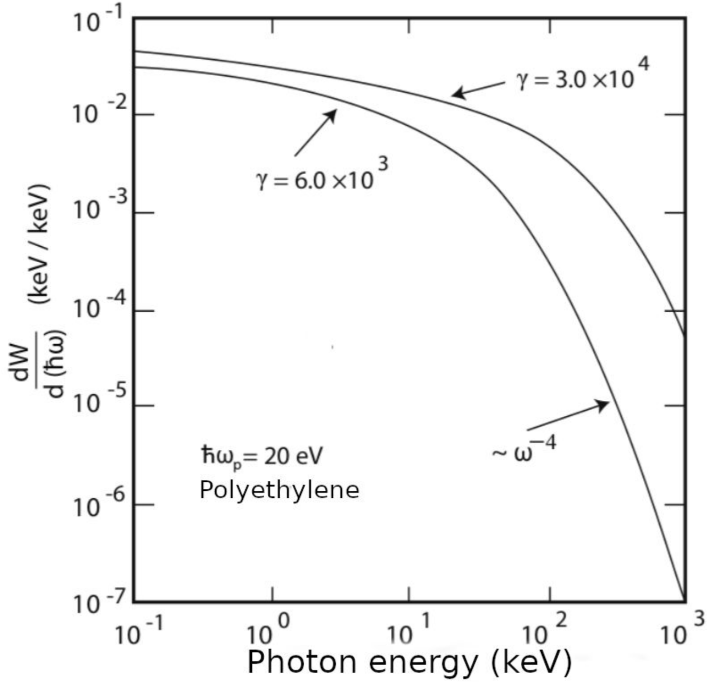

2.2.2 Modern particle detector

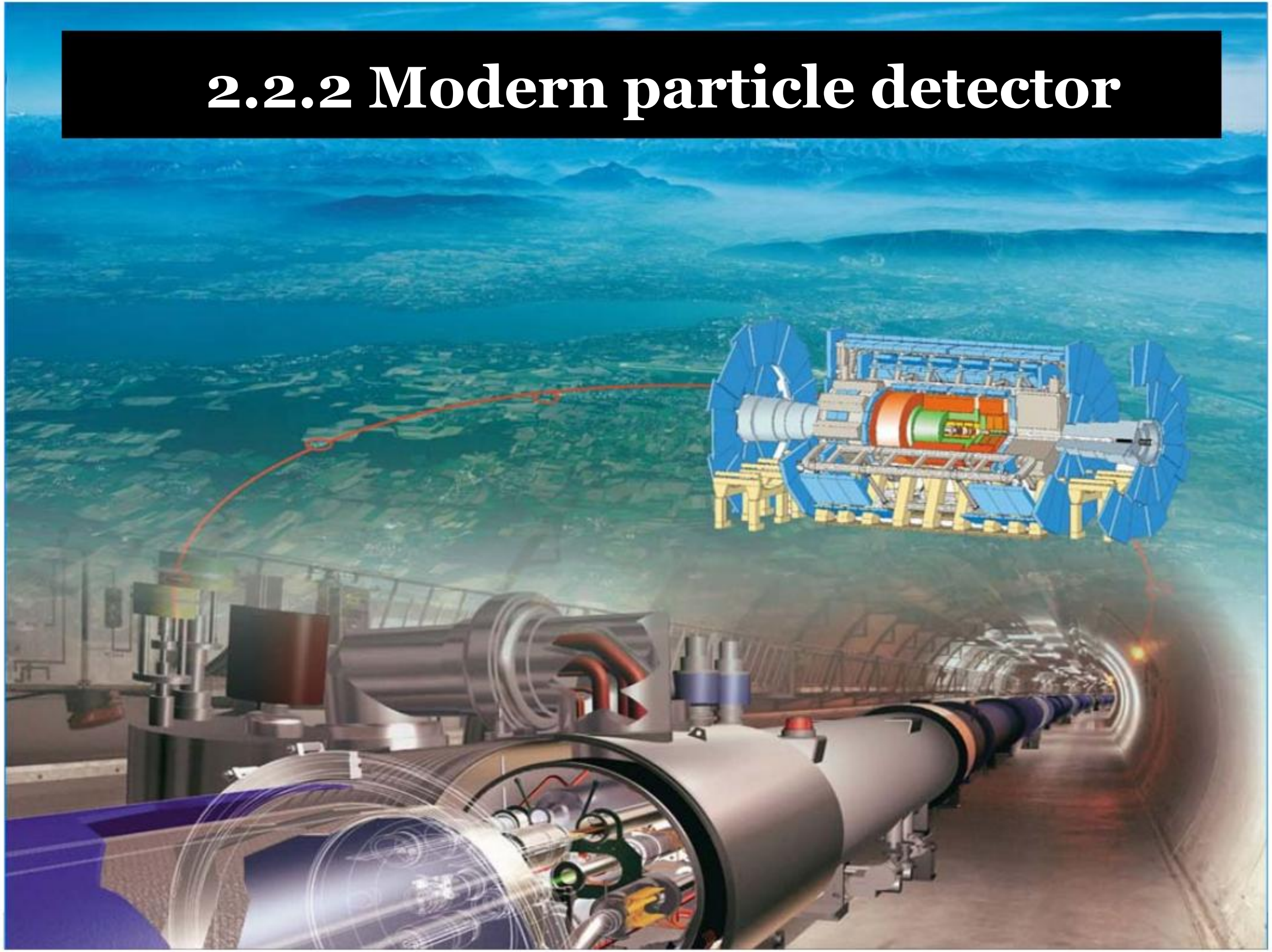

The ATLAS Detector

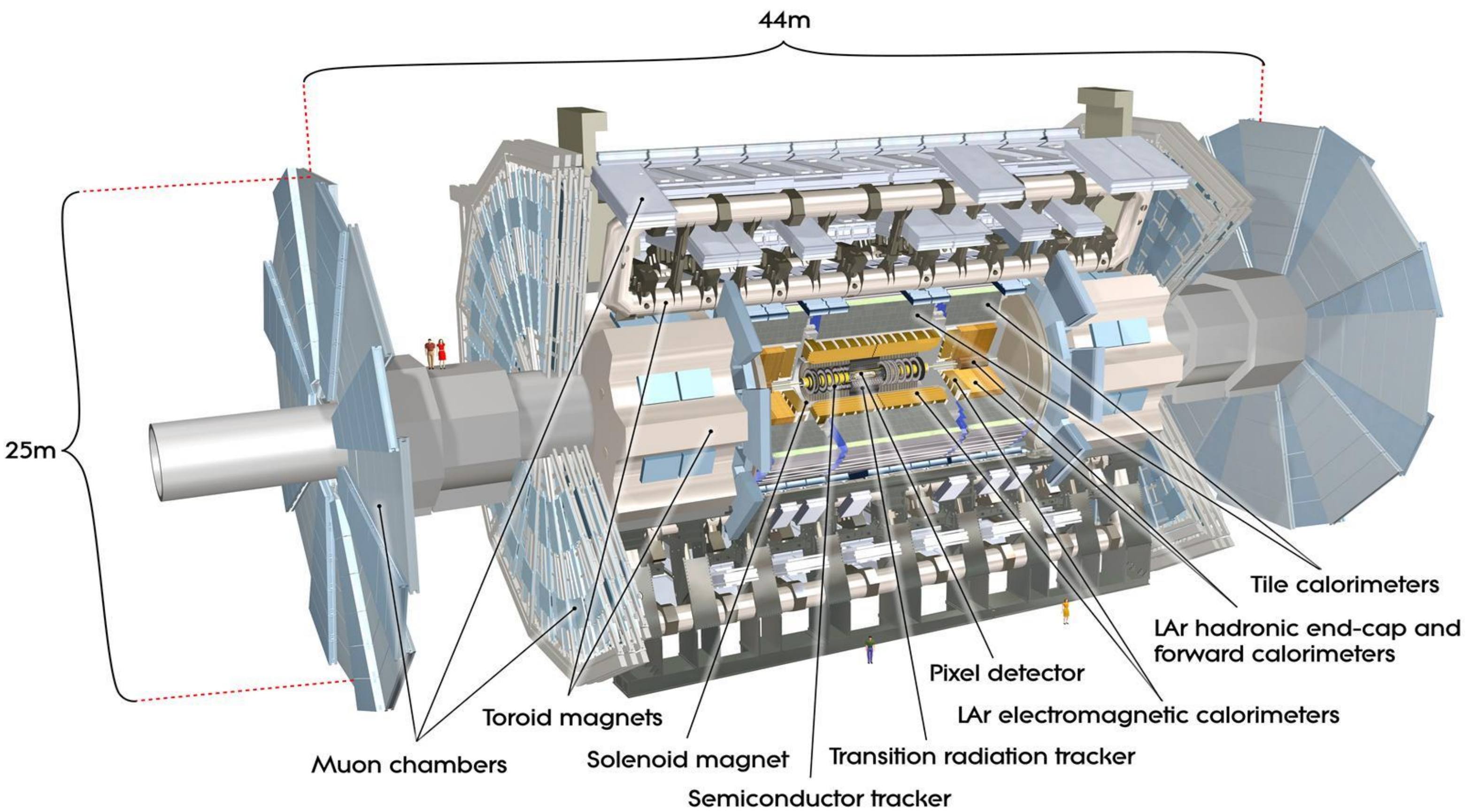

Inner Detector

- **Inner Detector** build up by three types of tracking detectors
  - Pixel
  - Semiconductor Tracker (SCT)
  - Transition Radiation Tracker (TRT)
- Dedicated to reconstruct trajectories of charged particles (tracking), charge identification and momentum measurement

$$\frac{\sigma_{p_T}}{p_T} = 0,05\% \cdot p_T \oplus 1\%$$

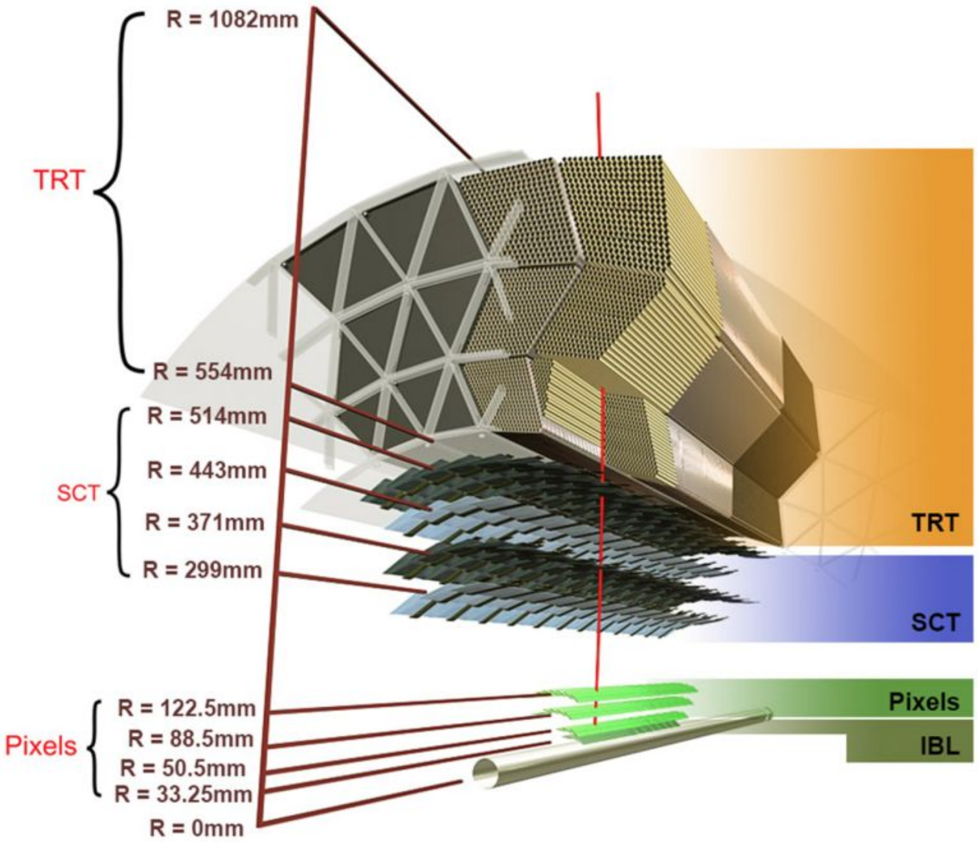

Inner Detector

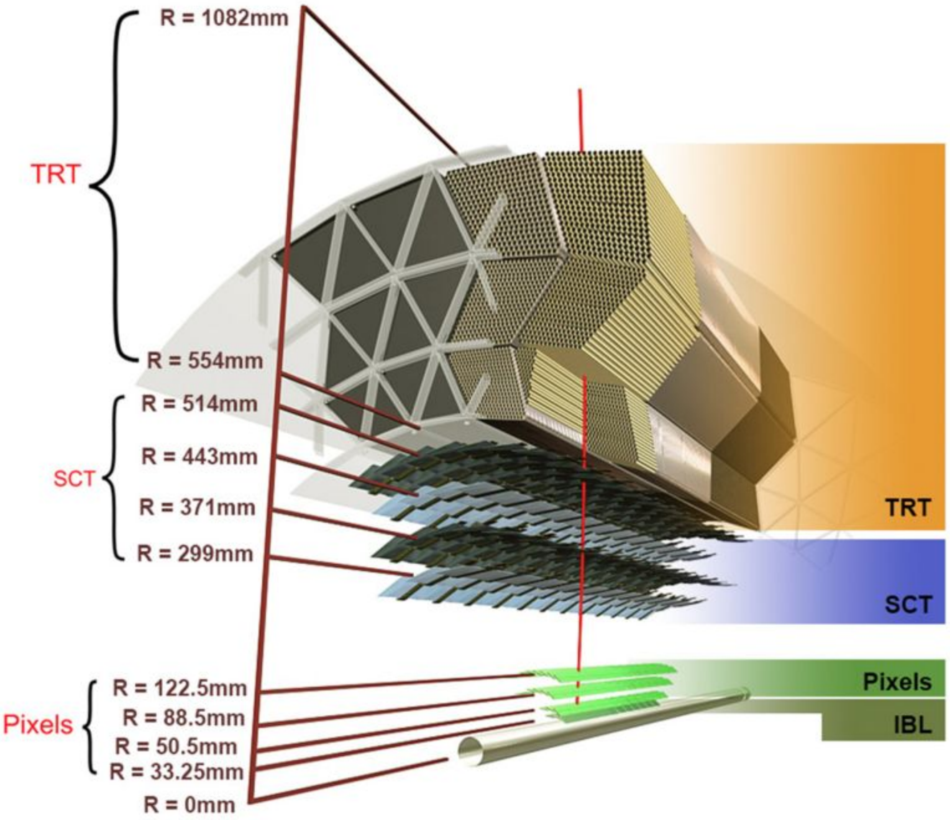

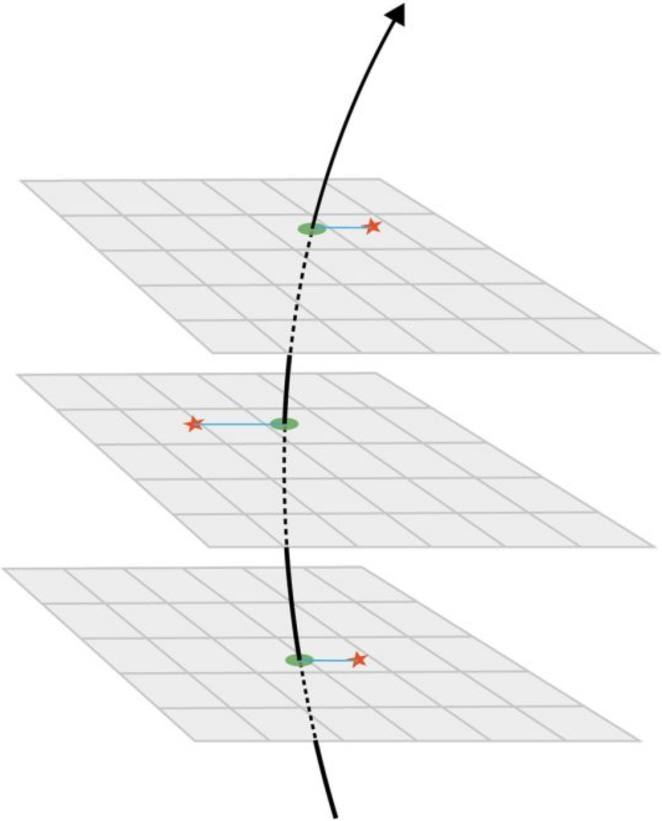

Inner Detector

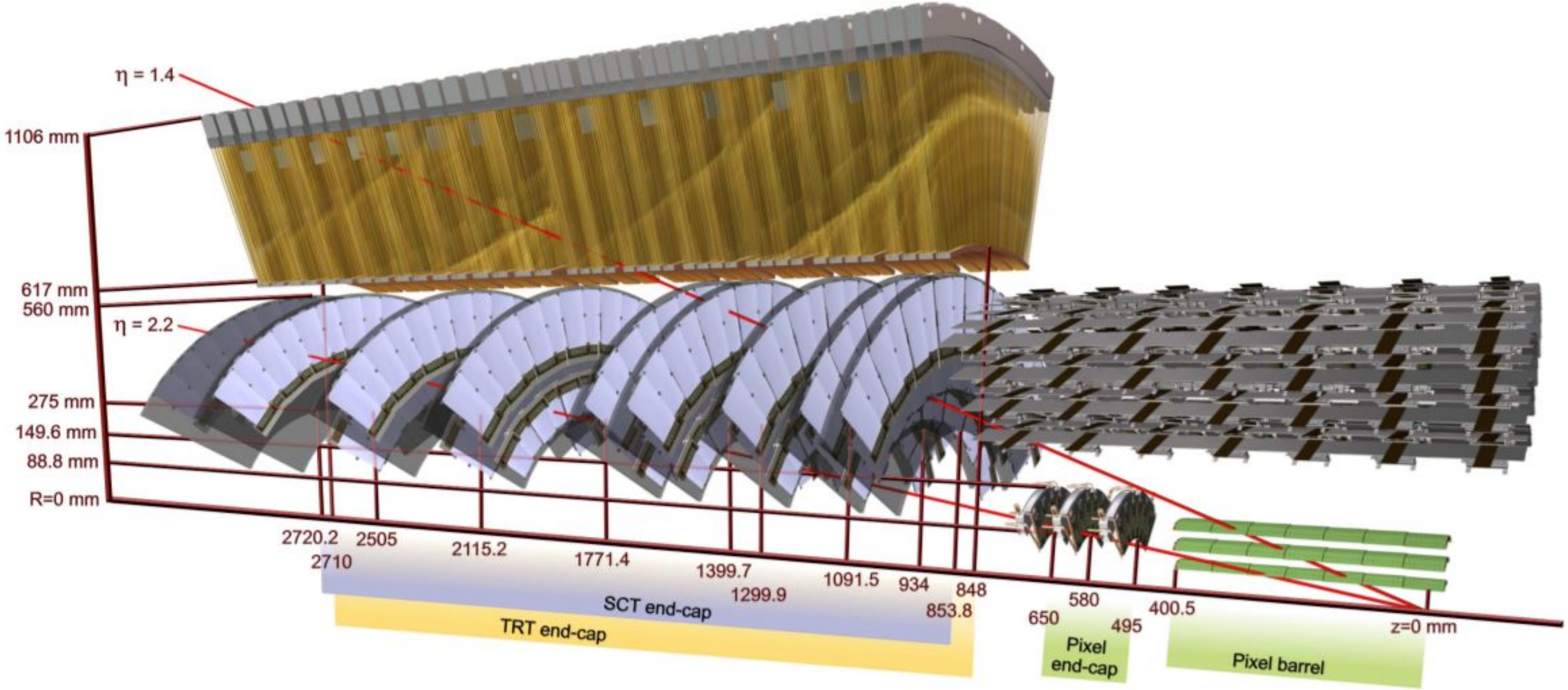

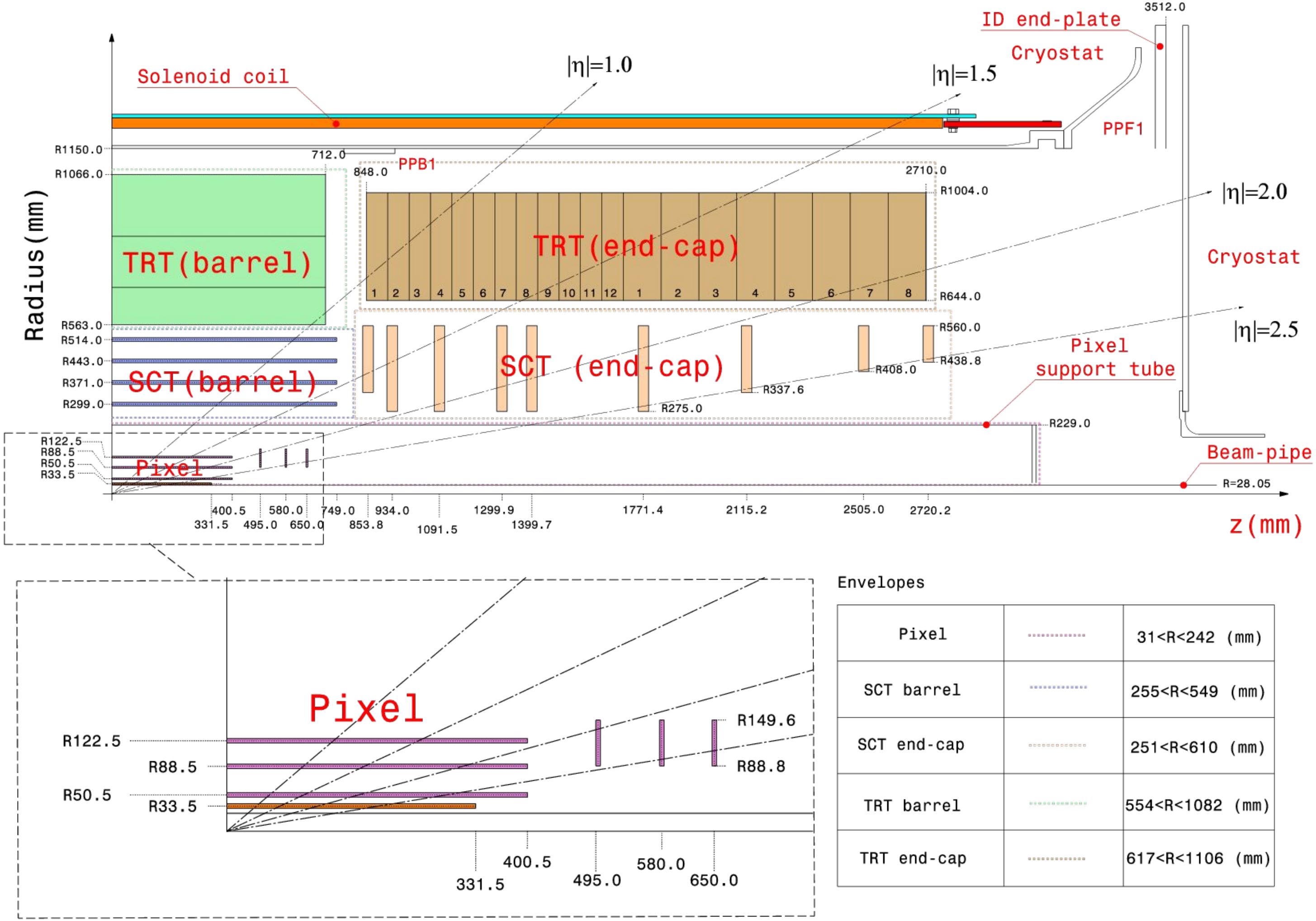

Radius(mm)
z(mm)
Solenoid coil
|η|=1.0
|η|=1.5
|η|=2.0
|η|=2.5
ID end-plate
Cryostat
3512.0
PPF1
PPB1
R1150.0
R1066.0
712.0
848.0
2710.0
R1004.0
R644.0
TRT(barrel)
TRT(end-cap)
1 2 3 4 5 6 7 8 9 10 11 12 1 2 3 4 5 6 7 8
Cryostat
R563.0
R514.0
R443.0
R371.0
R299.0
SCT(barrel)
SCT (end-cap)
R560.0
R438.8
R408.0
R337.6
R275.0
Pixel
support tube
R229.0
Beam-pipe
R=28.05
R122.5
R88.5
R50.5
R33.5
Pixel
400.5
331.5
580.0
495.0
650.0
749.0
934.0
853.8
1091.5
1299.9
1399.7
1771.4
2115.2
2505.0
2720.2
Pixel
R122.5
R88.5
R50.5
R33.5
R149.6
R88.8
400.5
331.5
495.0
580.0
650.0
Envelopes
Pixel 31<R<242 (mm)
SCT barrel 255<R<549 (mm)
SCT end-cap 251<R<610 (mm)
TRT barrel 554<R<1082 (mm)
TRT end-cap 617<R<1106 (mm)

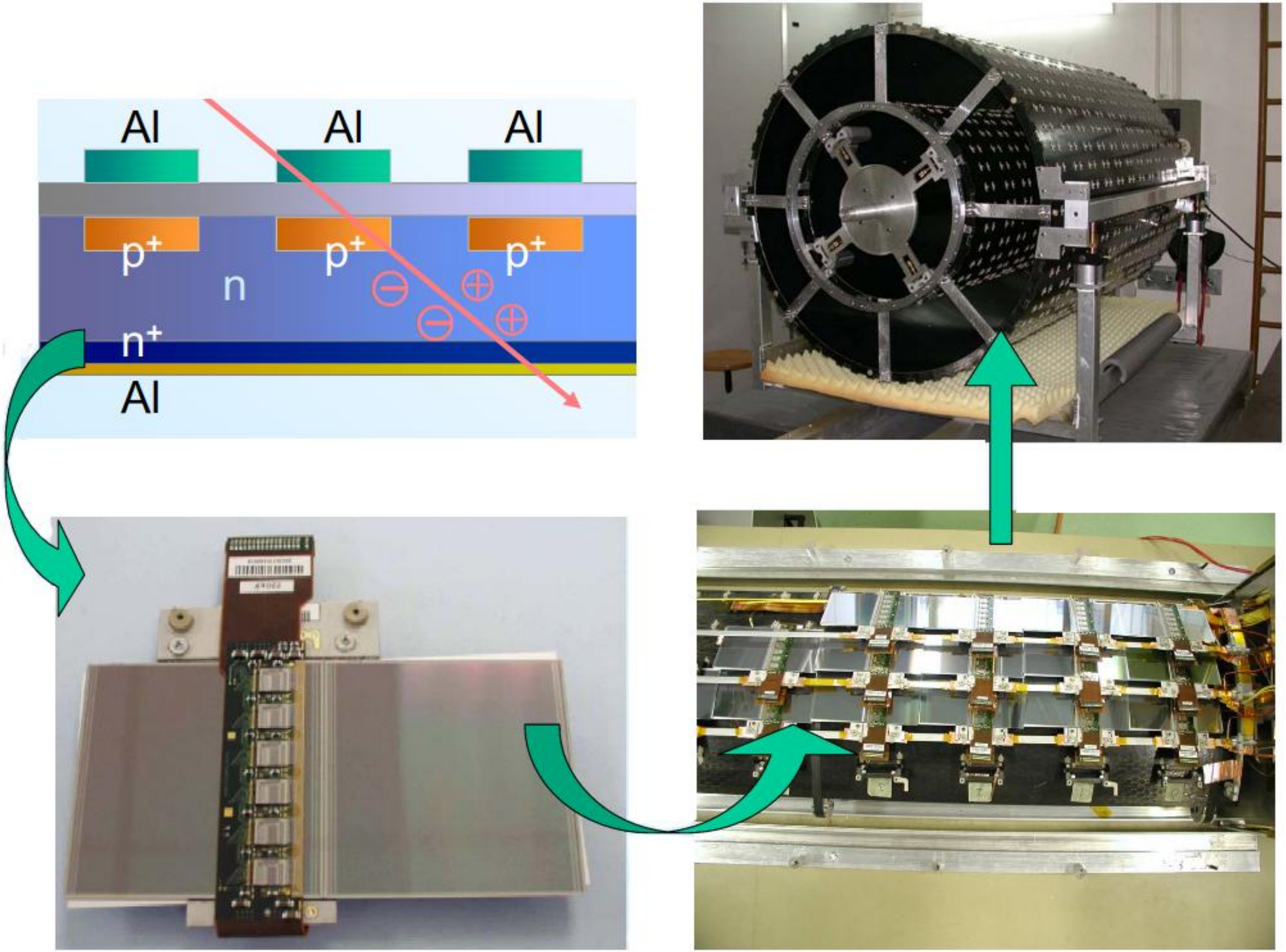
Al
Al
Al
p+
p+
p+
n
n+
Al

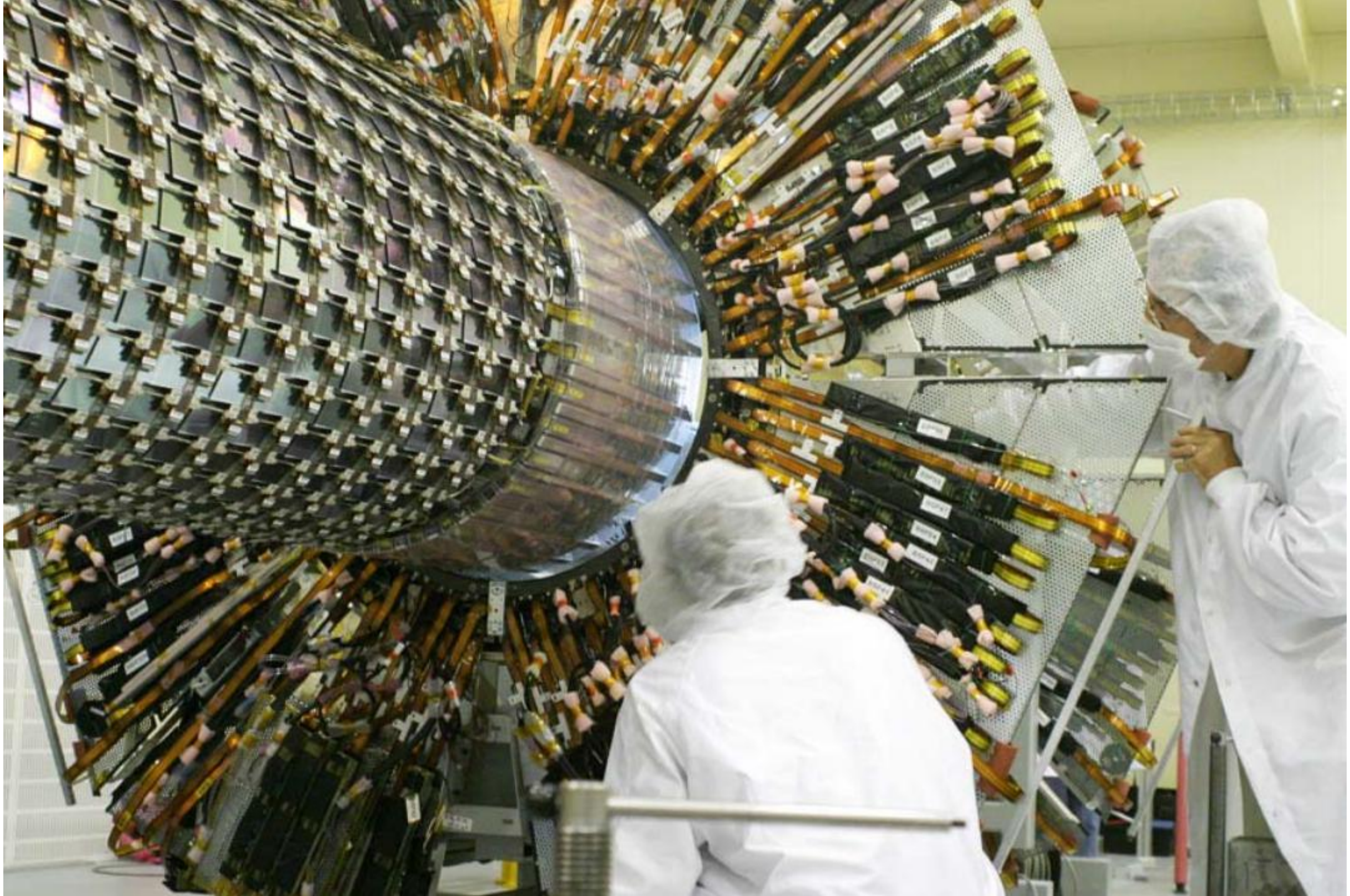

Inner Detector

	Intrinsic accuracy [μm]	
	Azimuthal (R-Φ)	Radial (R) / Axial (z)
	Pixel	
Layer-0	10 (R-Φ)	115 (z)
Layer-1 and -2	10 (R-Φ)	115 (z)
Disks	10 (R-Φ)	115 (R)
	SCT	
Barrel	17 (R-Φ)	580 (z)
Disks	17 (R-Φ)	580 (R)
	TRT	
Barrel/Disks	130 per straw	

Calorimeter system

- ATLAS calorimeters use so called sampling technique for **energy measurements**
  - Active material and absorber alternate
- **EM calorimeter:**
  - Active medium: **liquid argon**
  - Absorber: **Lead**

$$\frac{\sigma_E}{E} = \frac{10\%}{\sqrt{E}} \oplus 0.7\%$$

- **Hadronic calorimeter:**
  - Active medium: **scintillating plastic**
  - Absorber: **Steel**

$$\frac{\sigma_E}{E} = \frac{50\%}{\sqrt{E}} \oplus 3\% \quad \text{and} \quad \frac{\sigma_E}{E} = \frac{100\%}{\sqrt{E}} \oplus 10\%$$

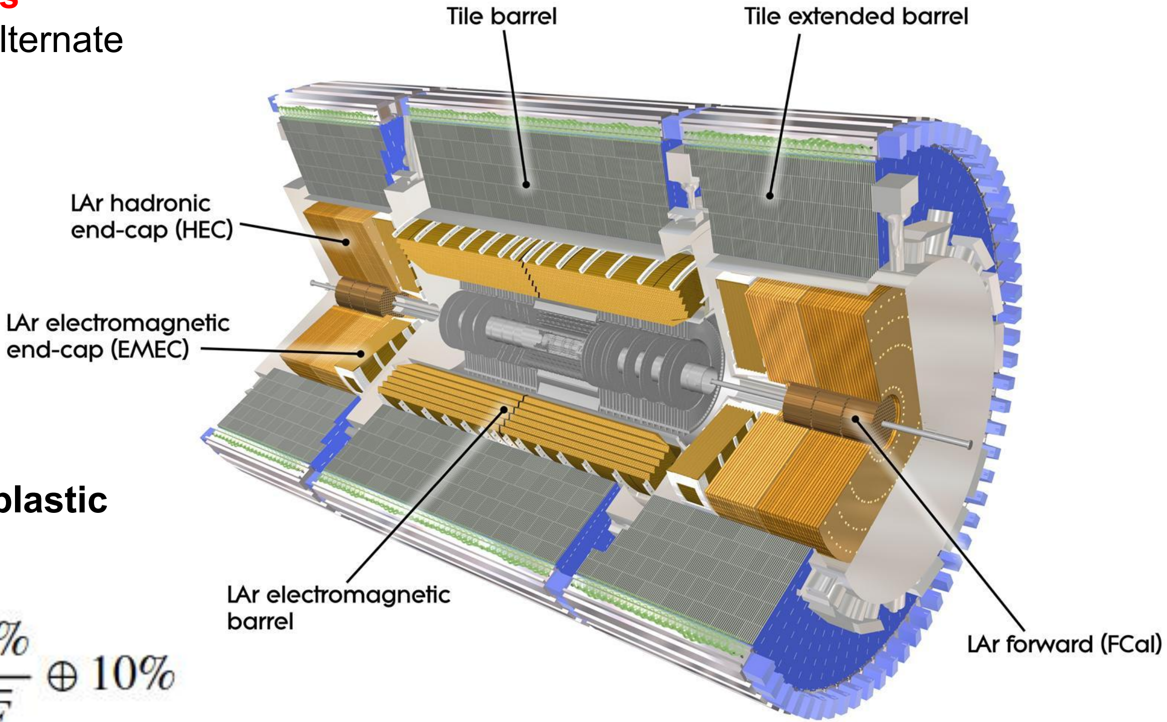

ATLAS calorimeter system

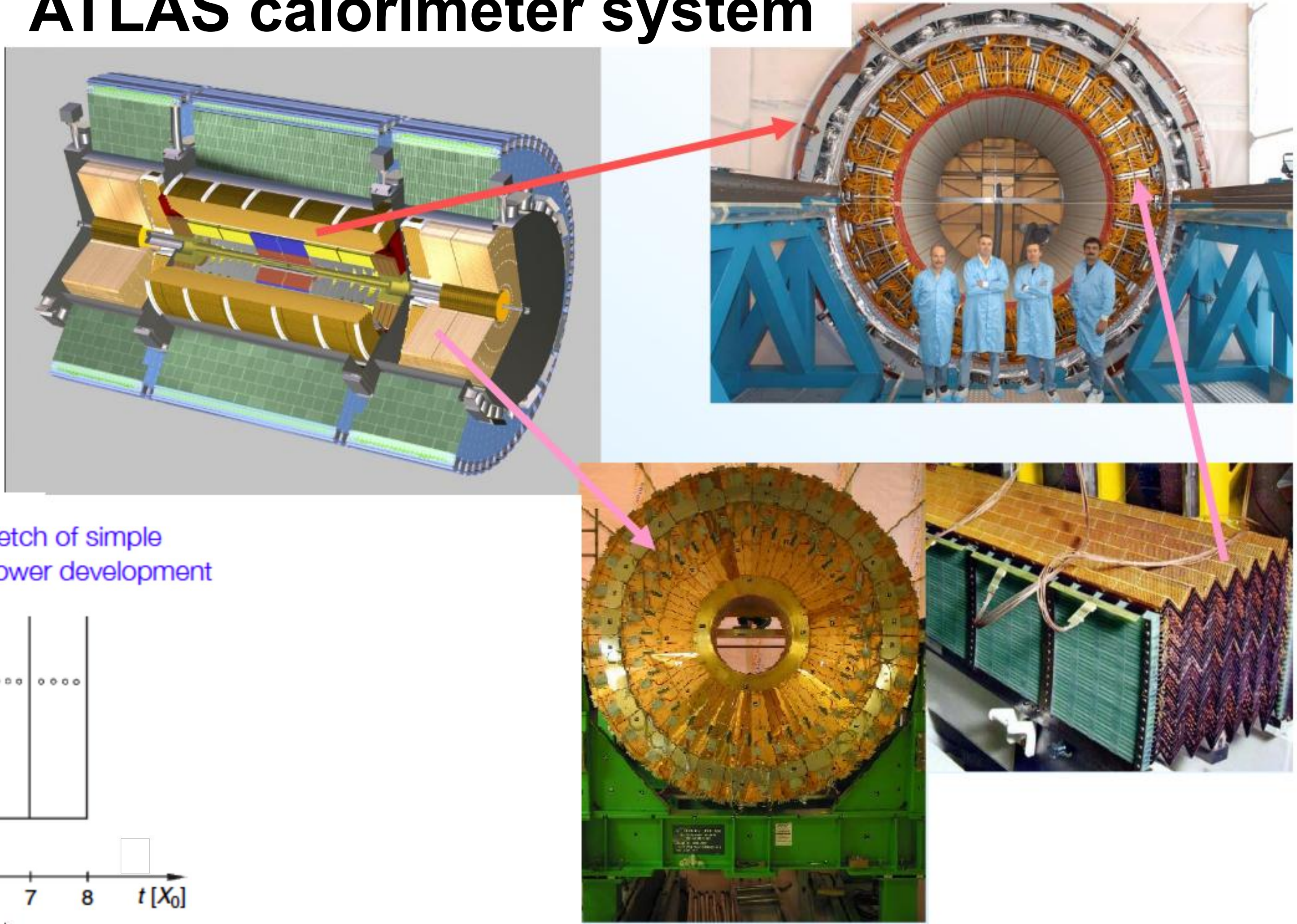

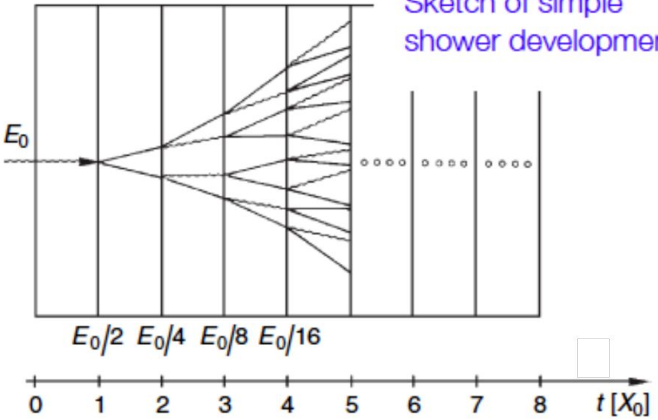

Sketch of simple shower development

EM calorimeter module

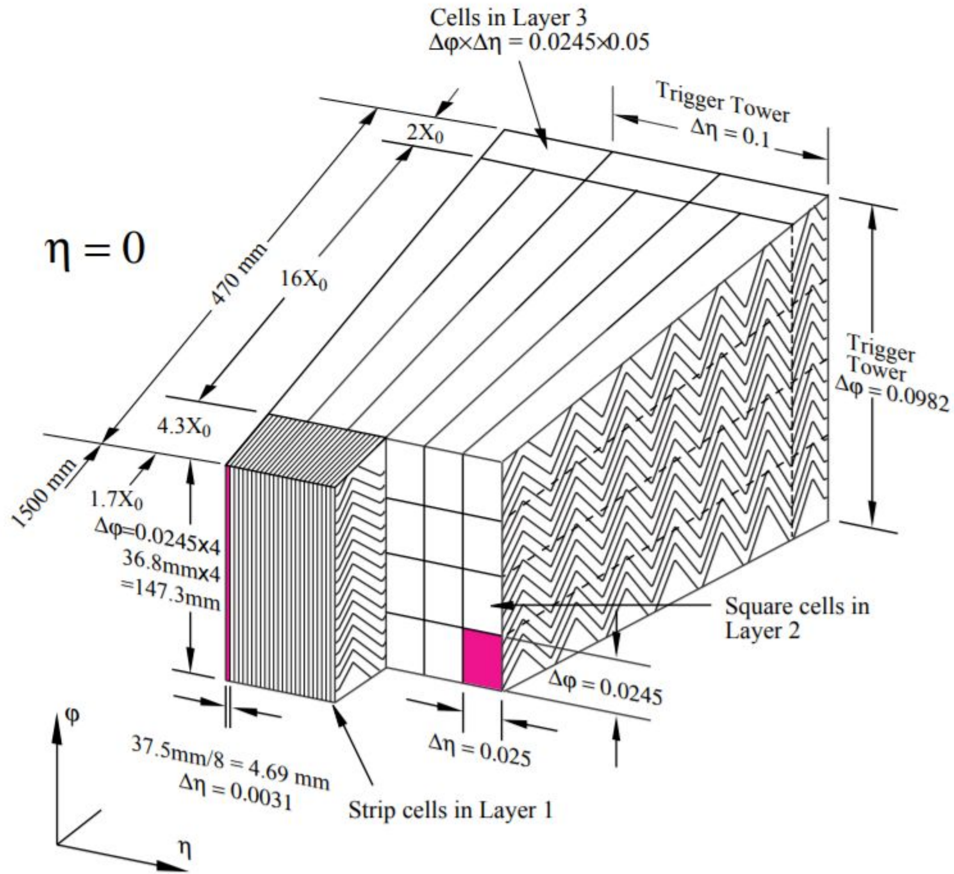

Calorimeter

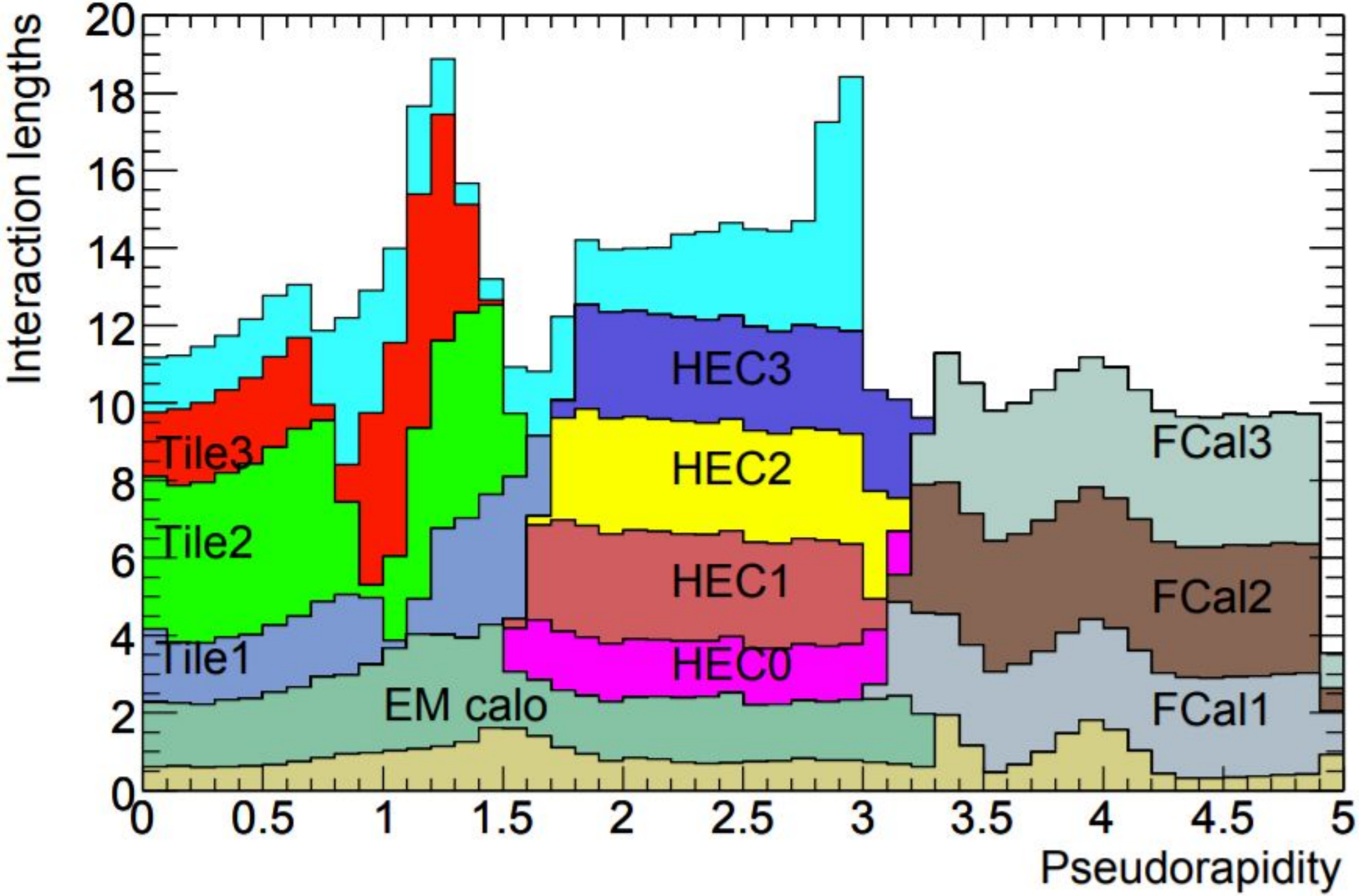

Muon spectrometer

- The muon spectrometer measures the deflection of the muon tracks in the magnetic field
  - Based on gaseous detectors for precision tracking and triggering
- Characteristics:
  - Momentum resolution of 2-10% for muons with a pT between 10GeV - 1TeV
  - Spatial resolution of 30 μm

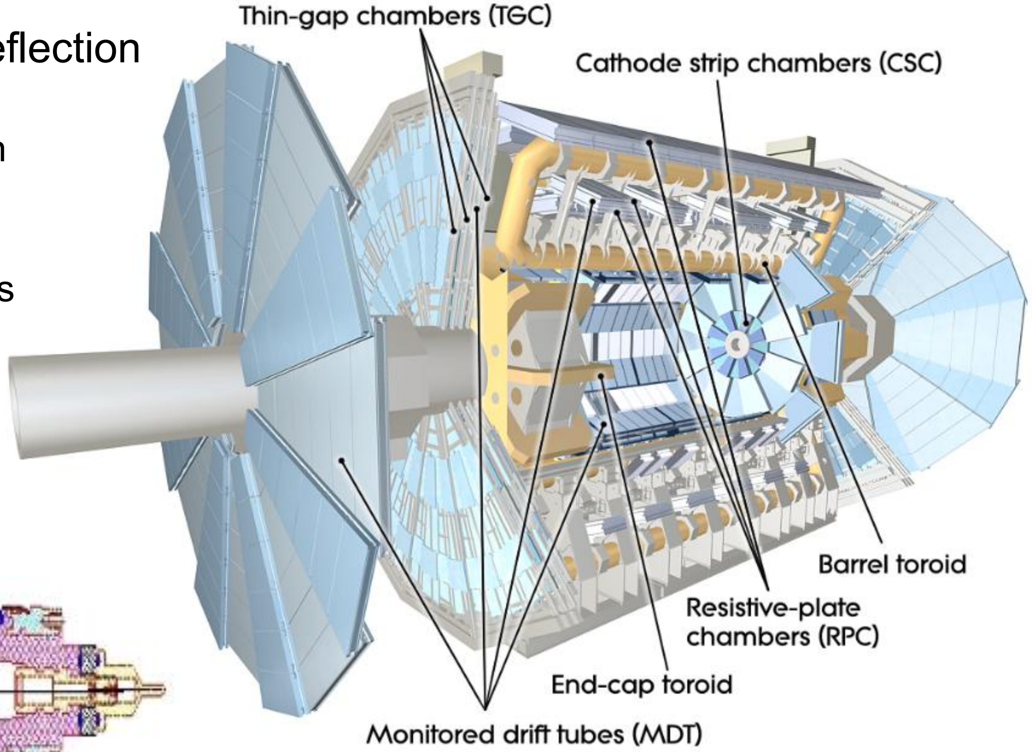

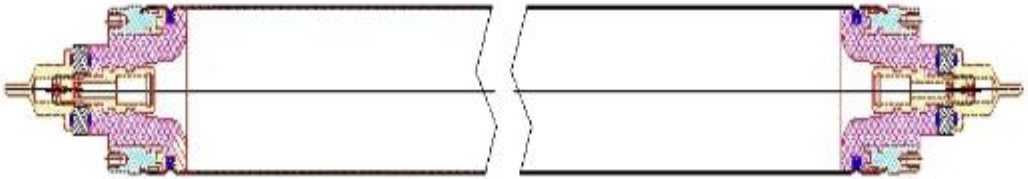

Muon spectrometer

- Each tube allows to measure one space point
  - Ensemble of space points is used to reconstruct muon tracks
- Drift time (of electrons/ions) is limiting factor for trigger rates

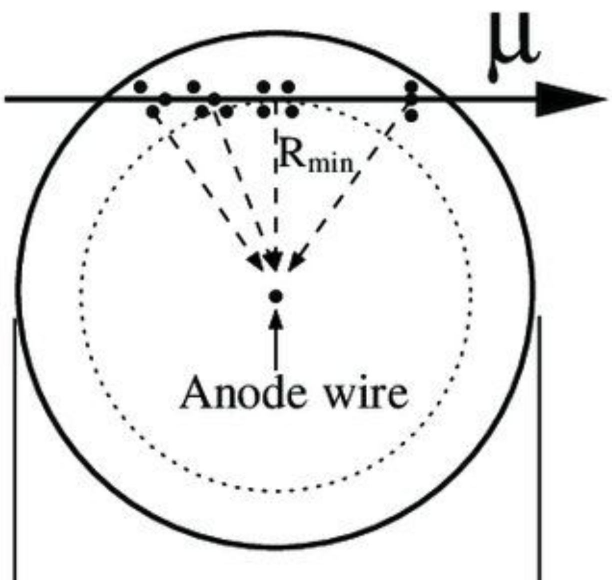

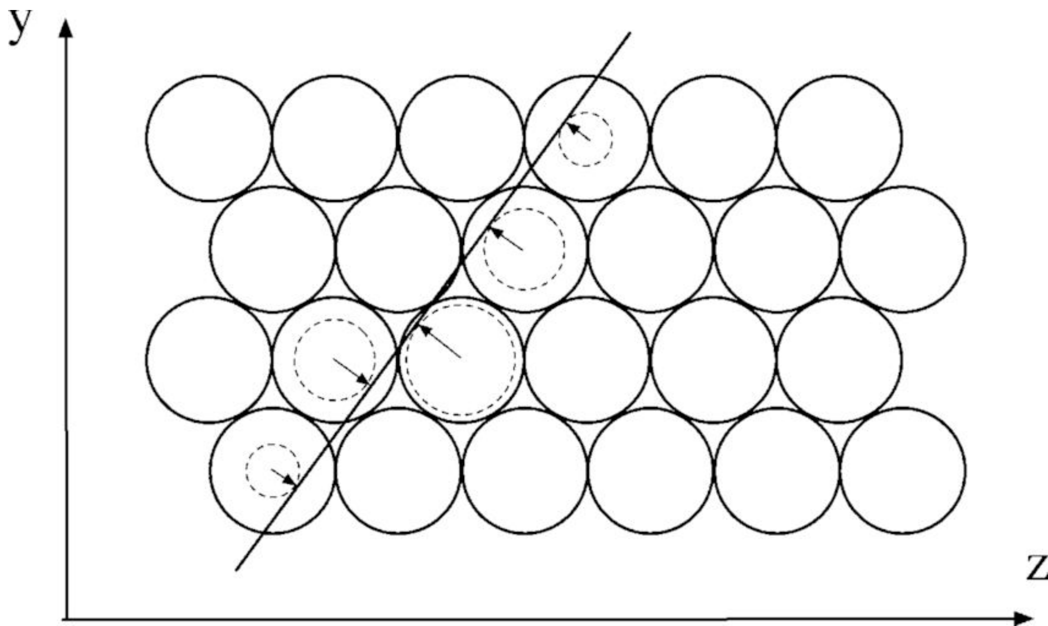

Construction of muon chambers

Magnet system

- **Toroids:**
  - Field strength: 4T
- **Solenoid**
  - Field strength: 2T
- **Responsible for bending trajectories of charged particles**
  - **Enables measurement of momenta**

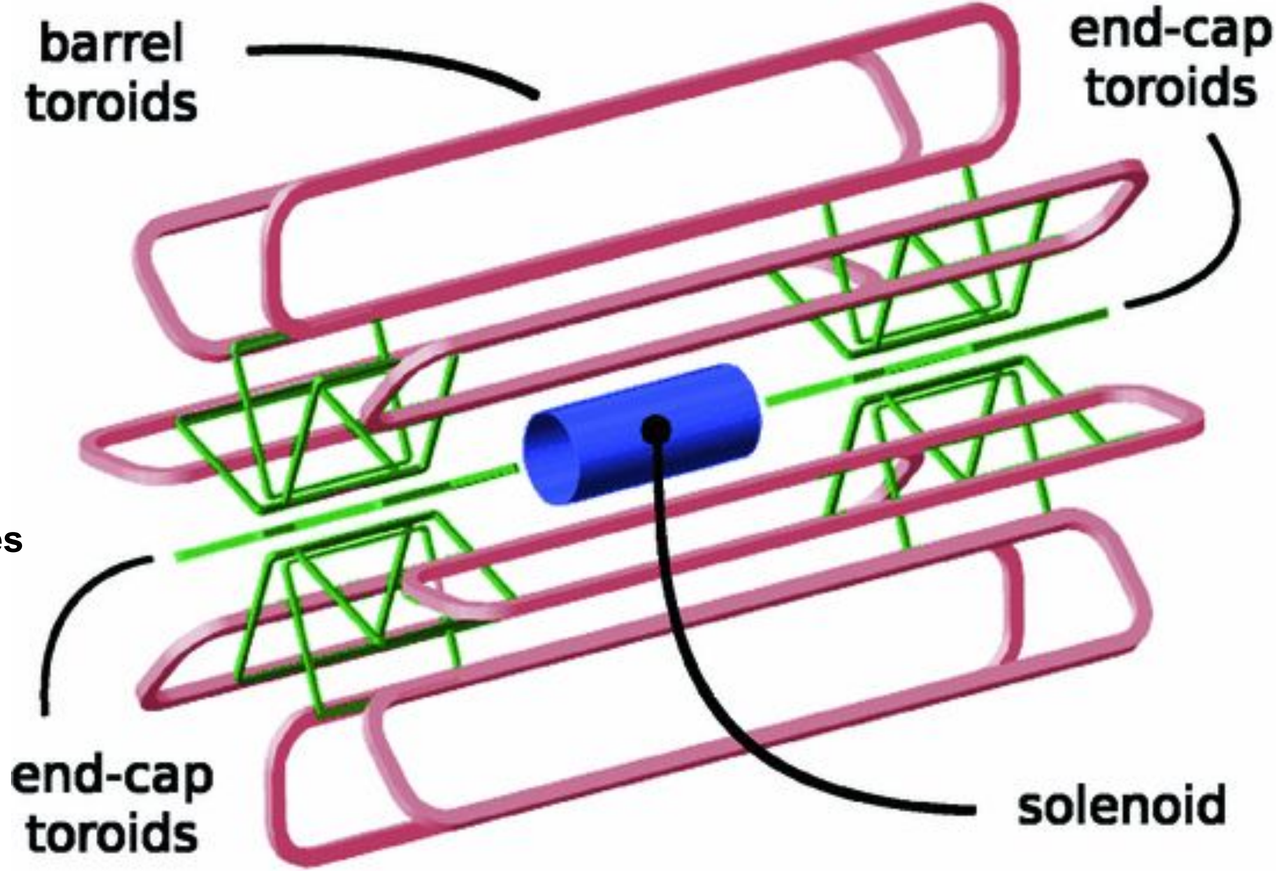

Construction

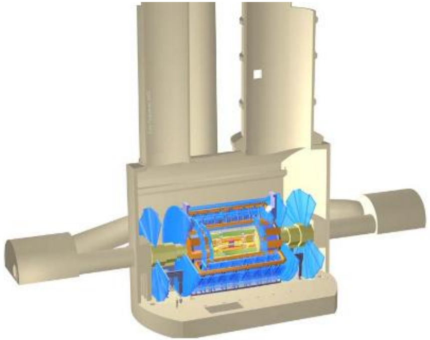


HWX 159

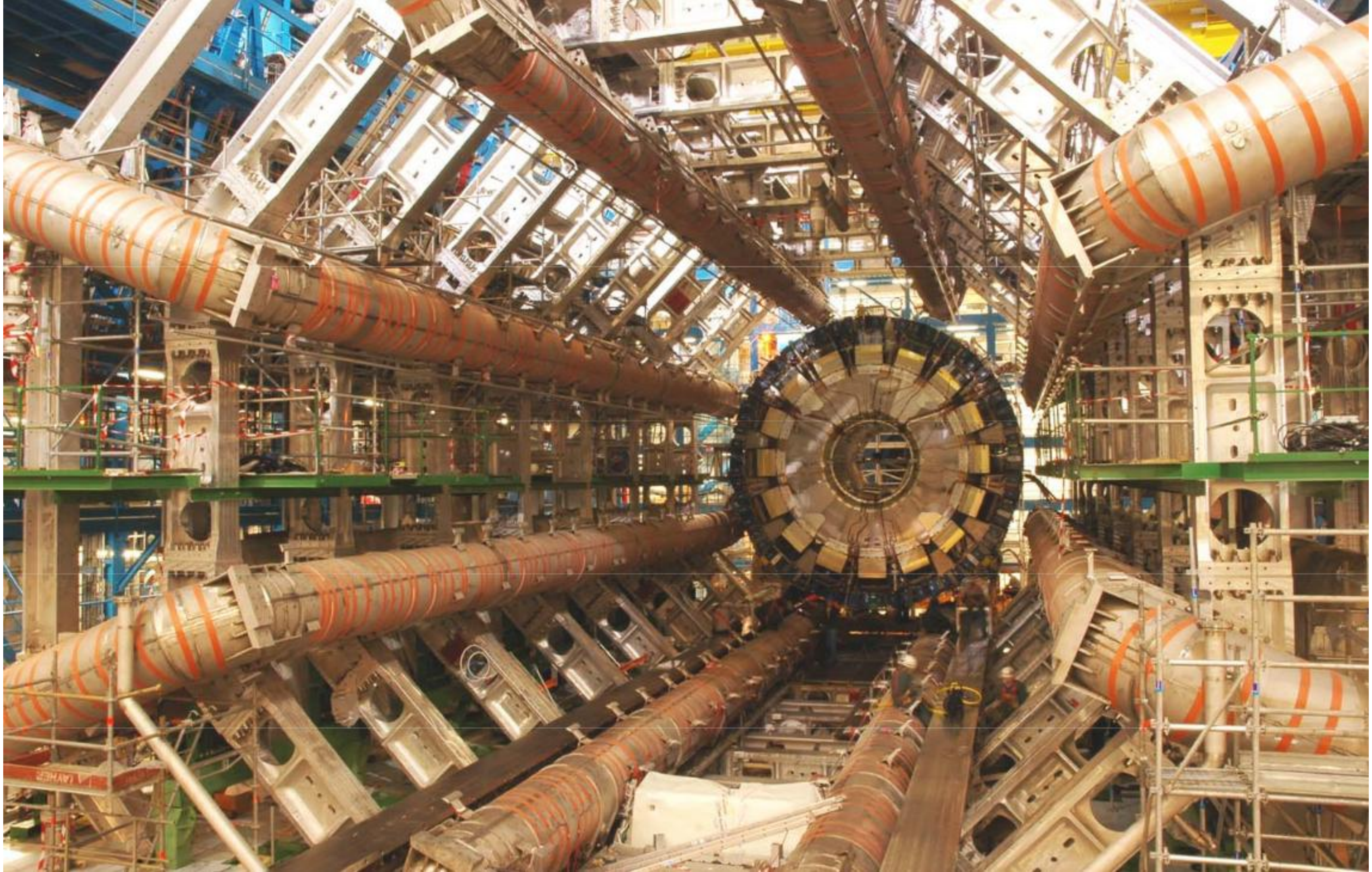

Trigger system

- **Trigger system filters out potentially interesting events**
  - Reduces the data to a more manageable amount

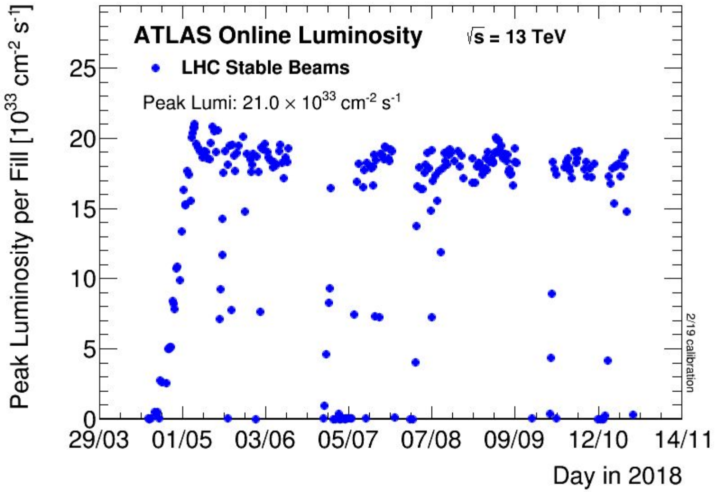

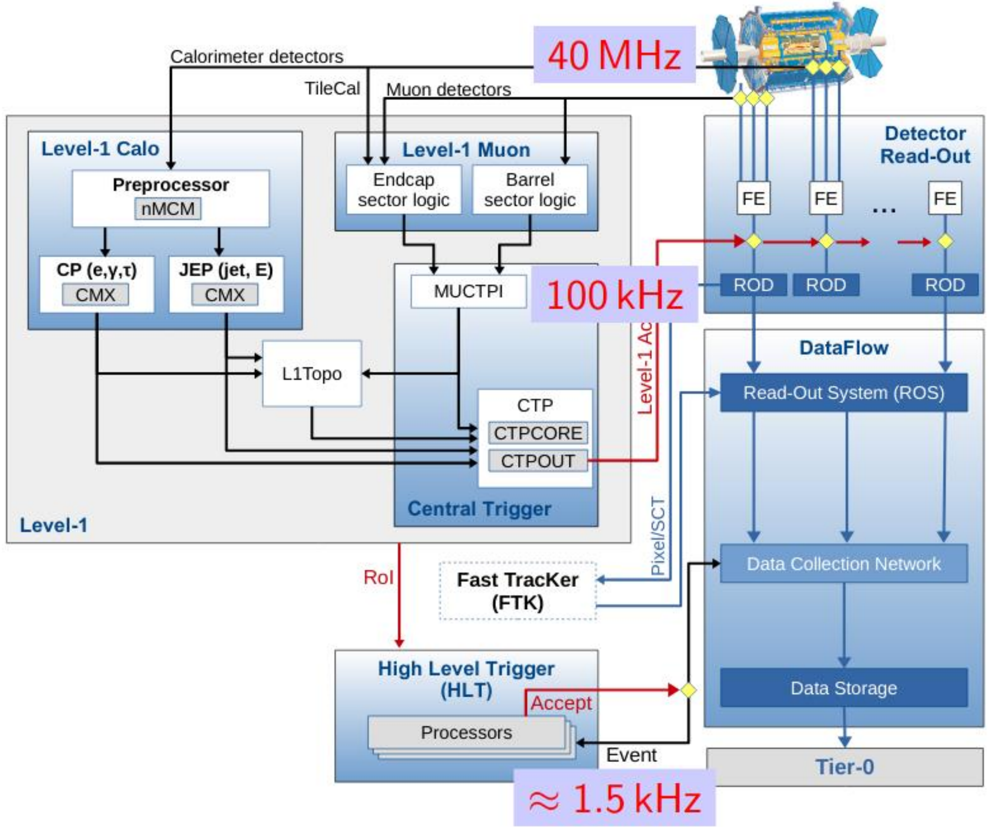

Data taking

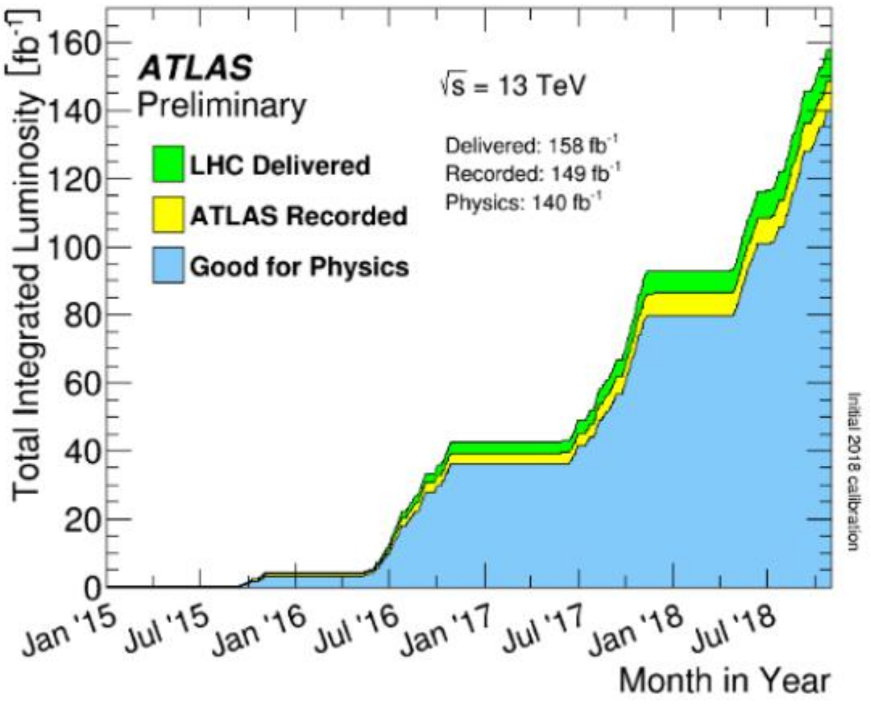

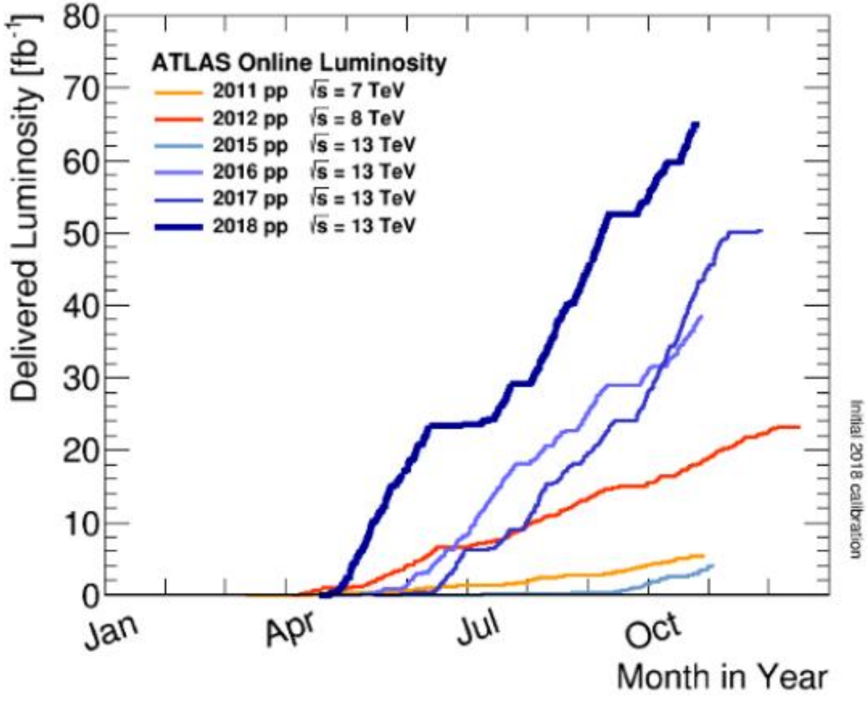

$$N = L \cdot \sigma$$

Data quality monitoring

Year	Dataset	Integrated Luminosity	
		Delivered	Recorded
2015	pp @ $\sqrt{s}$ = 13 TeV (50 ns)	102.2 pb^{-1}	94.5 pb^{-1}
	pp @ $\sqrt{s}$ = 13 TeV (25 ns)	3.88 fb^{-1}	3.63 fb^{-1}
	pp @ $\sqrt{s}$ = 5.02 TeV	26.1 pb^{-1}	25.6 pb^{-1}
	Pb-Pb @ $\sqrt{s_{NN}}$ = 5.02 TeV	0.51 nb^{-1}	0.50 nb^{-1}
2016	pp @ $\sqrt{s}$ = 13 TeV	38.0 fb^{-1}	35.5 fb^{-1}
	p-Pb @ $\sqrt{s_{NN}}$ = 8.16 TeV	170 nb^{-1}	167 nb^{-1}
	p-Pb @ $\sqrt{s_{NN}}$ = 5.02 TeV	0.44 nb^{-1}	0.43 nb^{-1}
2017	pp @ $\sqrt{s}$ = 13 TeV	49.0 fb^{-1}	46.4 fb^{-1}
	Xe-Xe @ $\sqrt{s_{NN}}$ = 5.44 TeV	1.97 nb^{-1}	1.96 nb^{-1}
	pp @ $\sqrt{s}$ = 5.02 TeV (μ = 2)	273 pb^{-1}	270 pb^{-1}
	pp @ $\sqrt{s}$ = 13 TeV (μ = 2)	150 pb^{-1}	148 pb^{-1}
2018	pp @ $\sqrt{s}$ = 13 TeV	62.1 fb^{-1}	60.0 fb^{-1}
	pp @ $\sqrt{s}$ = 13 TeV (μ = 2)	213 pb^{-1}	208 pb^{-1}
	Pb-Pb @ $\sqrt{s_{NN}}$ = 5.02 TeV	1.78 nb^{-1}	1.74 nb^{-1}

Taken from: https://arxiv.org/pdf/1911.04632.pdf

Data quality monitoring

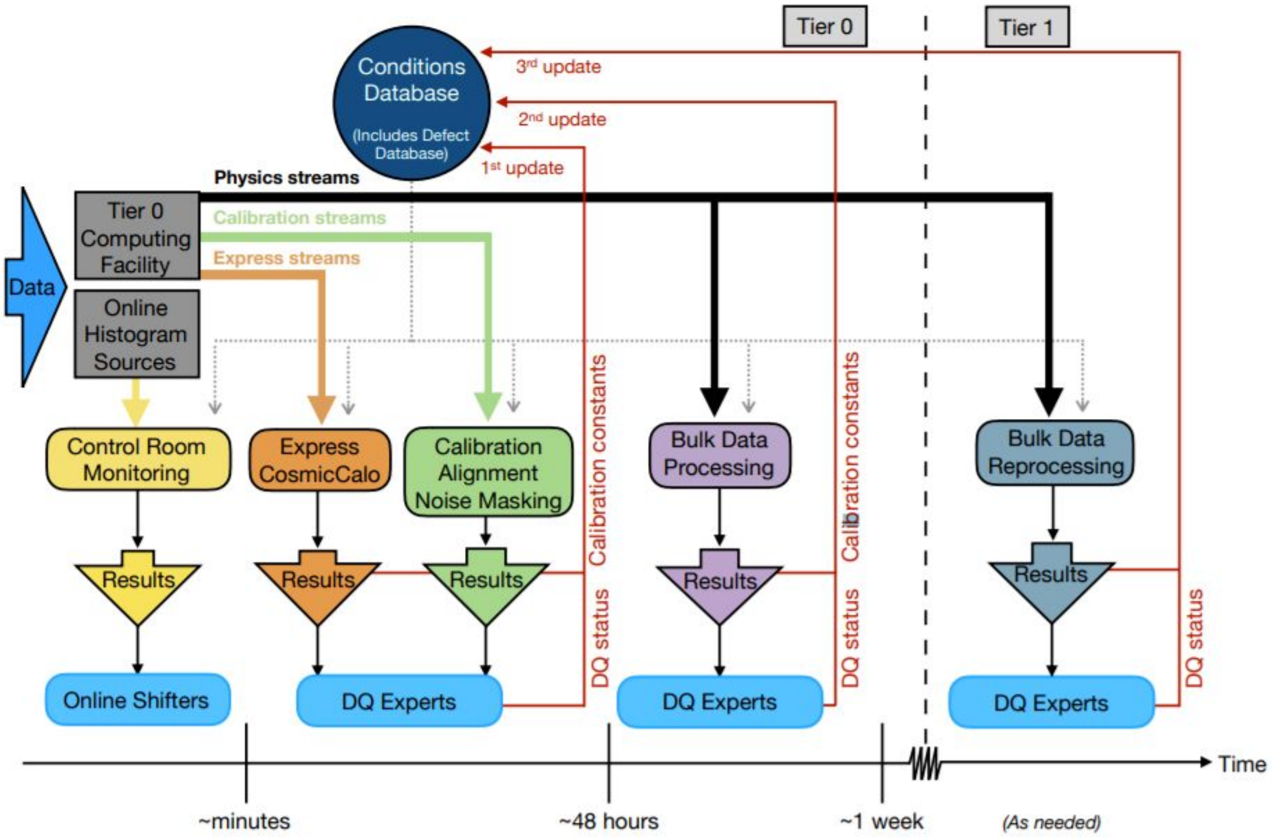

Taken from: https://arxiv.org/pdf/1911.04632.pdf

Data quality monitoring

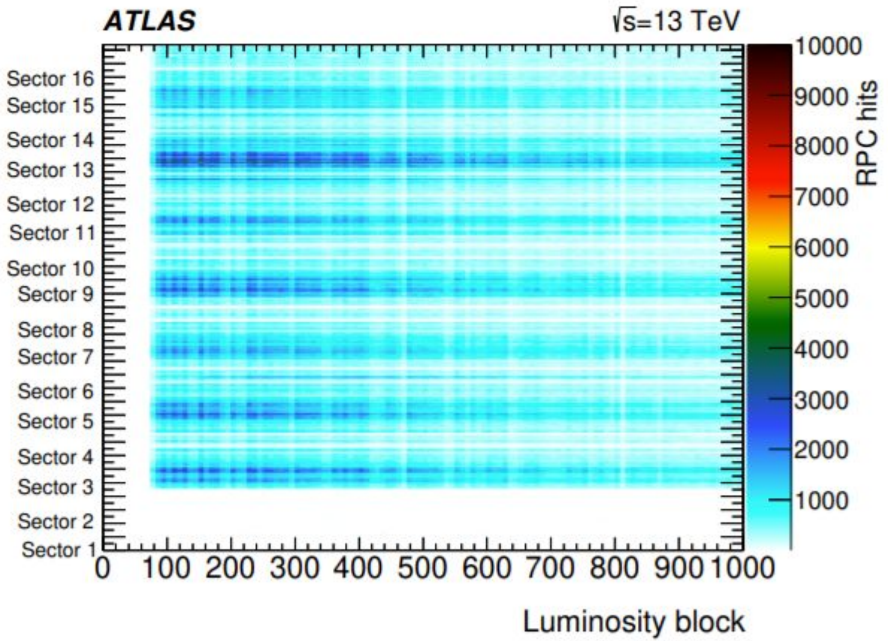

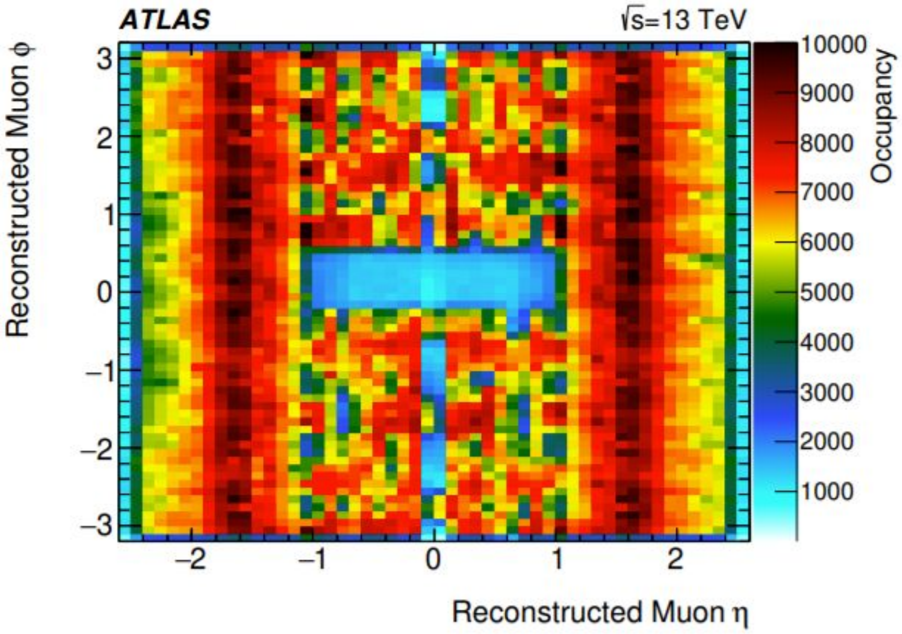

Taken from: https://arxiv.org/pdf/1911.04632.pdf

Data quality monitoring

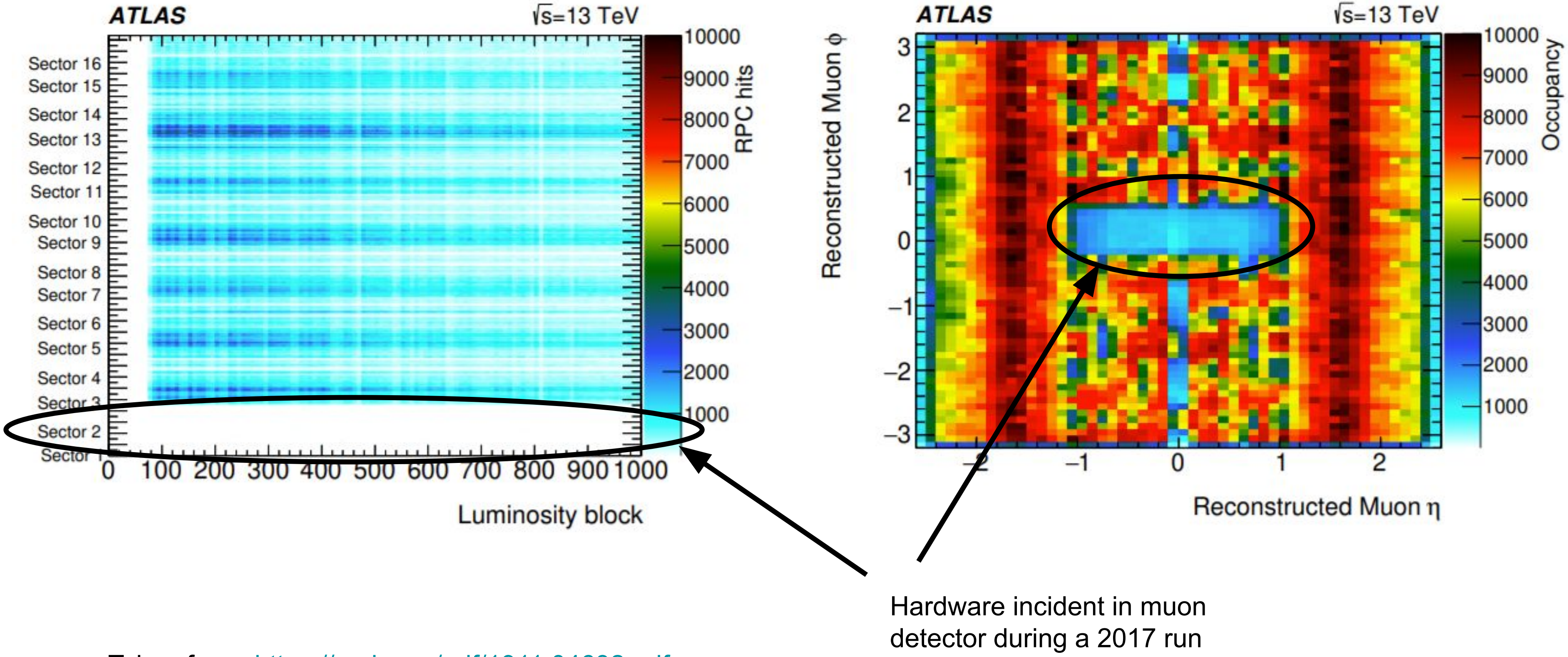

Taken from: https://arxiv.org/pdf/1911.04632.pdf

Data quality monitoring

2015 Data Quality Efficiency [%]

Dataset	Inner Tracker			Calorimeters		Muon Spectrometer				Magnets		Trigger	
	Pixel	SCT	TRT	LAr	Tile	MDT	RPC	CSC	TGC	Solenoid	Toroid	L1	HLT
pp @ 13 TeV (50 ns)	99.84	99.63	95.28	98.53	100	95.28	100	100	99.70	100	95.87	100	99.94
pp @ 13 TeV	93.84	99.77	98.29	99.54	100	100	99.96	100	99.97	100	97.79	99.97	99.76
pp @ 5.02 TeV	100	100	100	100	100	100	99.96	100	99.94	100	100	99.24	100
Pb-Pb @ 5.02 TeV	100	100	99.64	97.57	100	99.80	99.98	99.90	99.89	100	100	100	100

Dataset		Data Quality Efficiency [%]	Integrated Luminosity
pp @ 13 TeV (50 ns)	Good for Physics	88.77	83.9 pb^{-1}
pp @ 13 TeV		88.79	3.22 fb^{-1}
pp @ 5.02 TeV		99.14	25.3 pb^{-1}
Pb-Pb @ 5.02 TeV		96.76	0.49 nb^{-1}

2016 Data Quality Efficiency [%]

Dataset	Inner Tracker			Calorimeters		Muon Spectrometer				Magnets		Trigger	
	Pixel	SCT	TRT	LAr	Tile	MDT	RPC	CSC	TGC	Solenoid	Toroid	L1	HLT
pp @ 13 TeV	98.98	99.89	99.74	99.32	99.31	99.95	99.80	100	99.96	99.15	97.23	98.33	100
p-Pb @ 8.16 TeV	99.92	100	100	100	99.99	100	99.94	100	100	100	100	100	100
p-Pb @ 5.02 TeV	100	99.96	100	100	100	100	99.96	100	99.95	100	100	100	90.44

Dataset		Data Quality Efficiency [%]	Integrated Luminosity
pp @ 13 TeV	Good for Physics	93.07	33.0 fb^{-1}
p-Pb @ 8.16 TeV		98.35	165 nb^{-1}
p-Pb @ 5.02 TeV		82.93	0.36 nb^{-1}

Physics analyses use only events in which all ATLAS sub-detectors were fully operational

Taken from: https://arxiv.org/pdf/1911.04632.pdf

The CMS Detector

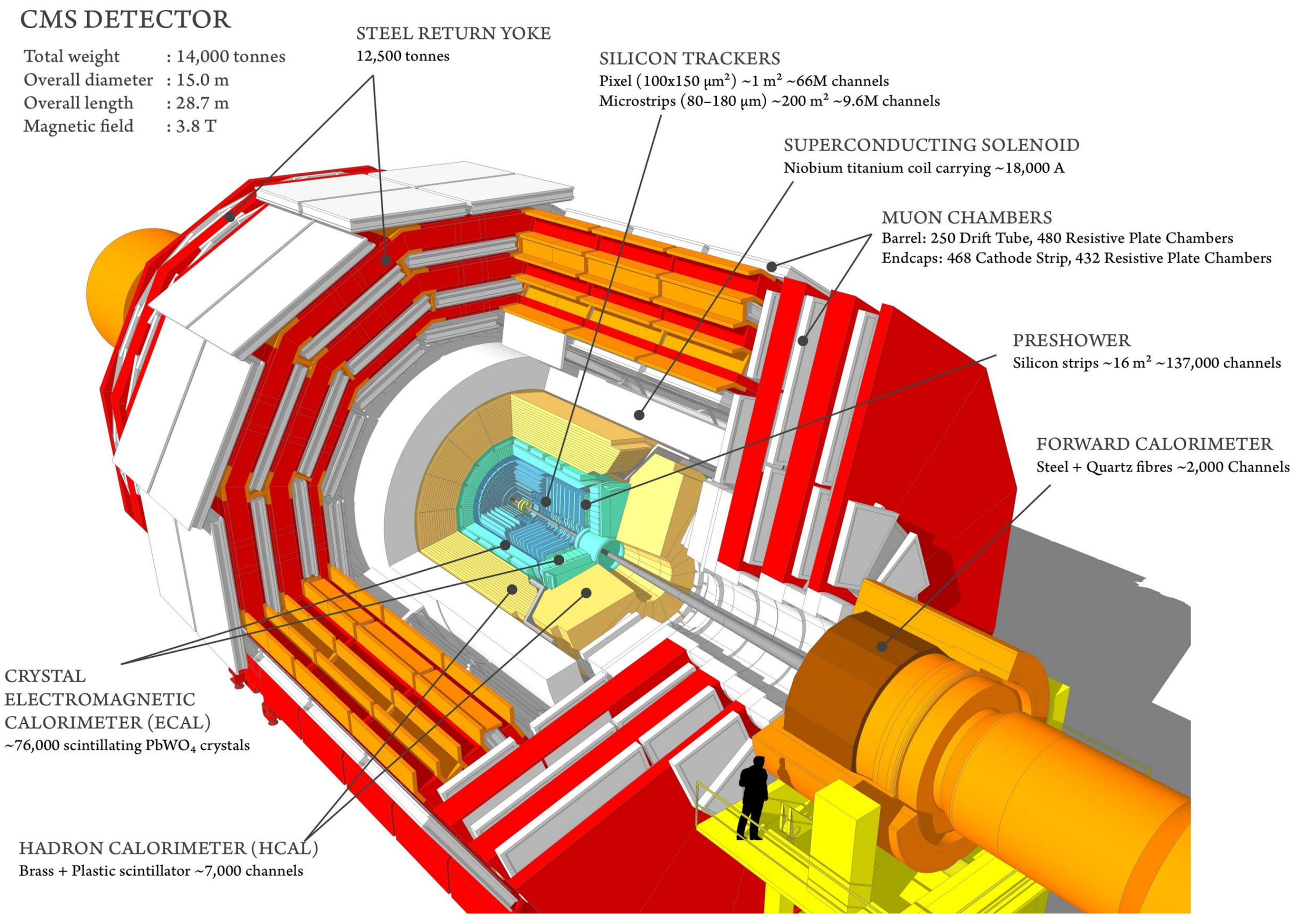

The CMS Detector

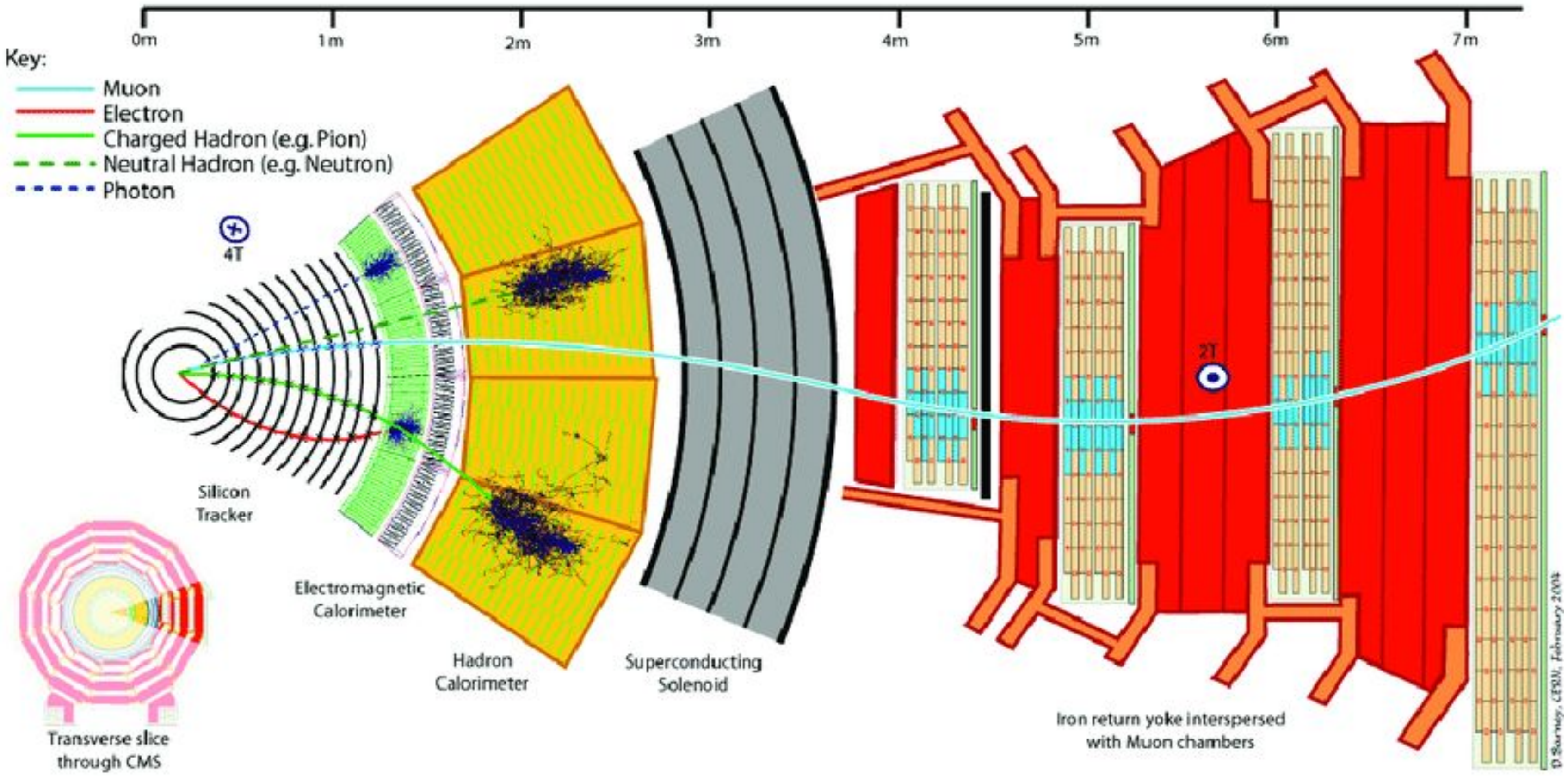

The CMS tracking detectors

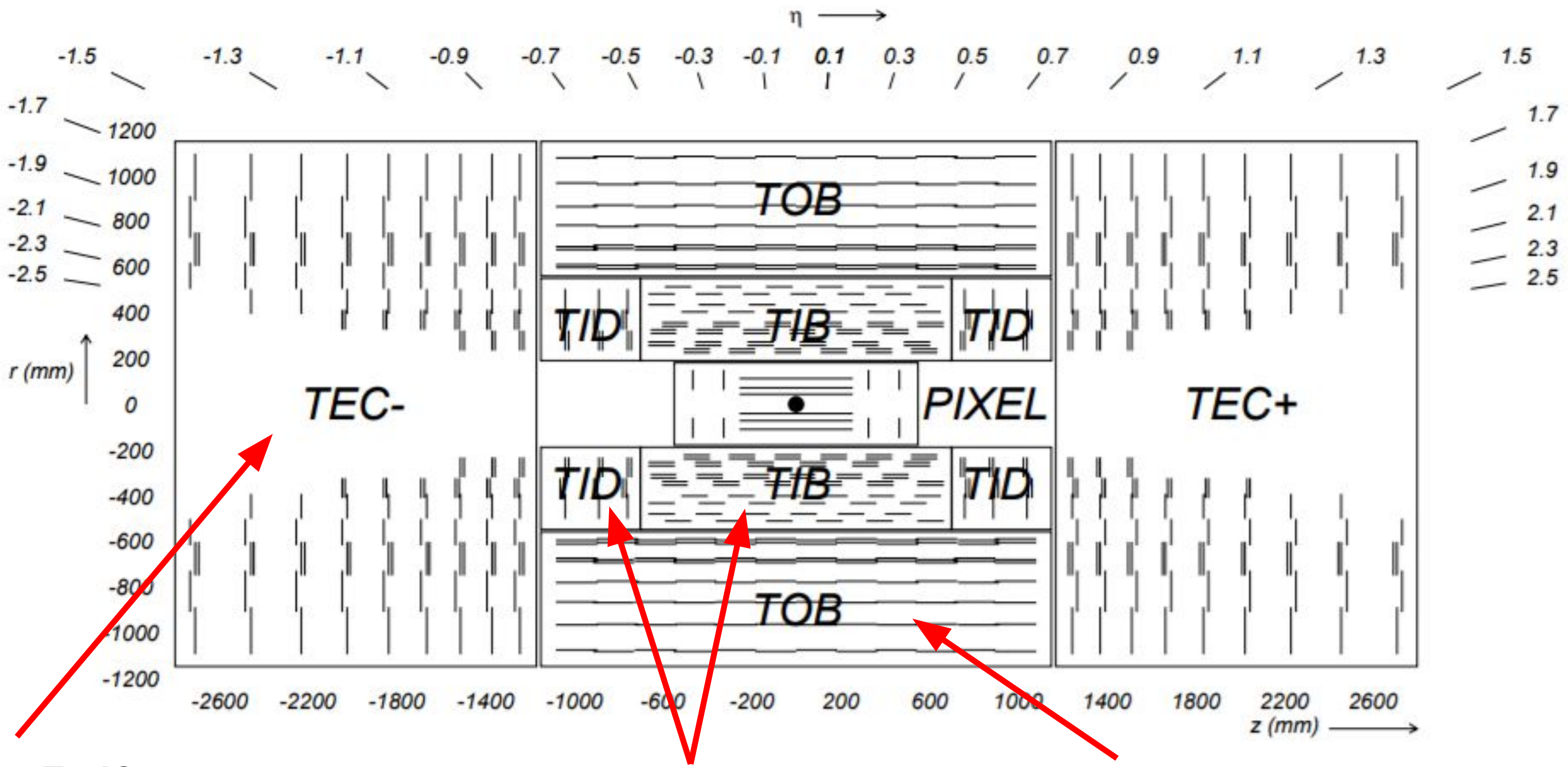

Tracker EndCaps

Tracker Inner Barrel and Disks

Tracker Outer Barrel

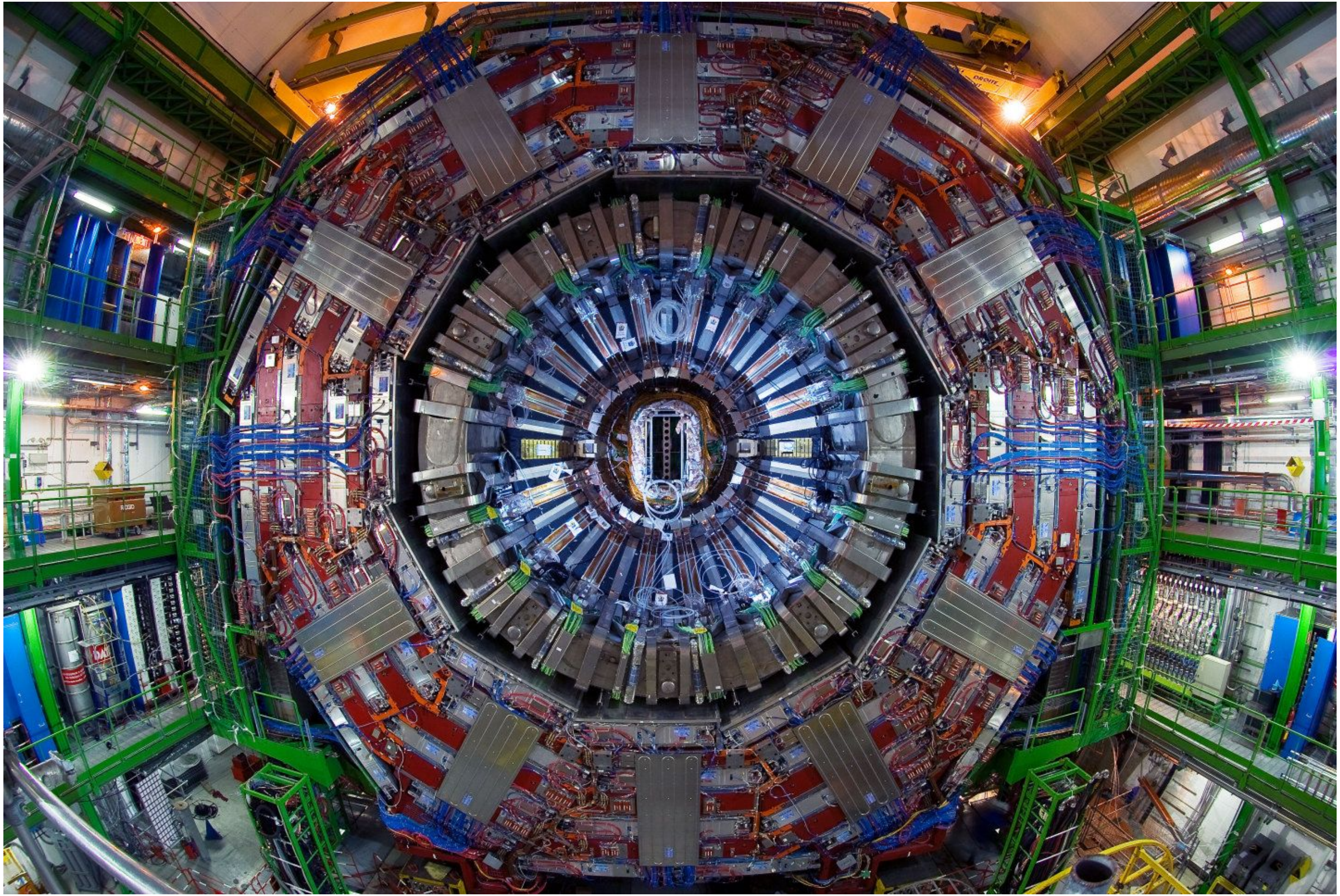

The ALICE Detector

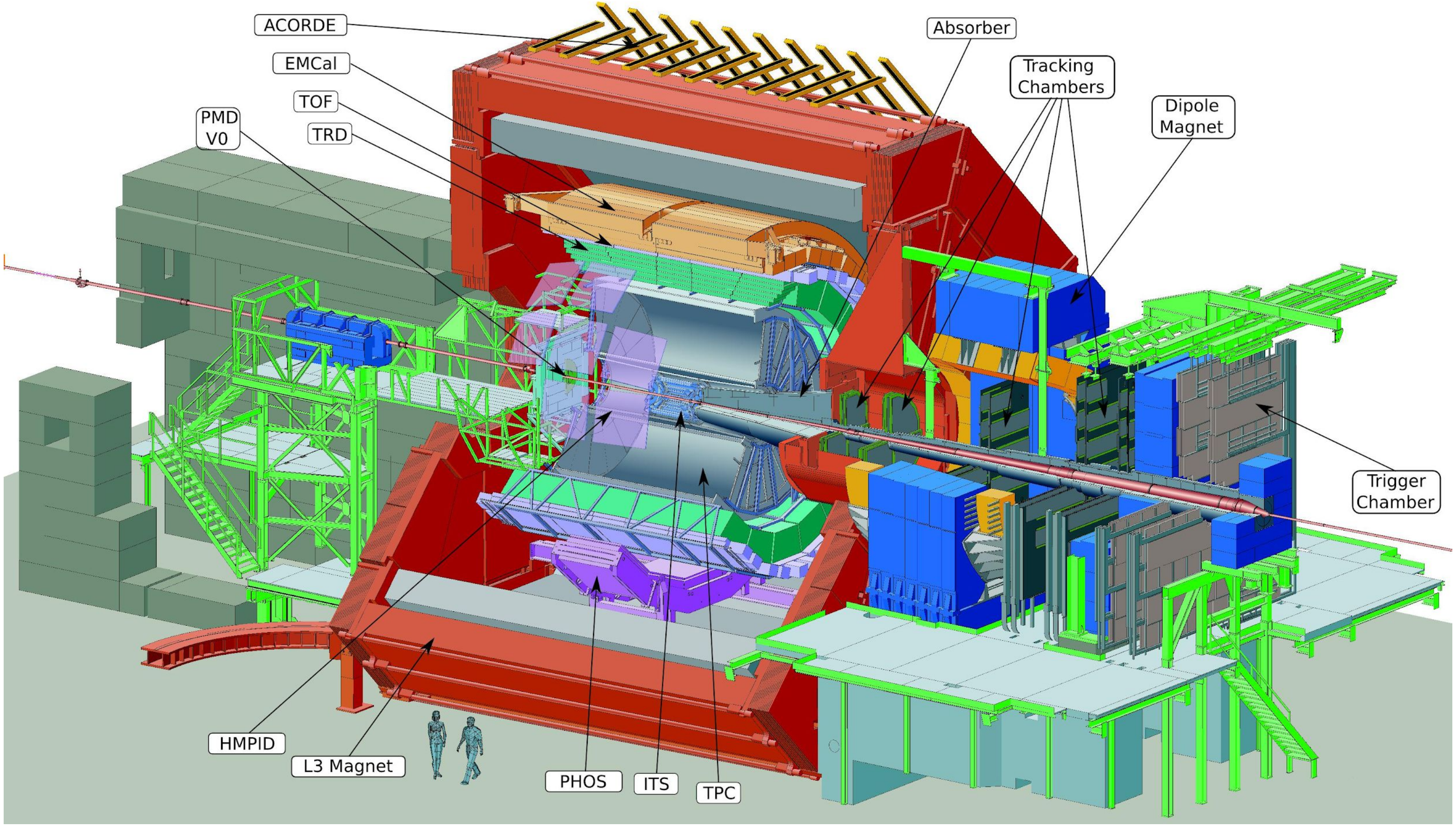

The ALICE Detector

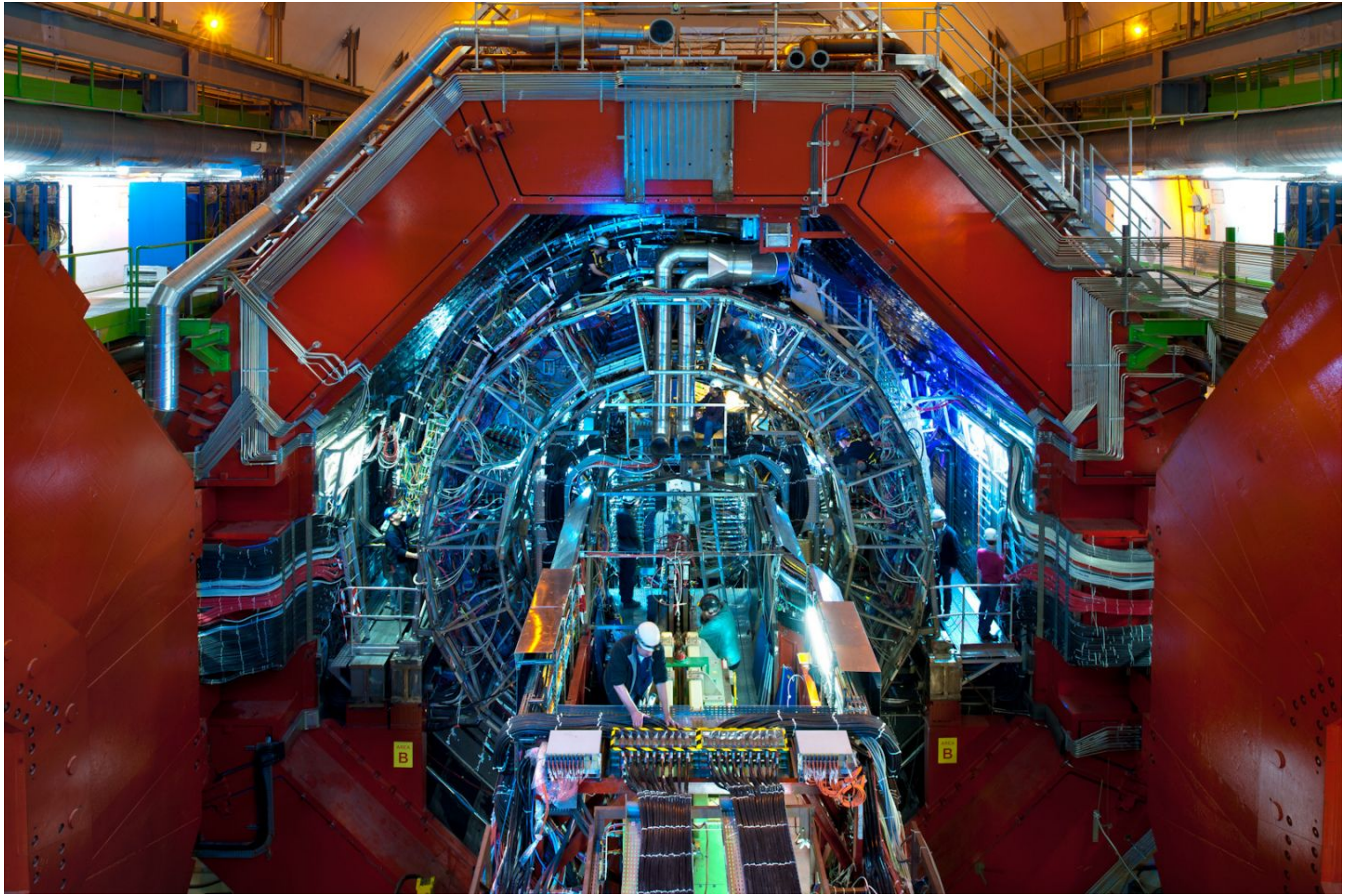

The LHCb Detector

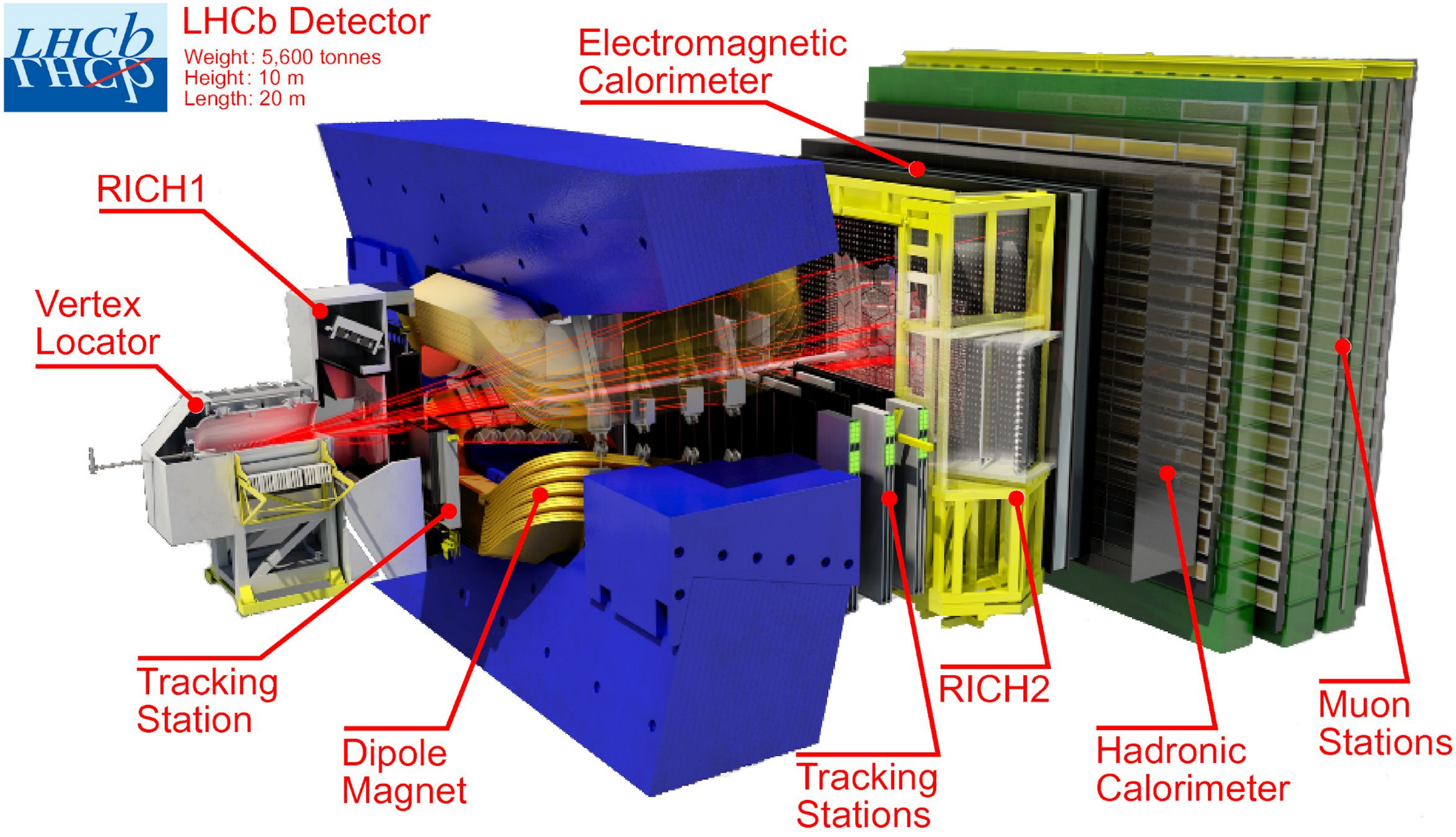

Belle II Detector

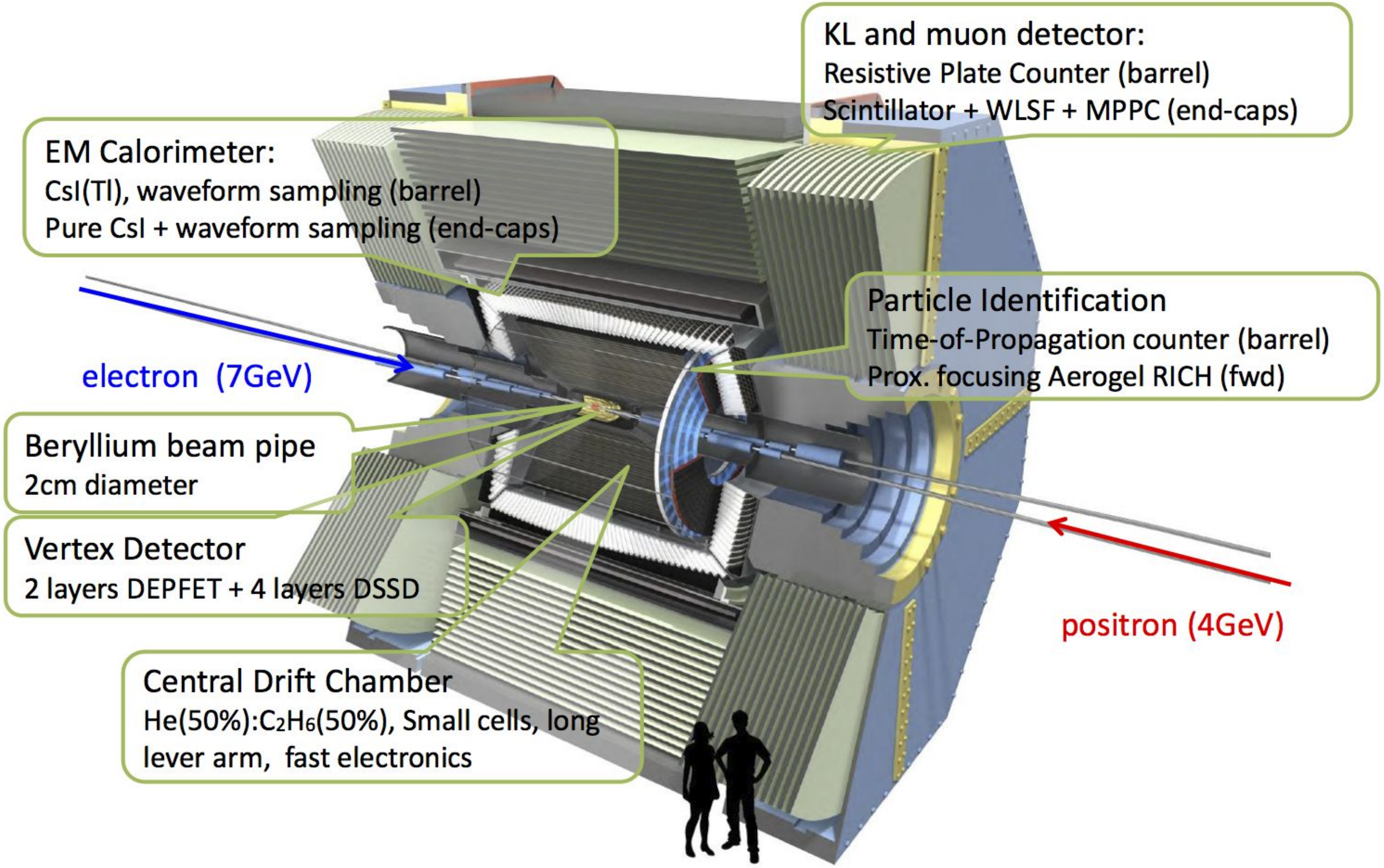

The IceCube Detector

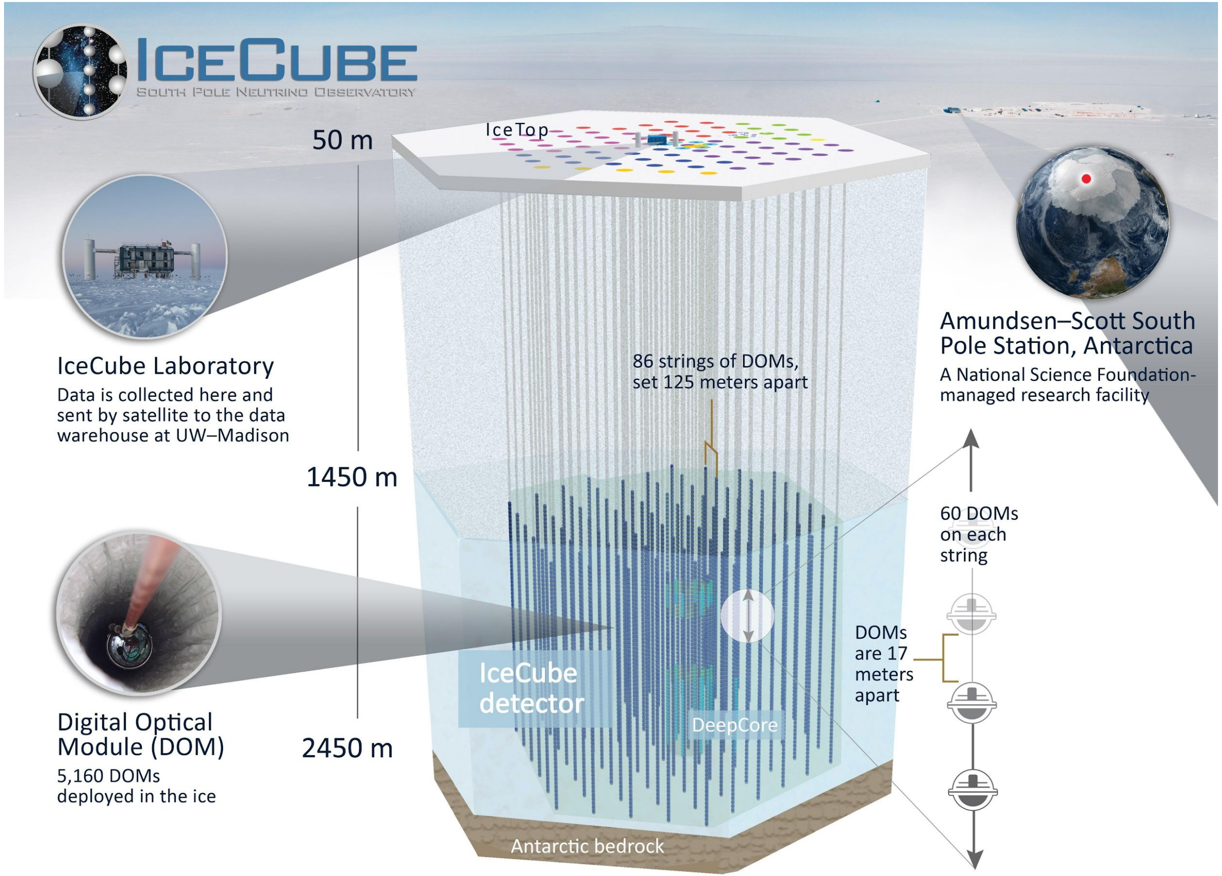

2.3 Computing

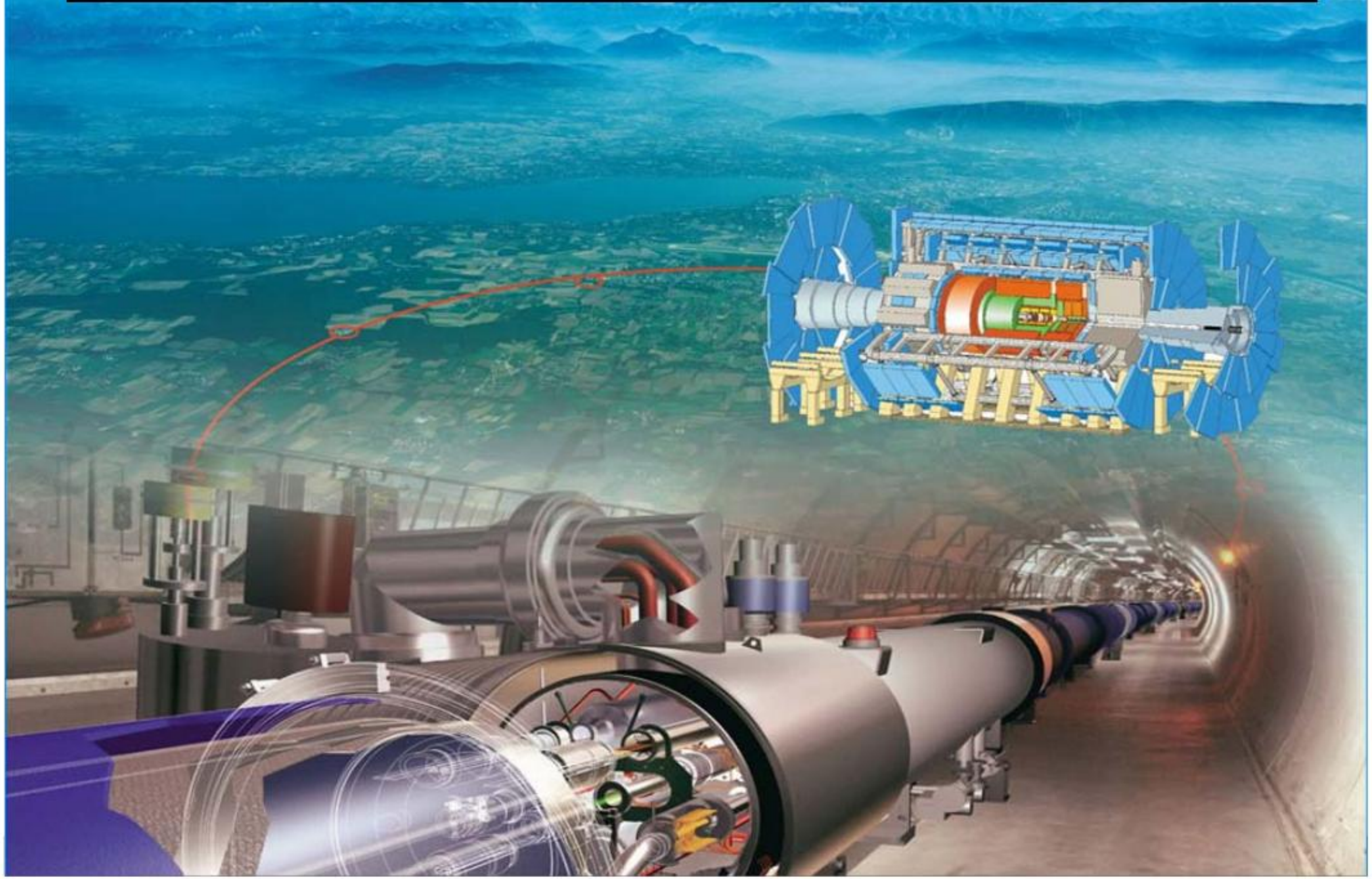

Grid computing

- Raw data from the experiments are written to tape at the Tier-0 center at CERN.
  - Afterwards the processed data is distributed to the various Tier-1 and Tier-2 centers.
    - Users send their software around the globe rather than downloading it to local facilities

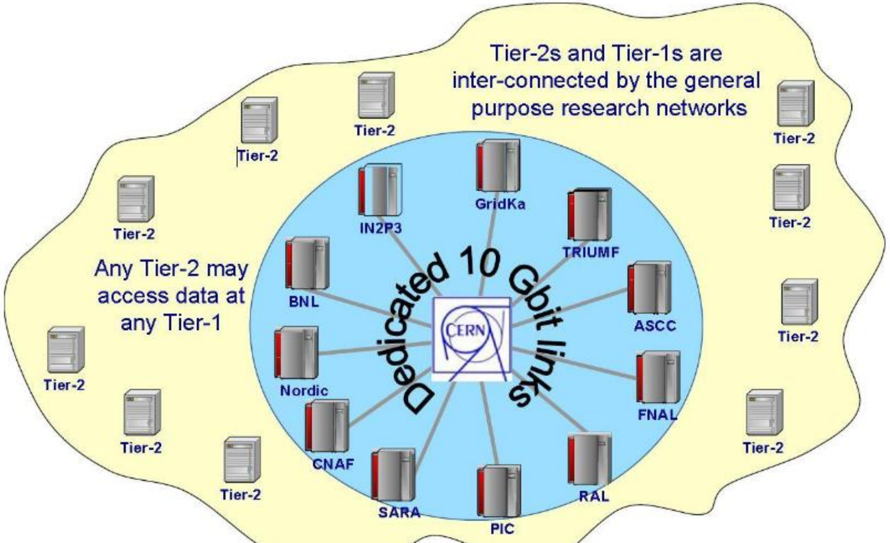

Grid computing

- Raw data from the experiments are written to tape at the Tier-0 center at CERN.
    - Afterwards the processed data is distributed to the various Tier-1 and Tier-2 centers.
        - Users send their software around the globe rather than downloading it to local facilities

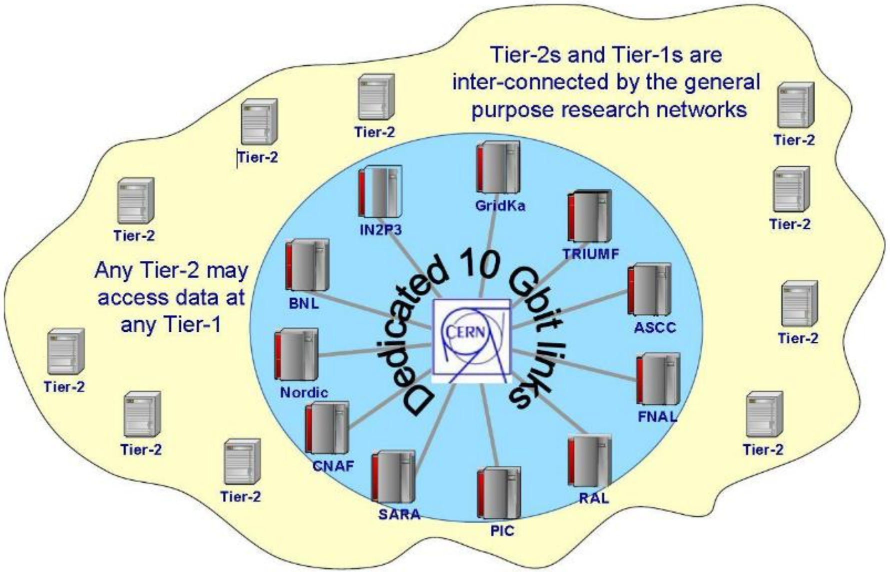

- ATLAS and CMS operate around 50-100 Tier-2 sites:
    - Each Tier-2 site provides around 200-300 TB for storage
    - To a large extend used for Monte Carlo production

2.4 Particle reconstruction and identification

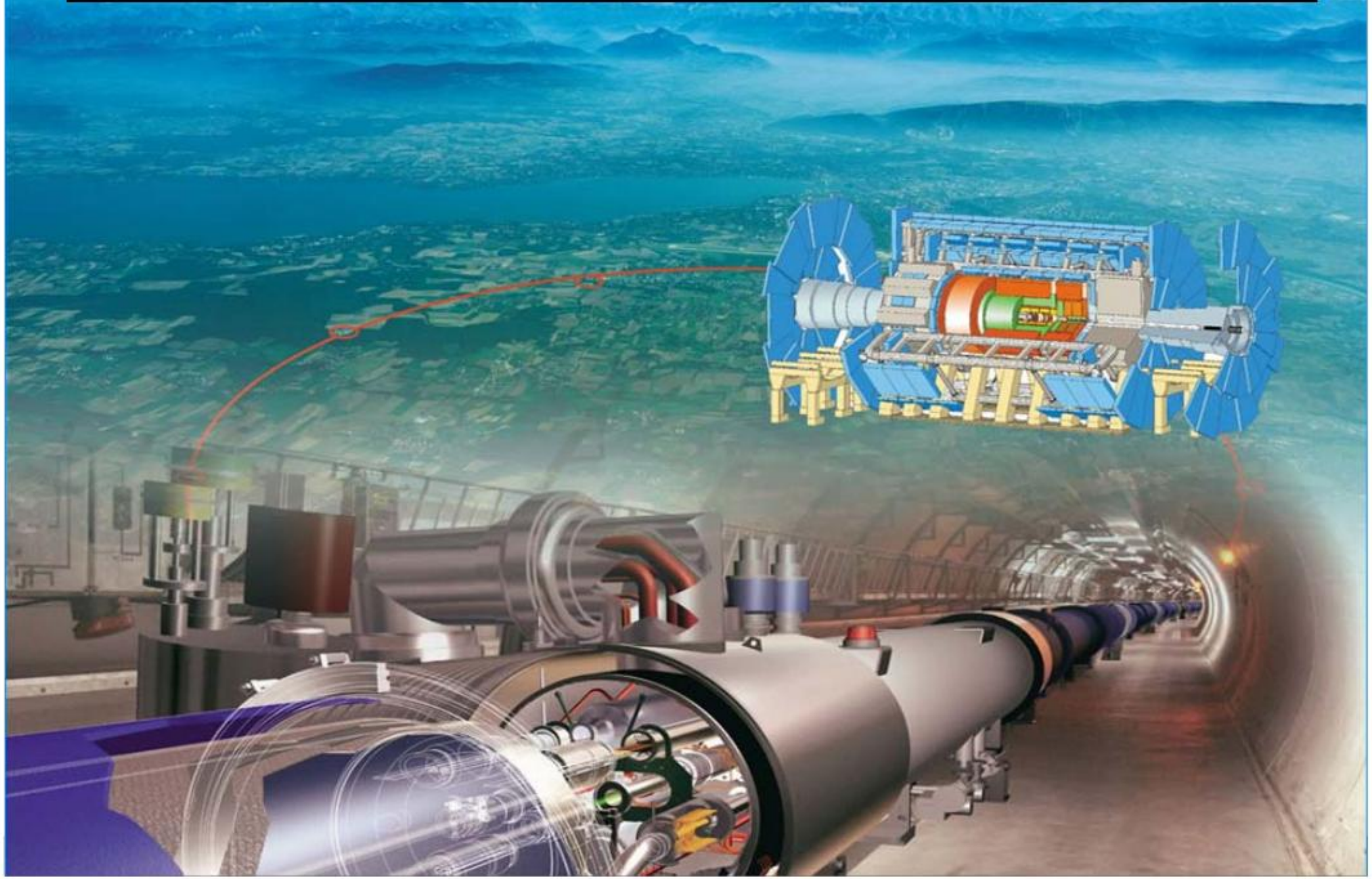

Particle identification

- **Hadronic particle shower**
  - Cone shaped jets build from calorimeter clusters or tracks
- **Muons**
  - Combined tracks from Inner Detector and Spectrometer
- **Electrons**
  - Inner Detector (ID) track
  - Energy clusters in calorimeter system
- **Taus**
  - Jets with either 1 or 3 ID tracks
- **Neutrinos**
  - Pass through the detector without leaving any trace.
  - Estimated from energy balance:

$$E_{\mathrm{X,Y}}^{\mathrm{mis}} = -\sum E_{\mathrm{X,Y}}^{\mathrm{obj.}} + E_{\mathrm{X,Y}}^{\mathrm{soft}}$$

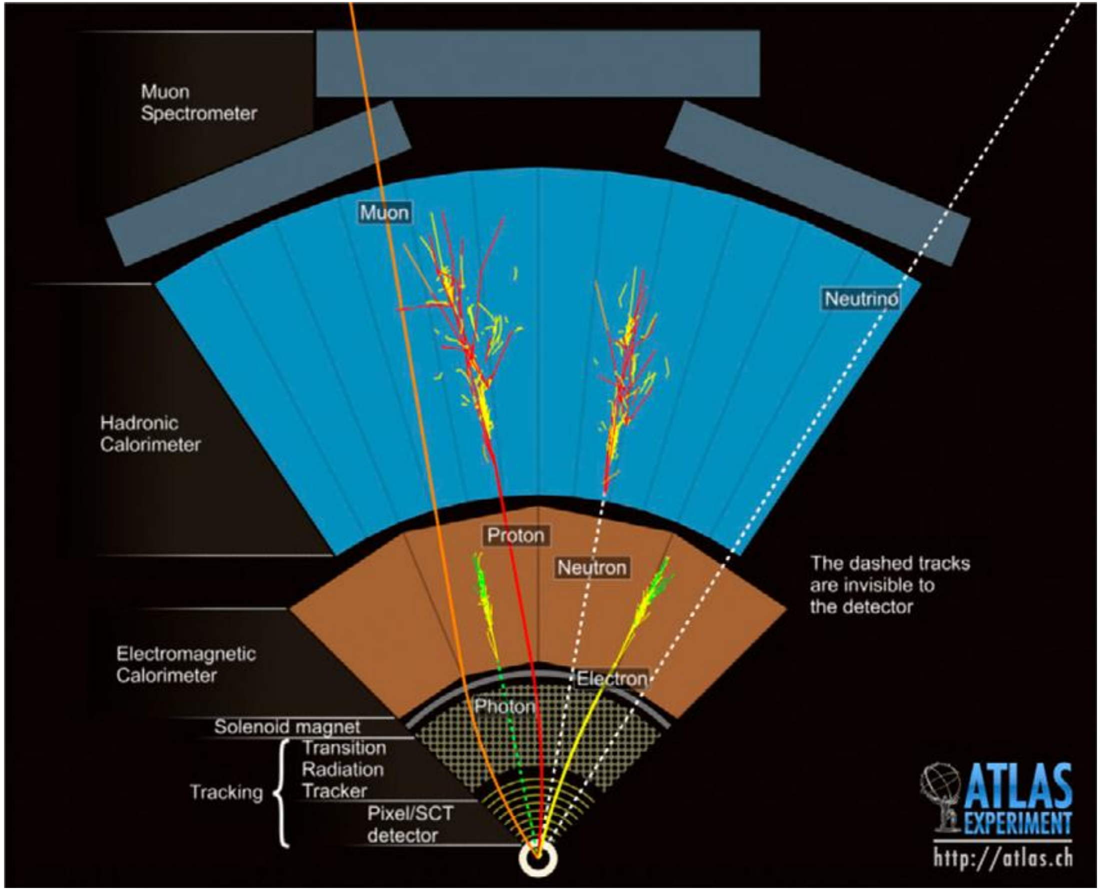

Tracking

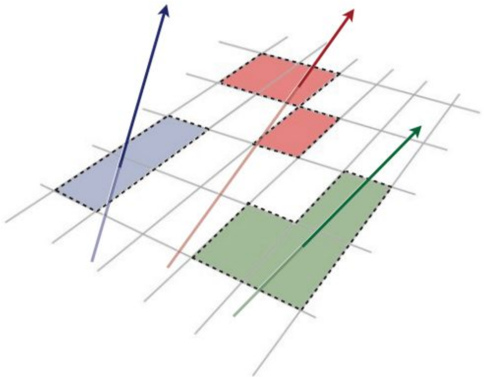

- **Track Finding:**
  - Clusterization
  - Iterative combinatorial track finding:
    - Track seeds are formed from sets of three space-points (assuming a perfect helical trajectory in a uniform magnetic field)
    - Track candidates are build from these seeds by incorporating additional space-points compatible with the preliminary trajectory
  - Track candidates and ambiguity solving
    - Low quality track candidates are sorted out
    - Number of shared clusters is reduced
  - Extension into TRT and track fit
    - Perform fit with all available information to precisely determine track properties

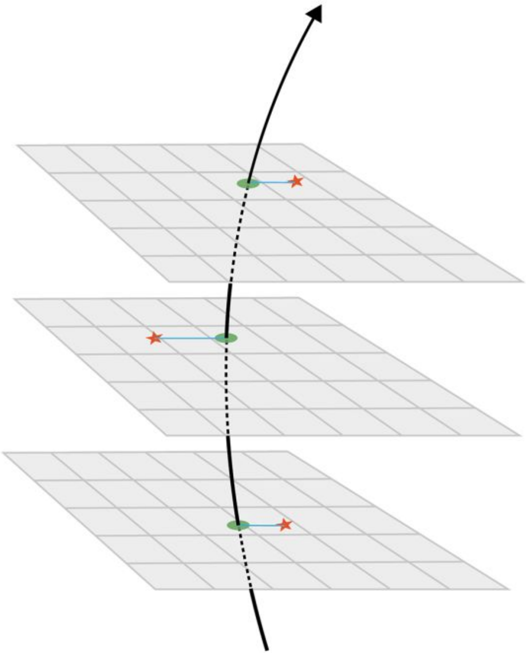

Tracking

- Pixel and SCT provide high spatial resolution
  - Pixel ~4 hits per track
  - SCT ~8 hits per track
- TRT contributes to track fit by large multiplicity of measurements

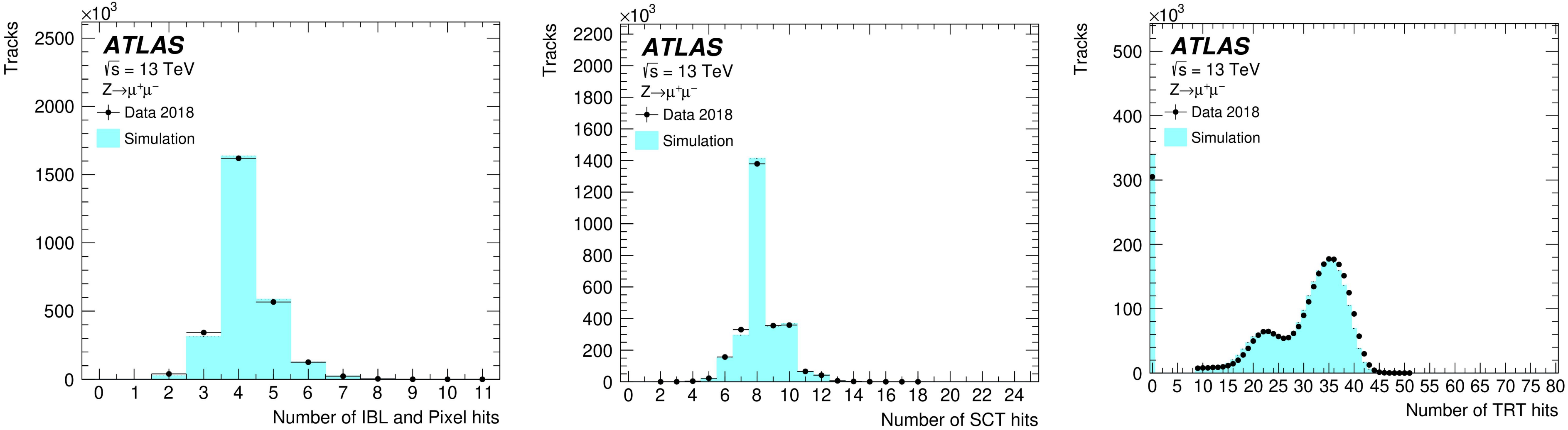

Track reconstruction efficiency

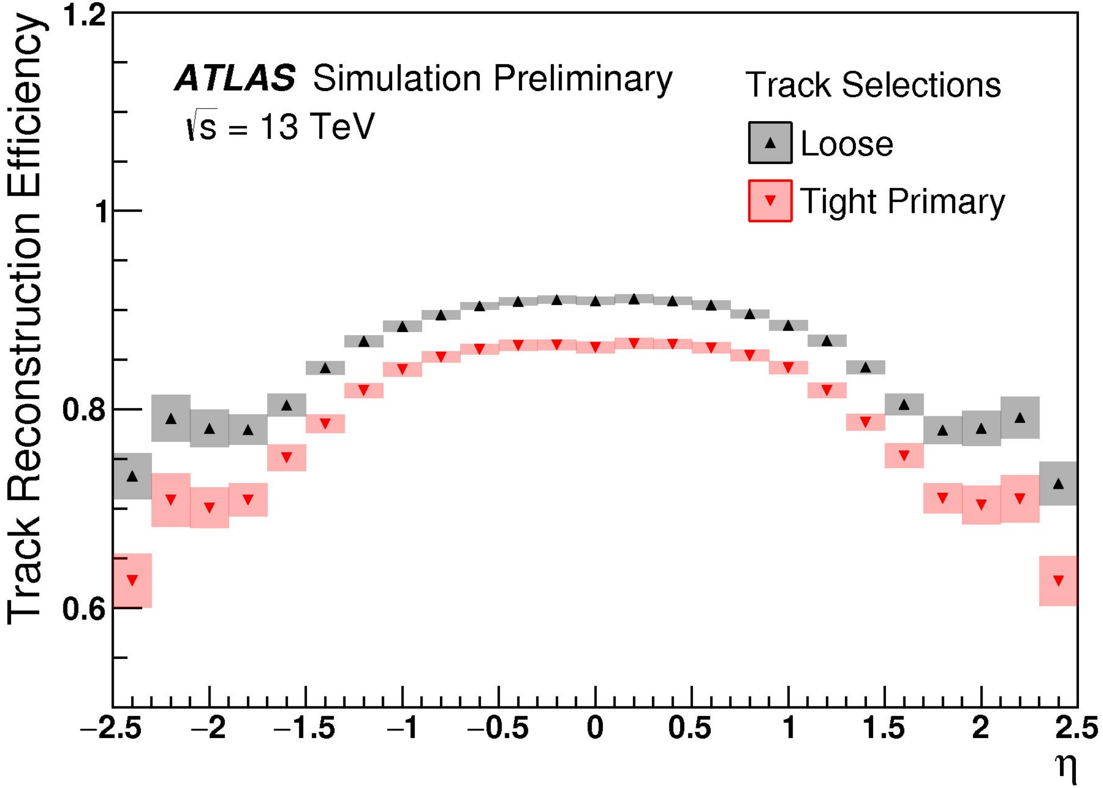

Electrons

- Electron candidates are reconstructed from tracks in the ID matched to clusters of energy deposits in the electromagnetic calorimeter system

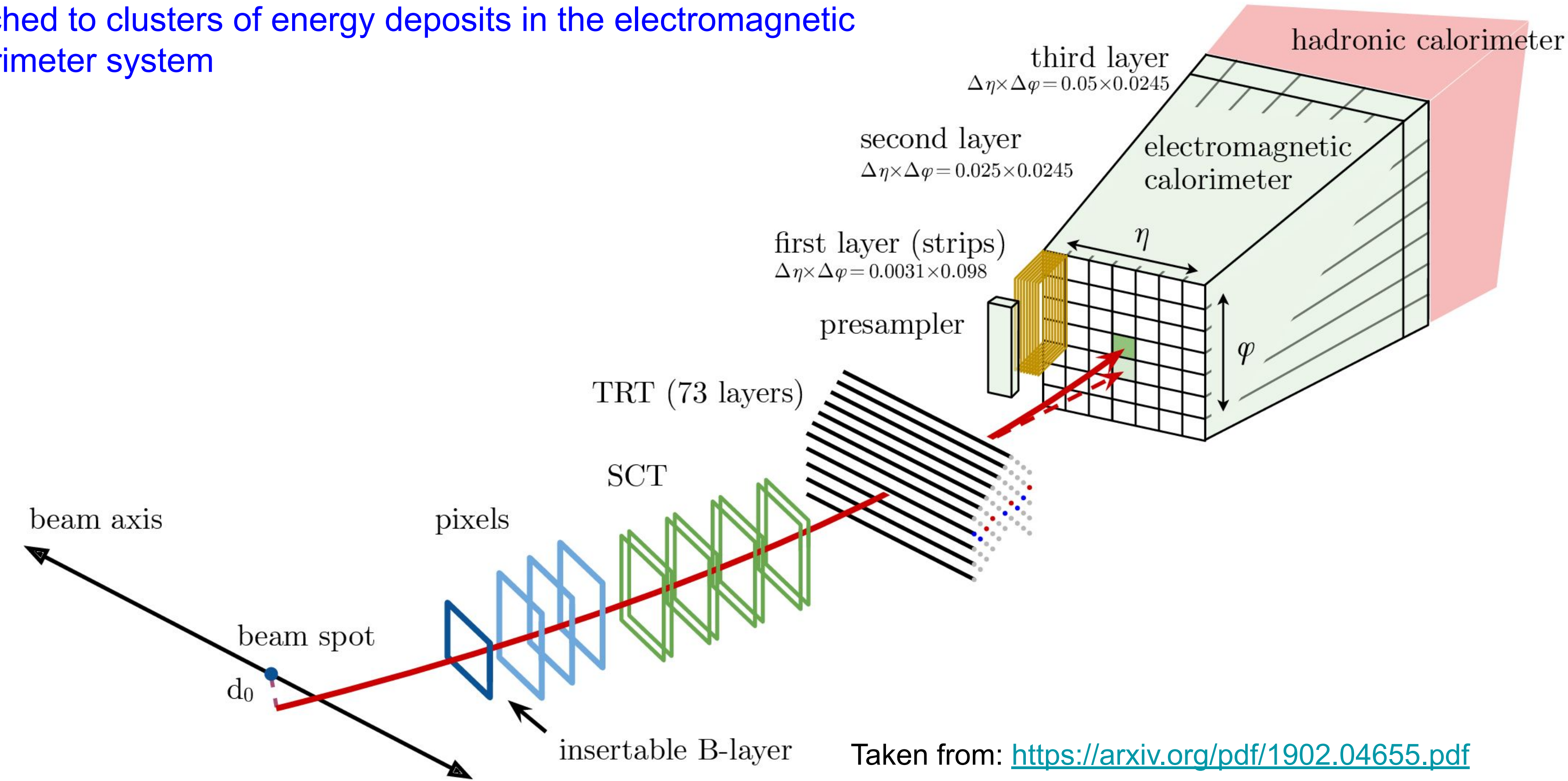

Taken from: https://arxiv.org/pdf/1902.04655.pdf

Electrons

- Identification of electrons is based on MVAs using information on the shower development as input

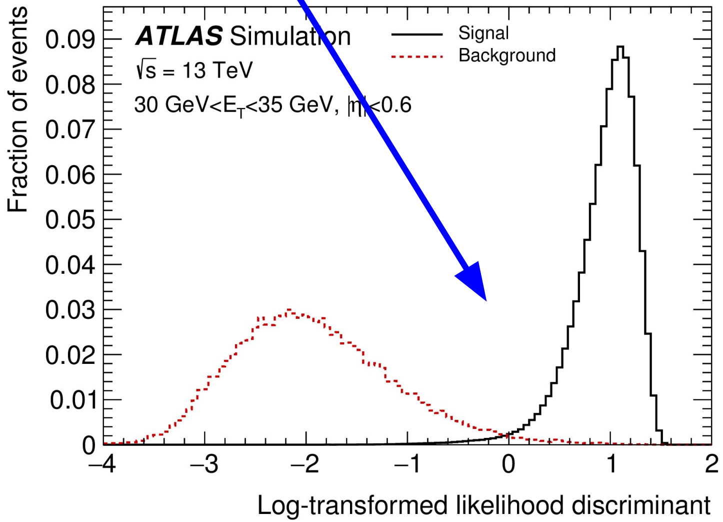

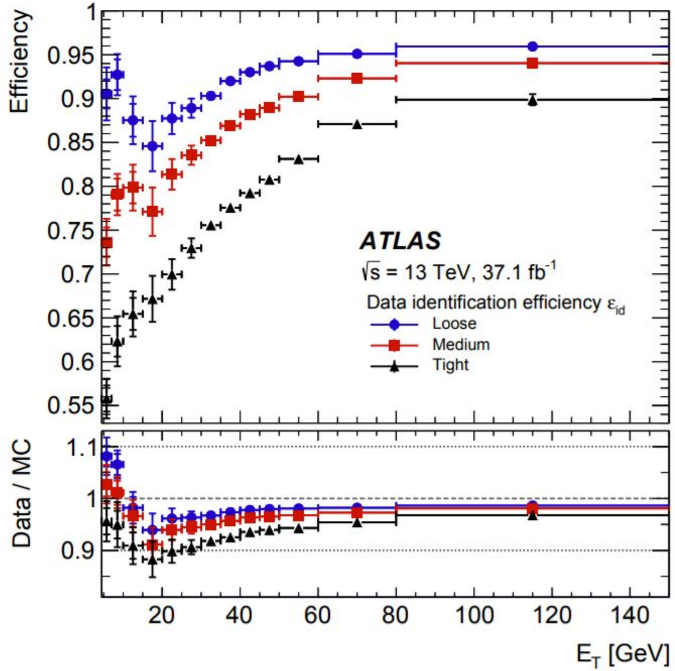

Taken from: https://arxiv.org/pdf/1902.04655.pdf

Photons

- Photon candidates are reconstructed from clusters of energy deposited in the EM calorimeter, and may have tracks and conversion vertices reconstructed in the ID.
    - Photon identification is based primarily on shower shapes in the calorimeter

- Converted photons:
    - Require ID tracks and conversion vertex

- Unconverted photons:
    - Only use shower shapes in the calorimeter system

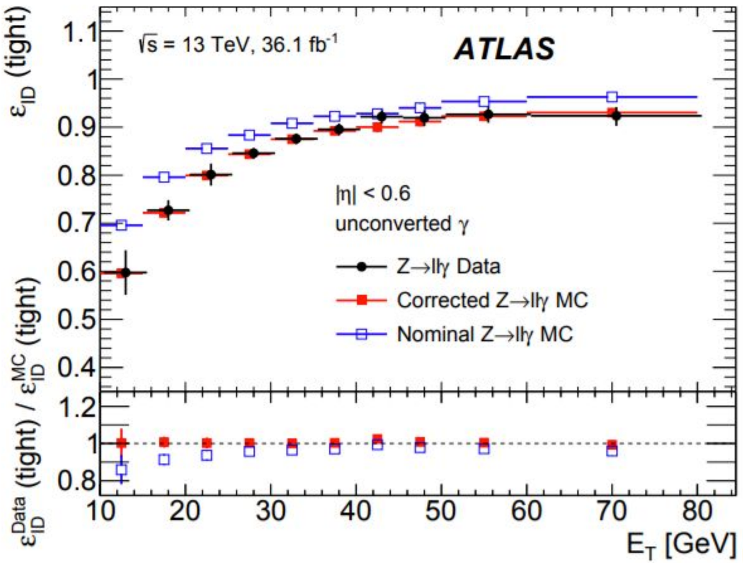

Taken from: https://arxiv.org/pdf/1810.05087.pdf

Muons

- **Reconstruction and identification:**
  - Muon candidates are reconstructed from combined tracks using information from both the Muon-Spectrometer and the Inner Detector
  - Identification is based on:
    - Track properties
    - Variables that test the compatibility of the individual measurements in the two detector systems

- **Calibration:**
  - Use Tag & Probe method based on di-muon events
  - Low mass muons can be calibrated using J/ψ or Υ(1S), while Z boson is used for medium and higher momenta

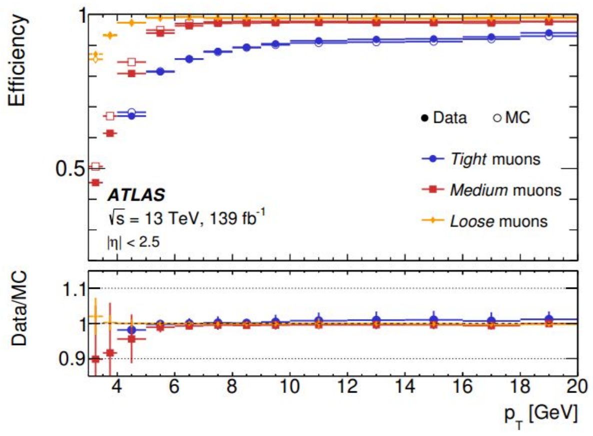

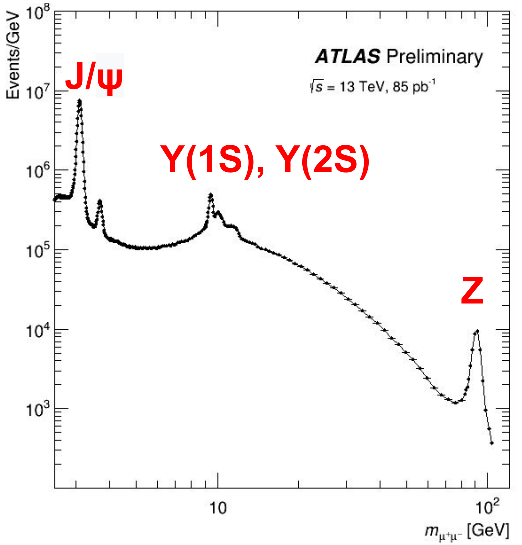

Jets

- **Jets:** Collimated bunches of stable hadrons, originating from partons (quarks and gluons) after fragmentation and hadronization
- Require collinear- and infrared-safety i.e. jets are unchanged by:
  - Collinear splitting
  - Soft emissions
- LHC experiments preferrably use so called **sequential clustering algorithms**
- Application: Calculate for all pairs of particles i an j:

$$d_{ij} = \min(k_{i,T}^{2p}, k_{j,T}^{2p}) \frac{\Delta_{ij}^2}{R^2}$$

$$d_{iB} = k_{i,T}^{2p}$$

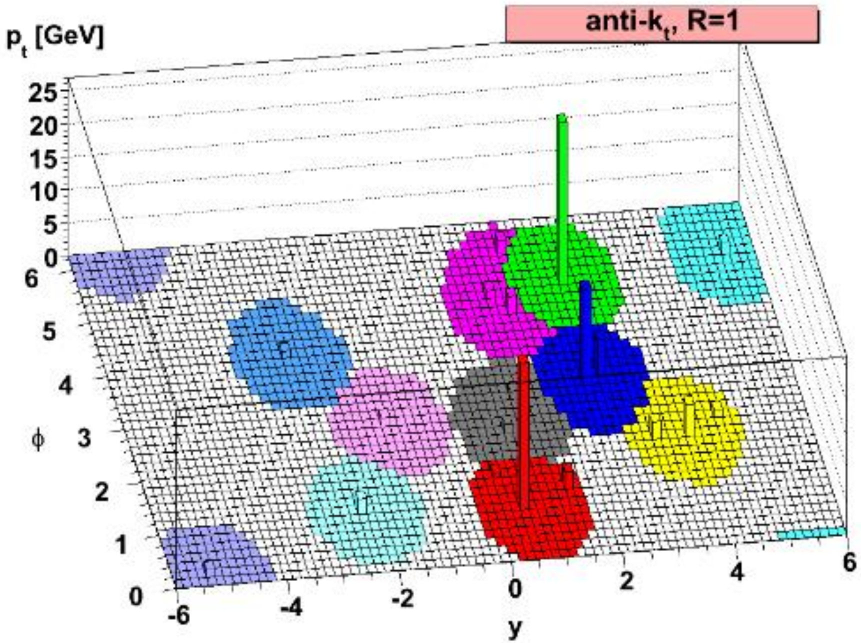

The pair with the smallest d_{ij} is clustered if $d_{ij} < d_{iB}$, for $d_{iB} < d_{ij}$ object i is called a jet

Jets

- **Jets:** Collimated bunches of stable hadrons, originating from partons (quarks and gluons) after fragmentation and hadronization
- Require collinear- and infrared-safety i.e. jets are unchanged by:
  - Collinear splitting
  - Soft emissions
- LHC experiments preferrably use so called **sequential clustering algorithms**
- Application: Calculate for all pairs of particles i an j:

$$d_{ij} = \min(k_{i.T}^{2p}, k_{j,T}^{2p}) \frac{\Delta_{ij}^2}{R^2}$$

$$d_{iB} = k_{i,T}^{2p}$$

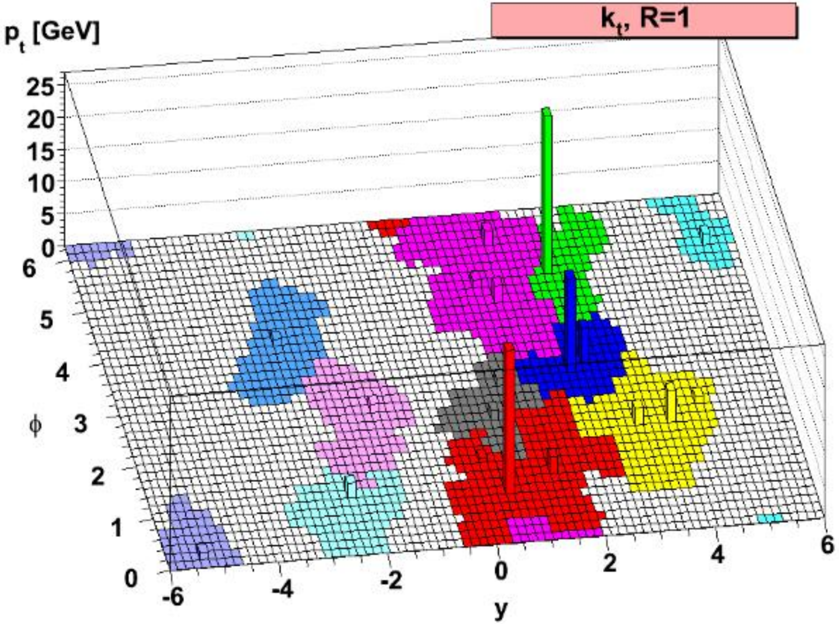

The pair with the smallest d_{ij} is clustered if $d_{ij} < d_{iB}$, for $d_{iB} < d_{ij}$ object i is called a jet

Jet energy scale

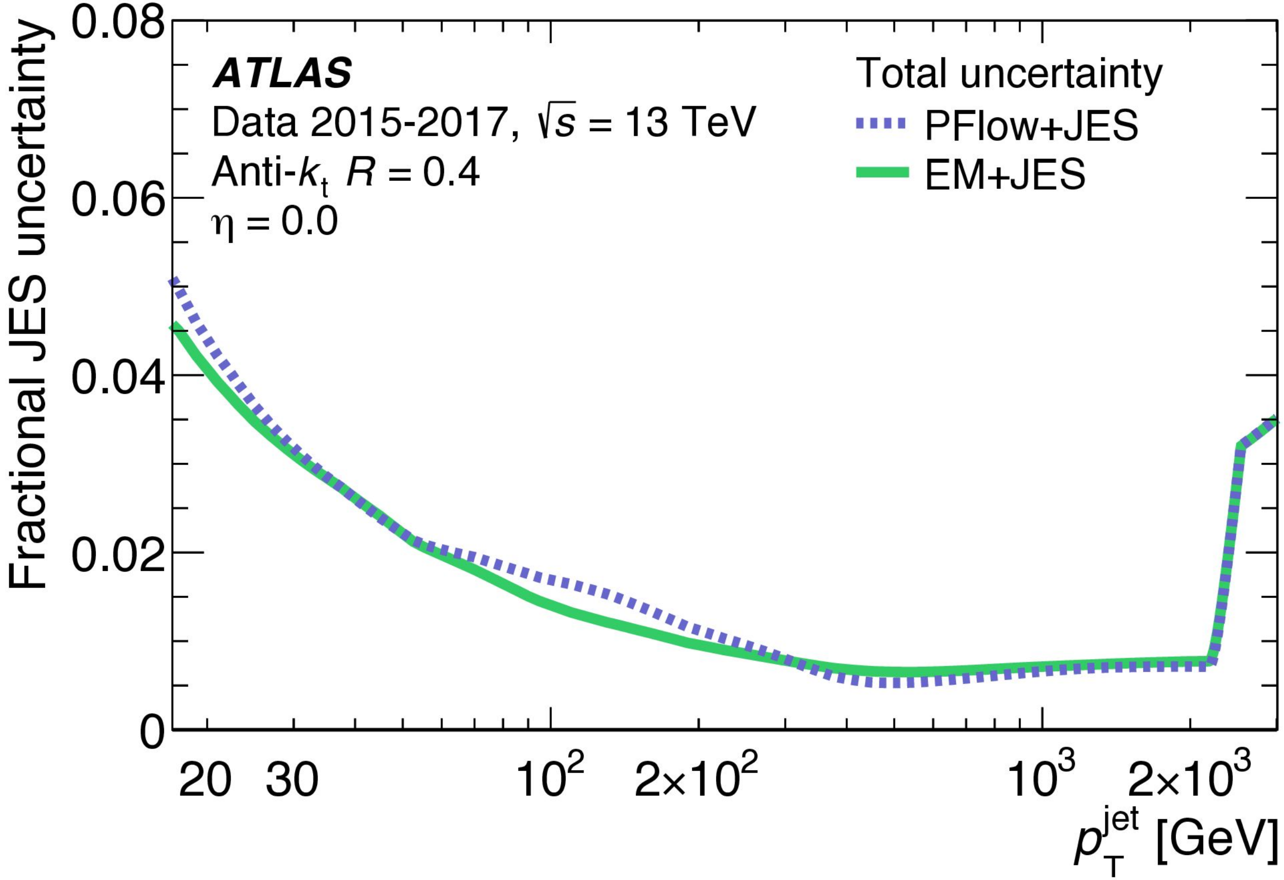

Jet energy calibration

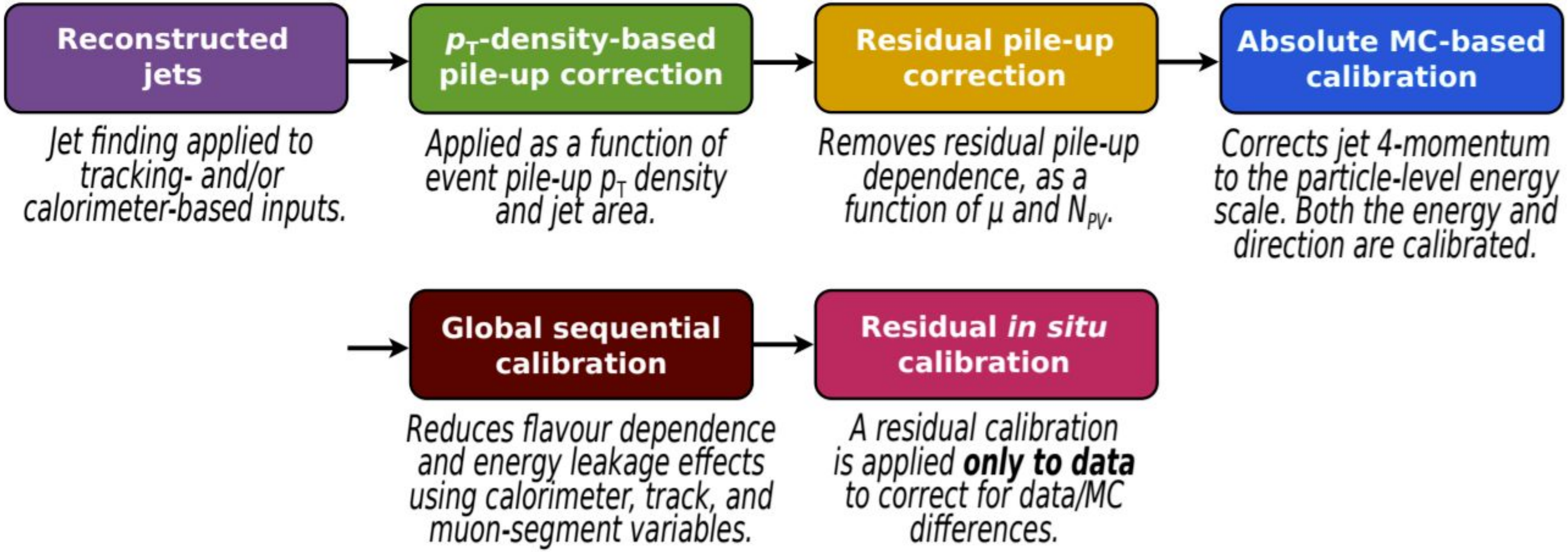

- The jet energy scale calibration aims to restore the jet energy to that of jets reconstructed at the particle level

Taken from https://arxiv.org/pdf/2007.02645.pdf

Flavour tagging (b-tagging)

- Low-level information for b-tagging algorithms:
  - **Lifetime of heavy flavour hadrons**
  - **Presence of soft leptons** (electrons or muons) as decay products of c- and b-hadrons
- b-tagging algorithms are based on MVAs using low-level information as inputs

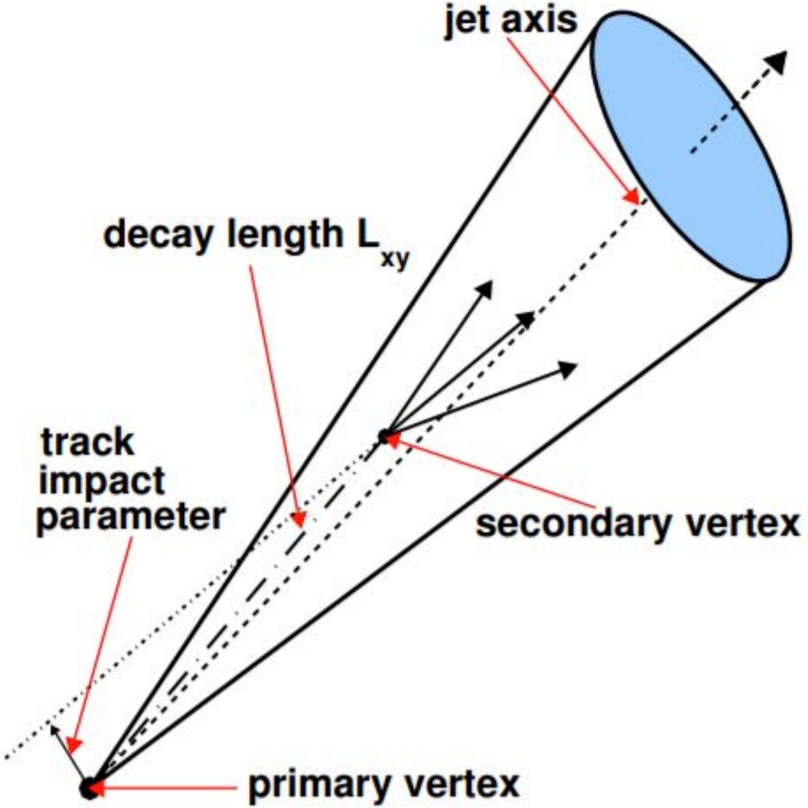

Particle	Content	Production fraction [%]	Mass [MeV]	Lifetime [ps]
B^+	ub	40.1 ± 0.8	5279.26 ± 0.17	1.641 ± 0.008
B^0	db	40.1 ± 0.8	5279.58 ± 0.17	1.519 ± 0.007
B_S	sb	10.5 ± 0.6	5366.77 ± 0.24	1.516 ± 0.011
B_c^+	cb	9.3 ± 1.6 (combined for B_c^+, Λ_b^0, Ξ_b^-, Ω_b^-)	6274.5 ± 1.8	0.452 ± 0.033
Λ_b^0	udb		5619.4 ± 1.6	1.425 ± 0.032
Ξ_b^-	dsb		5791.1 ± 2.2	$1.56^{+0.27}_{-0.25}$
Ω_b^-	ssb		6071 ± 40	$1.13^{+0.53}_{-0.40}$

Flavour tagging (b-tagging)

- b-tagging algorithms are based on MVAs using low-level information as inputs
- Inputs to MVAs are based on information from:
  - Track impact parameters
  - Secondary vertices

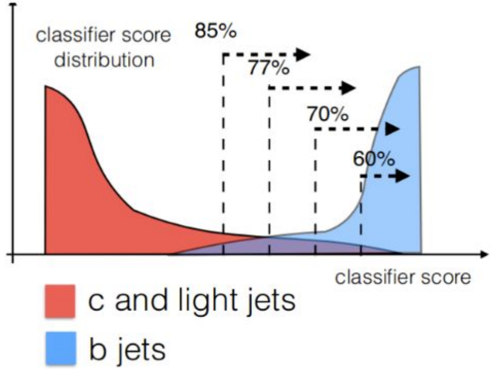

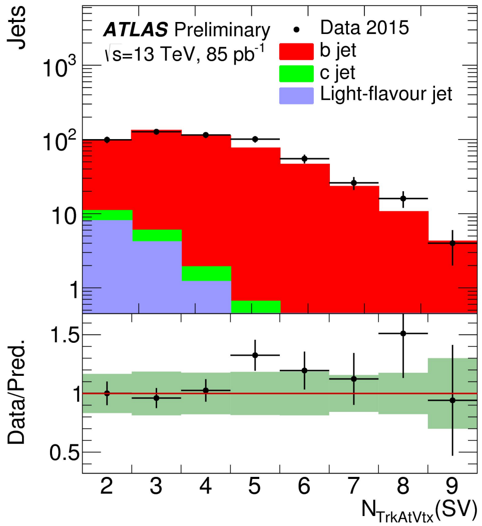

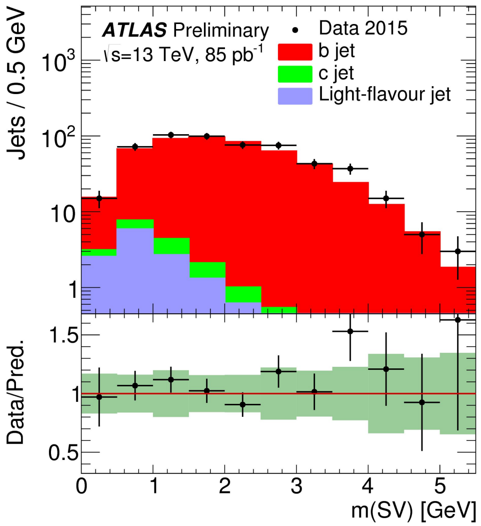

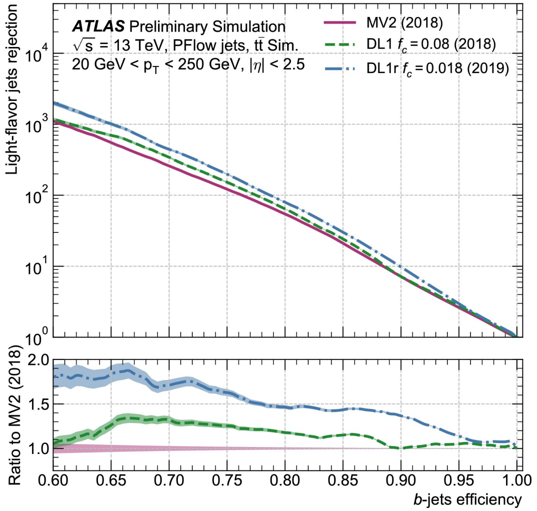

Flavour tagging (b-tagging)

- **Calibrations:**
  - Needed due to:
    - Imperfect modelling of the detector and its response to incoming particle showers
    - Use of approximations in the generation of the fragmentation and hadronisation
    - Monte Carlo models depend strongly on inputs from previous measurements
  - **Simulations are corrected by:**

$$SF = \frac{\varepsilon_i^{\text{data}}}{\varepsilon_i^{\text{MC}}} \text{ with } i = b, c, \text{light}$$

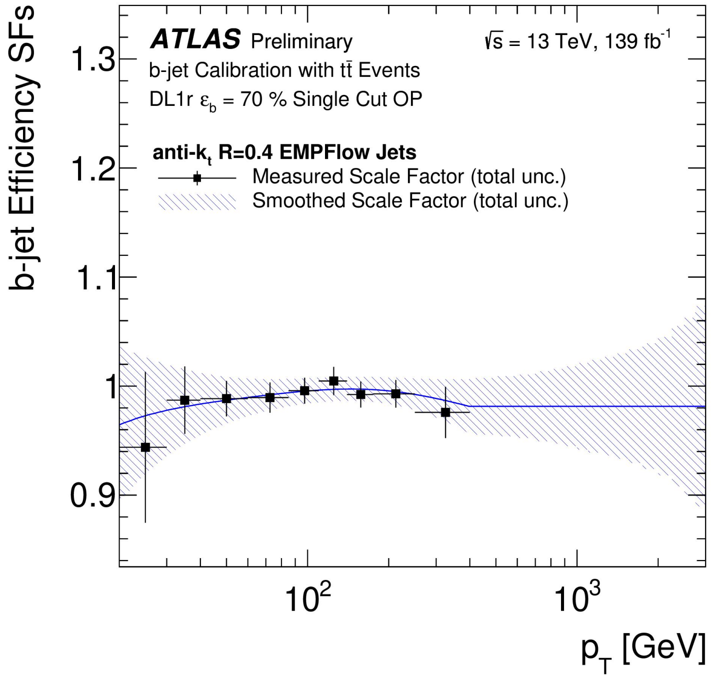

Taus

- **Taus reconstruction:**
  - Use jets with either one or three associated tracks
- **Tau identification via MVA:**
  - Inputs:
    - Track properties
    - Energy distribution

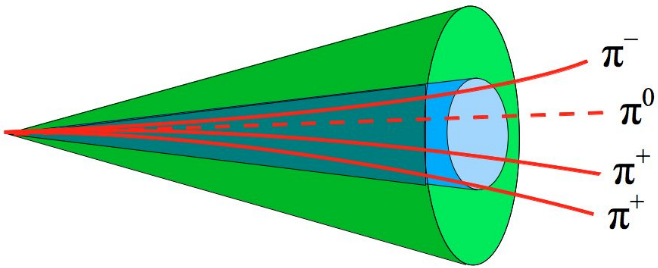

Decay Mode	BR
$\tau^- \to e^- \nu_e \nu_\tau$	$(17.83 \pm 0.04)\%$
$\tau^- \to \mu^- \nu_\mu \nu_\tau$	$(17.41 \pm 0.04)\%$
$\tau^- \to \pi^- \pi^0 \nu_\tau$	$(25.52 \pm 0.09)\%$
$\tau^- \to \pi^- \nu_\tau$	$(10.83 \pm 0.06)\%$
$\tau^- \to \pi^- \pi^0 \pi^0 \nu_\tau$	$(9.30 \pm 0.11)\%$
$\tau^- \to \pi^- \pi^+ \pi^- \nu_\tau$	$(8.99 \pm 0.05)\%$
$\tau^- \to \pi^- \pi^+ \pi^- \pi^0 \nu_\tau$	$(2.74 \pm 0.07)\%$
$\tau^- \to \pi^- \pi^0 \pi^0 \pi^0 \nu_\tau$	$(1.04 \pm 0.07)\%$

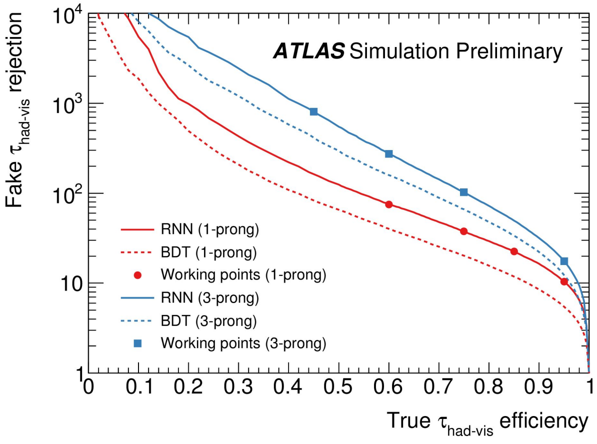

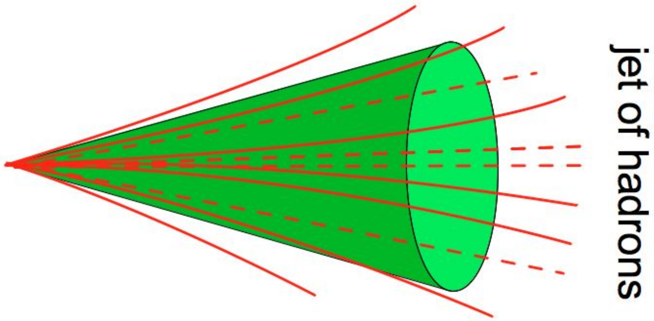

Missing transverse momentum

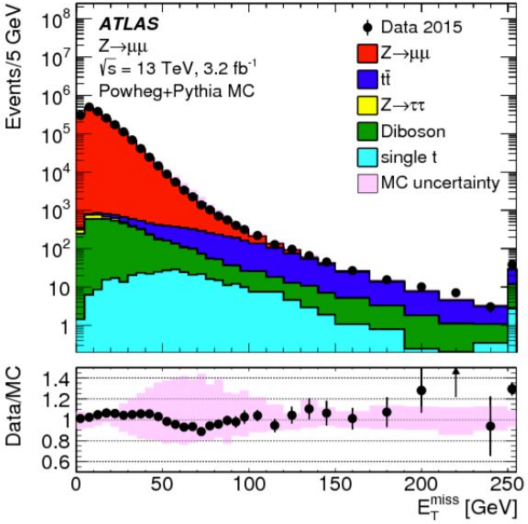

- **Indirect "identification" of neutrinos, WIMPs, DM particles, etc.:**
  - Use missing transverse momentum/energy
    - Momentum sum of reconstructed particles and soft component

$$\mathbf{E}_{\mathrm{T}}^{\mathrm{miss}} = \underbrace{\underbrace{-\sum_{\substack{\text{selected}\\\text{electrons}}} \mathbf{p}_{\mathrm{T}}^{e}}_{\mathbf{E}_{\mathrm{T}}^{\mathrm{miss},e}} \underbrace{-\sum_{\substack{\text{accepted}\\\text{photons}}} \mathbf{p}_{\mathrm{T}}^{\gamma}}_{\mathbf{E}_{\mathrm{T}}^{\mathrm{miss},\gamma}} \underbrace{-\sum_{\substack{\text{accepted}\\\tau\text{-leptons}}} \mathbf{p}_{\mathrm{T}}^{\tau_{\mathrm{had}}}}_{\mathbf{E}_{\mathrm{T}}^{\mathrm{miss},\tau_{\mathrm{had}}}} \underbrace{-\sum_{\substack{\text{selected}\\\text{muons}}} \mathbf{p}_{\mathrm{T}}^{\mu}}_{\mathbf{E}_{\mathrm{T}}^{\mathrm{miss},\mu}} \underbrace{-\sum_{\substack{\text{accepted}\\\text{jets}}} \mathbf{p}_{\mathrm{T}}^{\mathrm{jet}}}_{\mathbf{E}_{\mathrm{T}}^{\mathrm{miss},\mathrm{jet}}}}_{\text{hard term}} \underbrace{\underbrace{-\sum_{\substack{\text{unused}\\\text{tracks}}} \mathbf{p}_{\mathrm{T}}^{\mathrm{track}}}_{\mathbf{E}_{\mathrm{T}}^{\mathrm{miss},\mathrm{soft}}}}_{\text{soft term}}$$

Taken from: https://arxiv.org/pdf/1802.08168.pdf

Boosted topologies

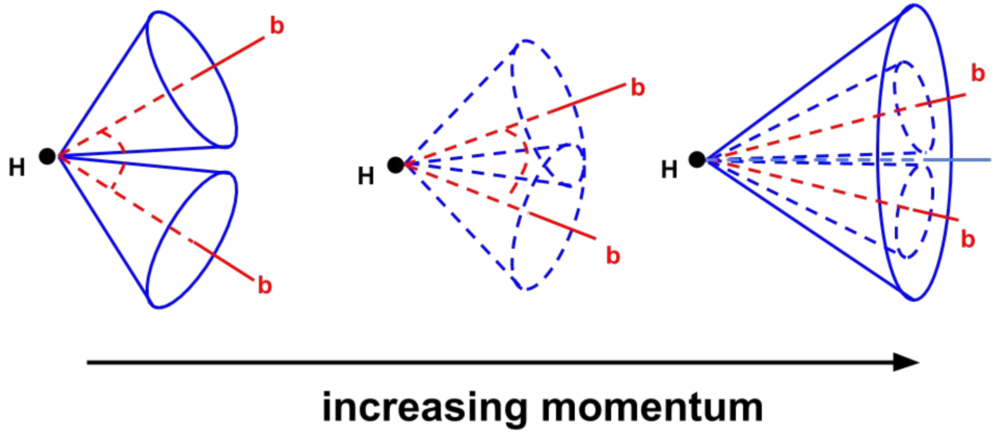

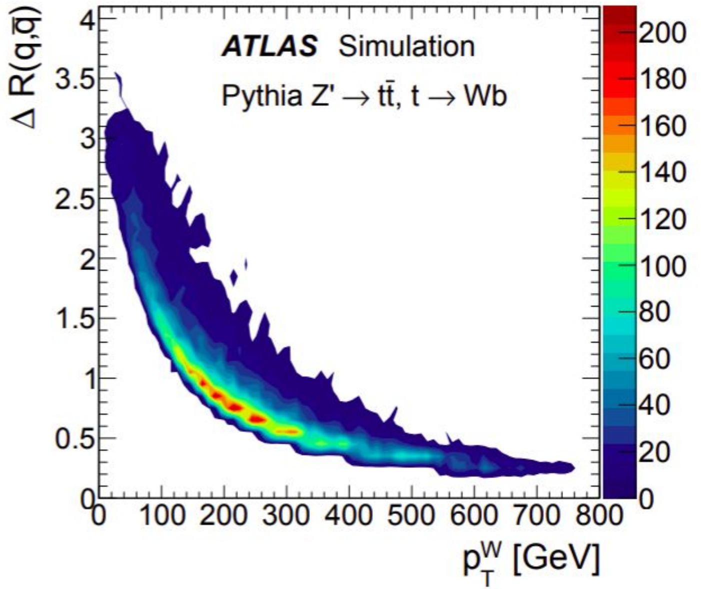

- **Decay products of boosted particles tend to be collimated**
- For p_T^{top} > 450GeV and p_T^{Higgs} > 300GeV decay products tend to have an angular separation smaller than 0.8
  - Partonic structure of decays can no longer be sufficiently described by R=0.4 jets
    - Use R=1.0 jets instead

$$\Delta R \approx \frac{2m}{p_T}$$

Identification of hadronically decaying massive particles

- The identification of hadronic jets originating from the decay of boosted W, Z, and Higgs bosons or top quarks is based on the use of **observables describing the substructure or kinematics of a jet.**

- Jet substructure observables describe:
  - Angular correlations between the constituents of a jet
  - Multiplicity of subjets
  - Jet shapes

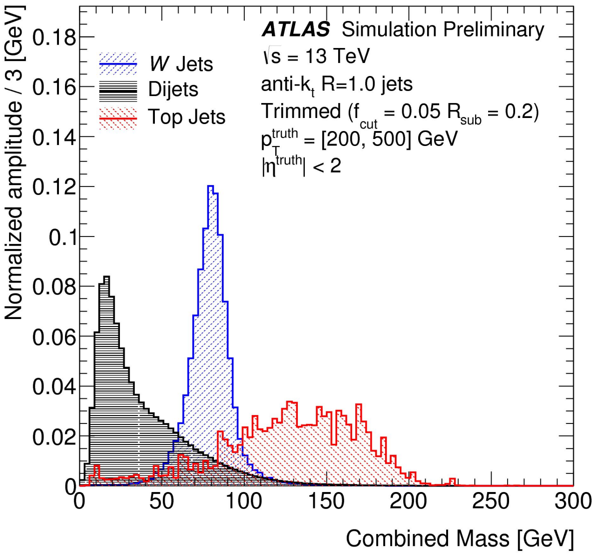

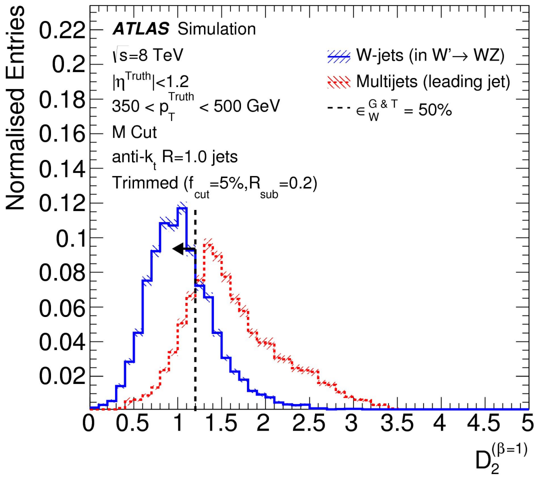

Example:

- Energy correlation functions:

$$D_2^{(\beta)} = \frac{e_3^{(\beta)}}{(e_2^{(\beta)})^3}$$

$$e_2^{(\beta)} = \frac{1}{p_{TJ}^2} \sum_{1\leq i<j\leq n_J} p_{Ti} p_{Tj} R_{ij}^{\beta} \,,$$

$$e_3^{(\beta)} = \frac{1}{p_{TJ}^3} \sum_{1\leq i<j<k\leq n_J} p_{Ti} p_{Tj} p_{Tk} R_{ij}^{\beta} R_{ik}^{\beta} R_{jk}^{\beta}$$

Jet substructure observables

Observable	Variable	Reference
Calibrated jet kinematics	p_T , m^{comb}	https://cds.cern.ch/record/2200211
Energy correlation ratios	e_3, C_2, D_2	https://arxiv.org/abs/1409.6298
N-subjettiness	τ_1, τ_2, τ_{21}, τ_3, τ_{32}	https://arxiv.org/abs/1011.2268
Fox-Wolfram moment	R^{FW}	https://arxiv.org/abs/1112.2567
Splitting measures	$z_{cut}, \sqrt{d_{12}}, \sqrt{d_{23}}$	https://arxiv.org/abs/1302.1415
Planar flow	P	https://arxiv.org/abs/0810.0934
Angularity	a_3	https://arxiv.org/abs/1206.5369
Aplanarity	A	https://arxiv.org/abs/1112.2567
KtDR	KtDR	https://doi.org/10.1016/0550-3213(93)90166-M
Q_W	Q_W	https://arxiv.org/abs/0806.0023

Jet substructure observables

- The width of a jet is defined via:

$$\text{width} = \frac{\sum_{i=1}^{N} p_{\mathrm{T}}^{i} \Delta R(i, \text{jet})}{\sum_{i=1}^{N} p_{\mathrm{T}}^{i}}$$

- N-subjettiness is defined via:

$$\tau_N = \frac{1}{\sum_{i=1}^{N} p_{\mathrm{T}}^{i} R_0} \sum_{i=1}^{N} p_{\mathrm{T}}^{i} \min\{\Delta R_{S_1 i}, \Delta R_{S_2 i}, \ldots, \Delta R_{S_N i}\}$$

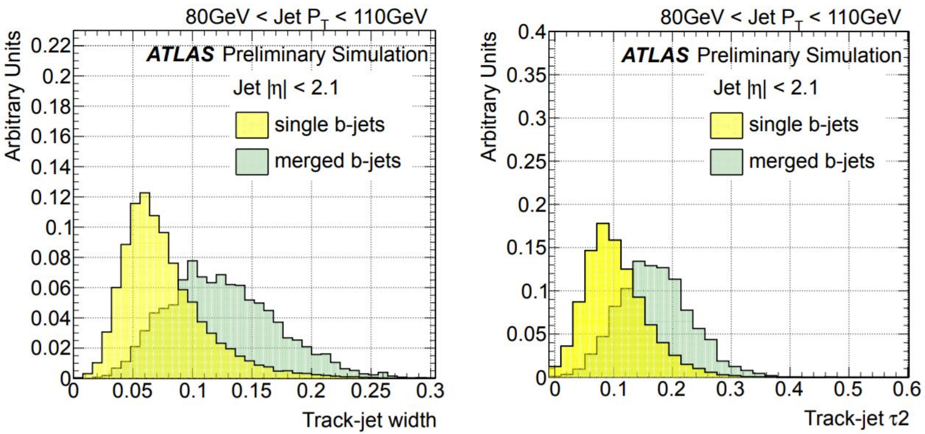

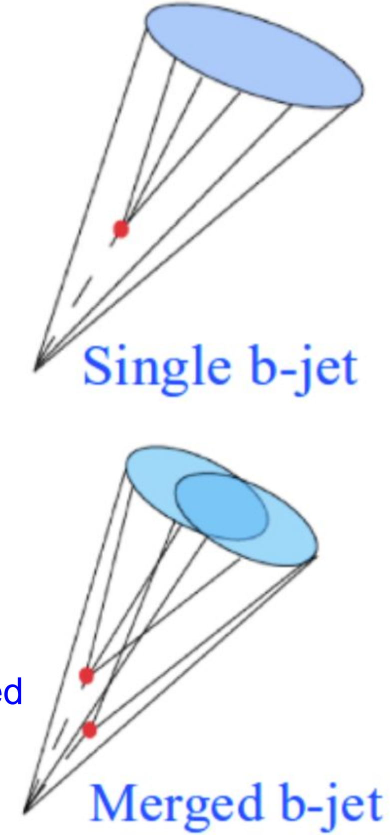

Jet substructure can be calculated by tracks or energy clusters

Jet substructure observables

- The width of a jet is defined via:

$$\text{width} = \frac{\sum_{i=1}^{N} p_{\mathrm{T}}^{i} \Delta R(i, \text{jet})}{\sum_{i=1}^{N} p_{\mathrm{T}}^{i}}$$

Sum over jet constituents

- N-subjettiness is defined via:

$$\tau_N = \frac{1}{\sum_{i=1}^{N} p_{\mathrm{T}}^{i} R_0} \sum_{i=1}^{N} p_{\mathrm{T}}^{i} \min\{\Delta R_{S_1 i}, \Delta R_{S_2 i}, ..., \Delta R_{S_N i}\}$$

Angular distance between constituents of jets and axis of i-th subjet

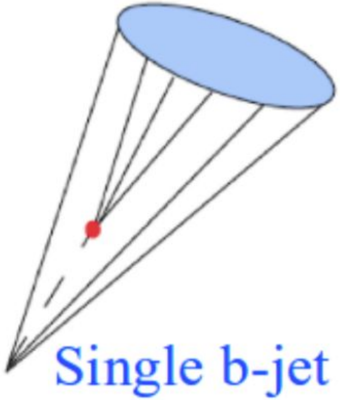

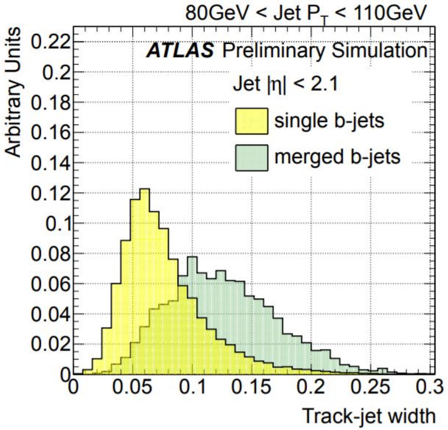

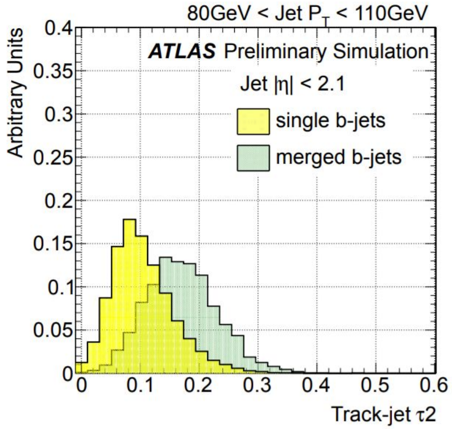

Jet substructure can be calculated by tracks or energy clusters

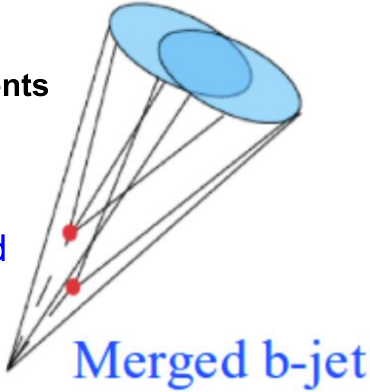

W/Z & top tagging

- Identification of hadronically decaying W/Z bosons and top quarks is done via p_T dependent rectangular cuts or MVAs

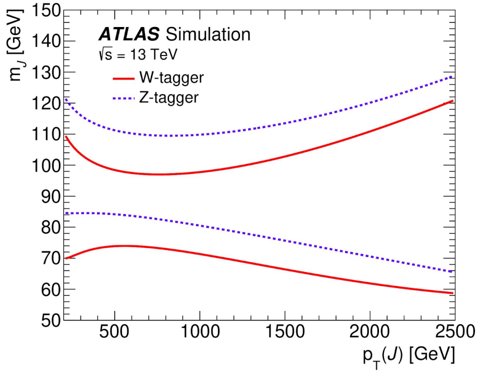

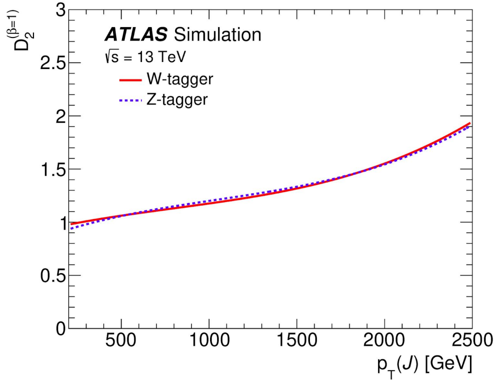

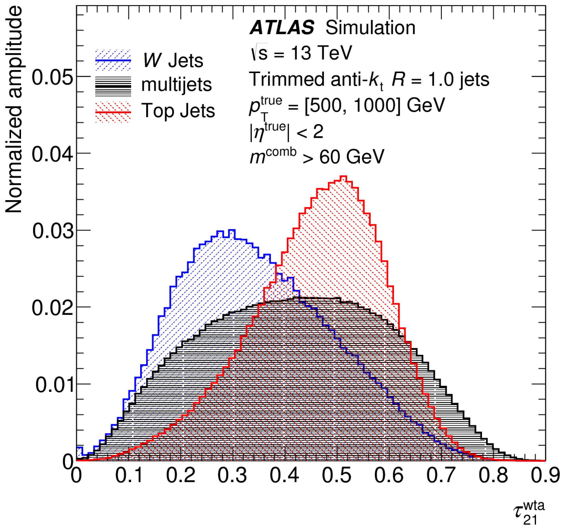

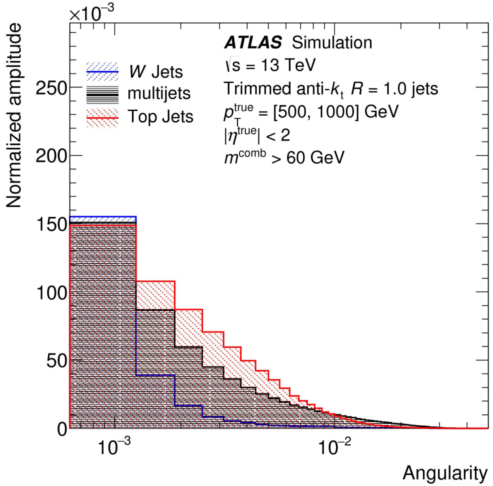

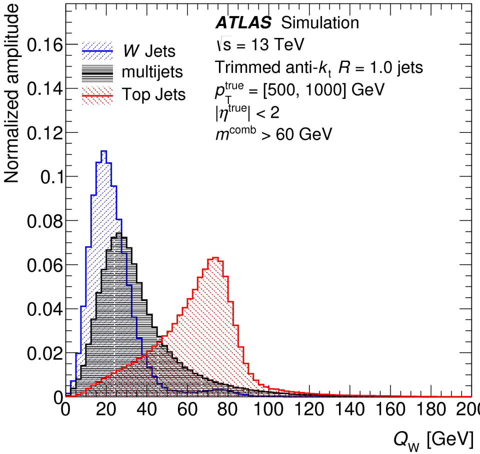

W tagging

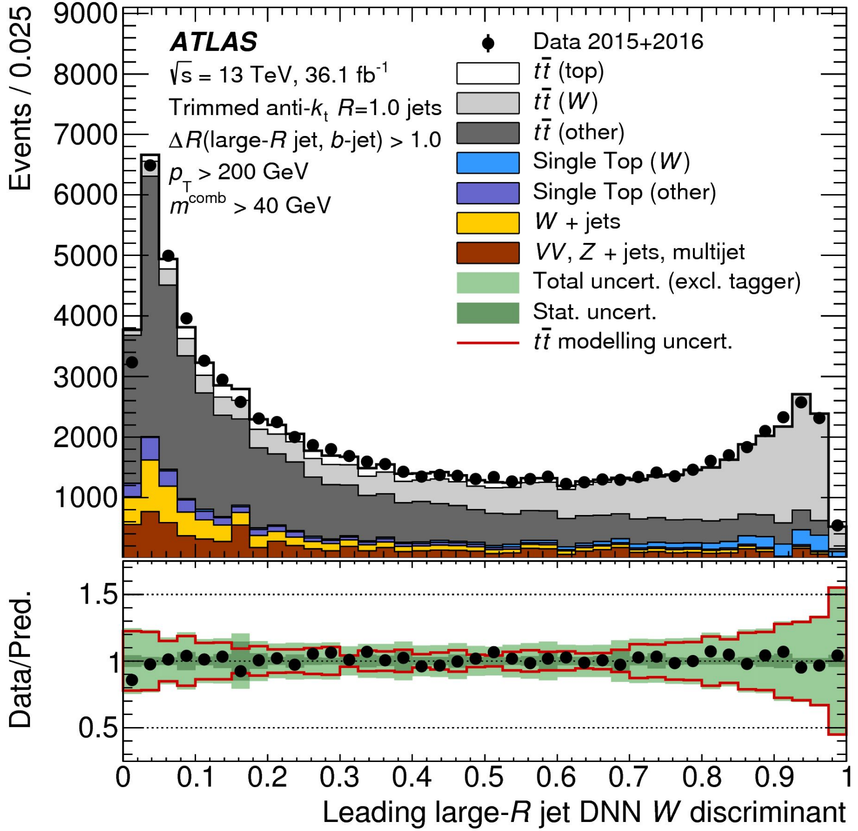
ATLAS
$\sqrt{s}$ = 13 TeV, 36.1 fb^{-1}
Trimmed anti-k_t R=1.0 jets
ΔR(large-R jet, b-jet) > 1.0
p_T > 200 GeV
m^{comb} > 40 GeV
Data 2015+2016
$t\bar{t}$ (top)
$t\bar{t}$ (W)
$t\bar{t}$ (other)
Single Top (W)
Single Top (other)
W + jets
VV, Z + jets, multijet
Total uncert. (excl. tagger)
Stat. uncert.
$t\bar{t}$ modelling uncert.
Events / 0.025
Data/Pred.
Leading large-R jet DNN W discriminant

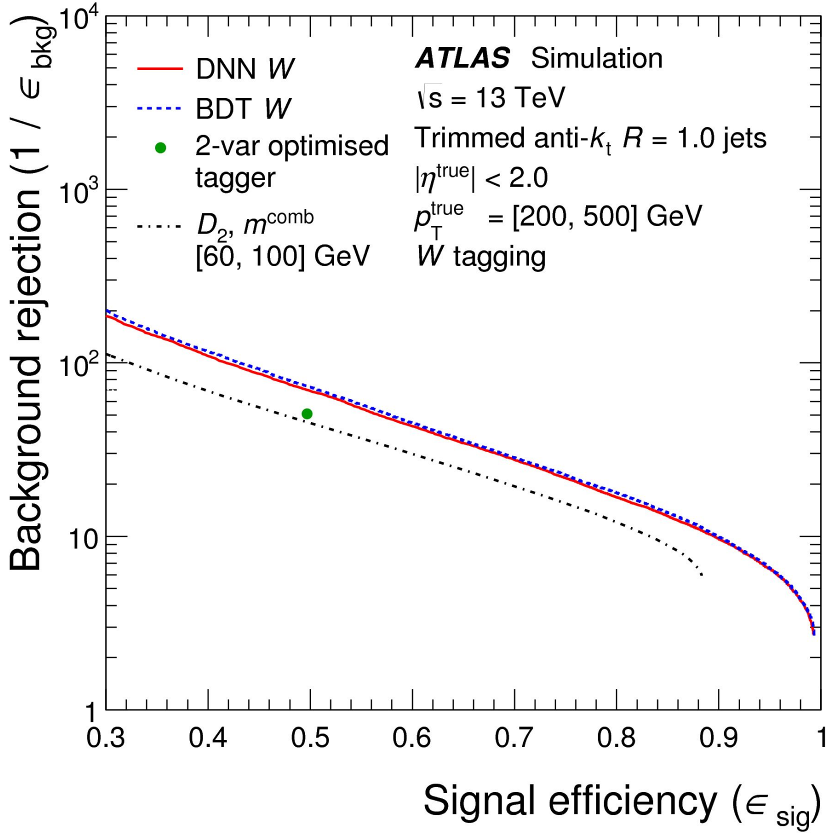
DNN W
BDT W
2-var optimised tagger
D_2, m^{comb} [60, 100] GeV
ATLAS Simulation
$\sqrt{s}$ = 13 TeV
Trimmed anti-k_t R = 1.0 jets
$|\eta^{true}|$ < 2.0
p_T^{true} = [200, 500] GeV
W tagging
Background rejection (1 / ϵ_{bkg})
Signal efficiency (ϵ_{sig})

top tagging

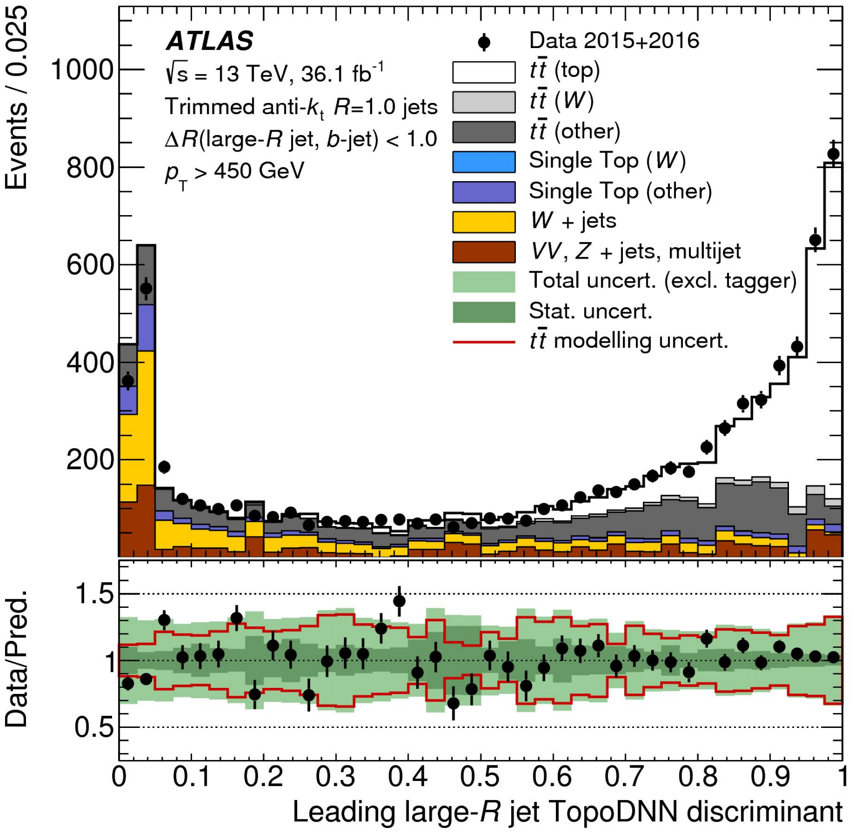

ATLAS
√s = 13 TeV, 36.1 fb-1
Trimmed anti-kt R=1.0 jets
ΔR(large-R jet, b-jet) < 1.0
pT > 450 GeV
Data 2015+2016
tt̄ (top)
tt̄ (W)
tt̄ (other)
Single Top (W)
Single Top (other)
W + jets
VV, Z + jets, multijet
Total uncert. (excl. tagger)
Stat. uncert.
tt̄ modelling uncert.
Events / 0.025
Data/Pred.
Leading large-R jet TopoDNN discriminant

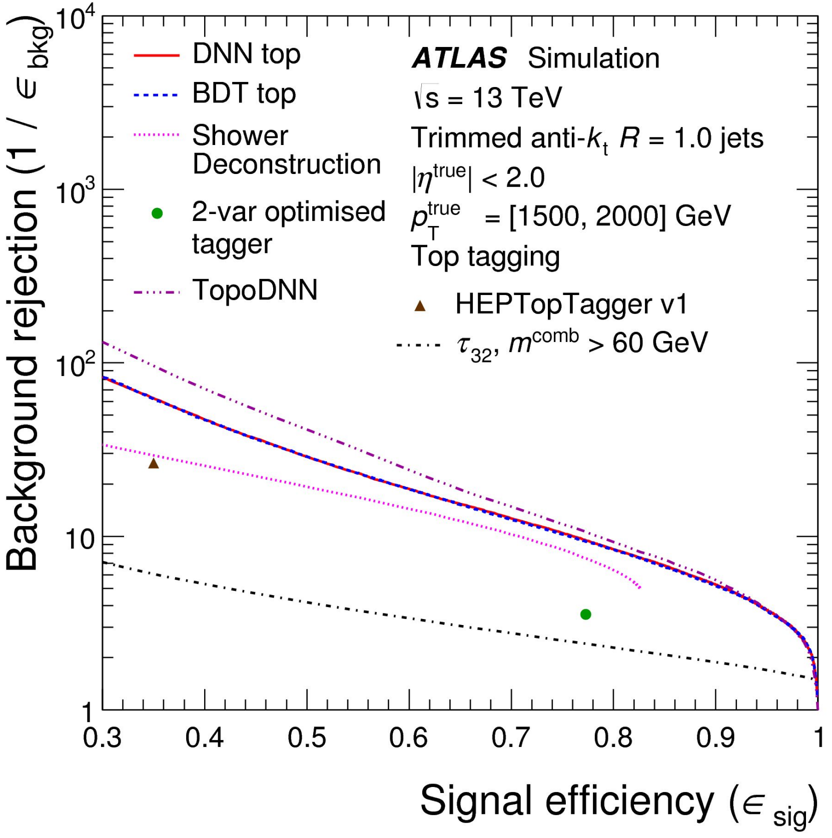

DNN top
BDT top
Shower Deconstruction
2-var optimised tagger
TopoDNN
ATLAS Simulation
√s = 13 TeV
Trimmed anti-kt R = 1.0 jets
|η^true| < 2.0
pT^true = [1500, 2000] GeV
Top tagging
HEPTopTagger v1
τ32, m^comb > 60 GeV
Background rejection (1 / ϵ bkg)
Signal efficiency (ϵ sig)

Higgs tagging

- Higgs tagging is mainly based on flavour tagging information
  - In contrast to W/Z and top tagging

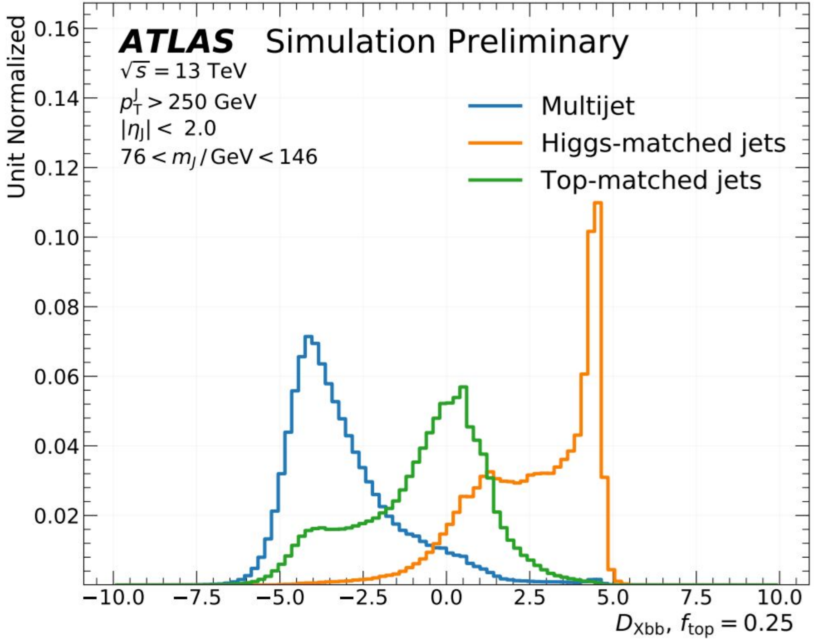

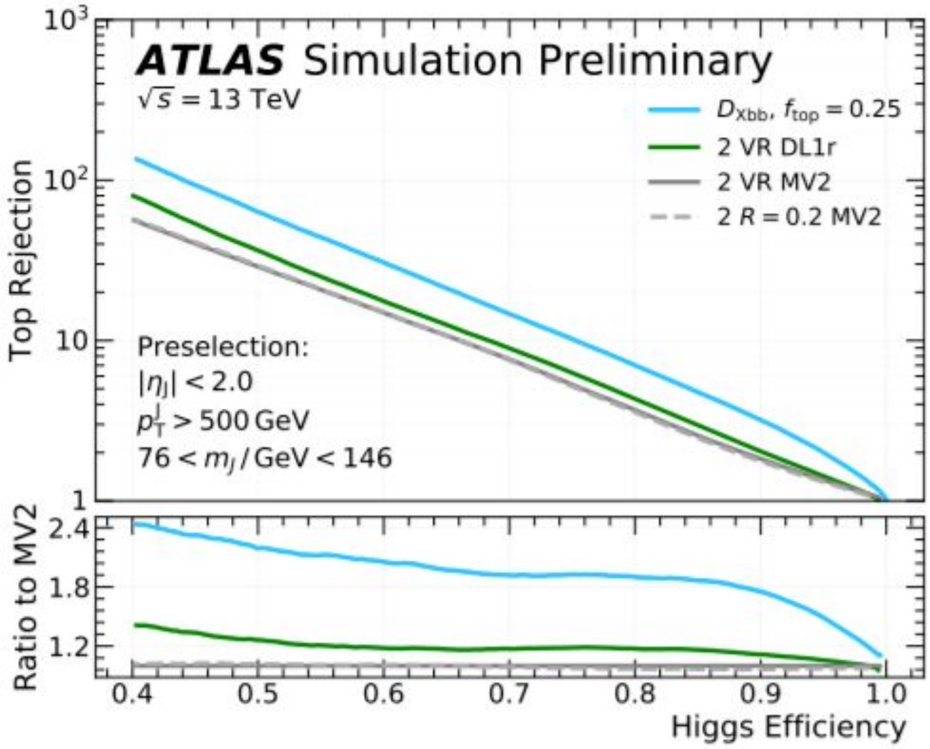

Removal of soft radiation and pile-up

- Jet grooming algorithms:
  - Mass-drop Filtering (https://arxiv.org/abs/0802.2470)
  - Pruning (https://arxiv.org/abs/0912.0033)
  - **Trimming (https://arxiv.org/pdf/0912.1342.pdf)**
    - Current default in ATLAS

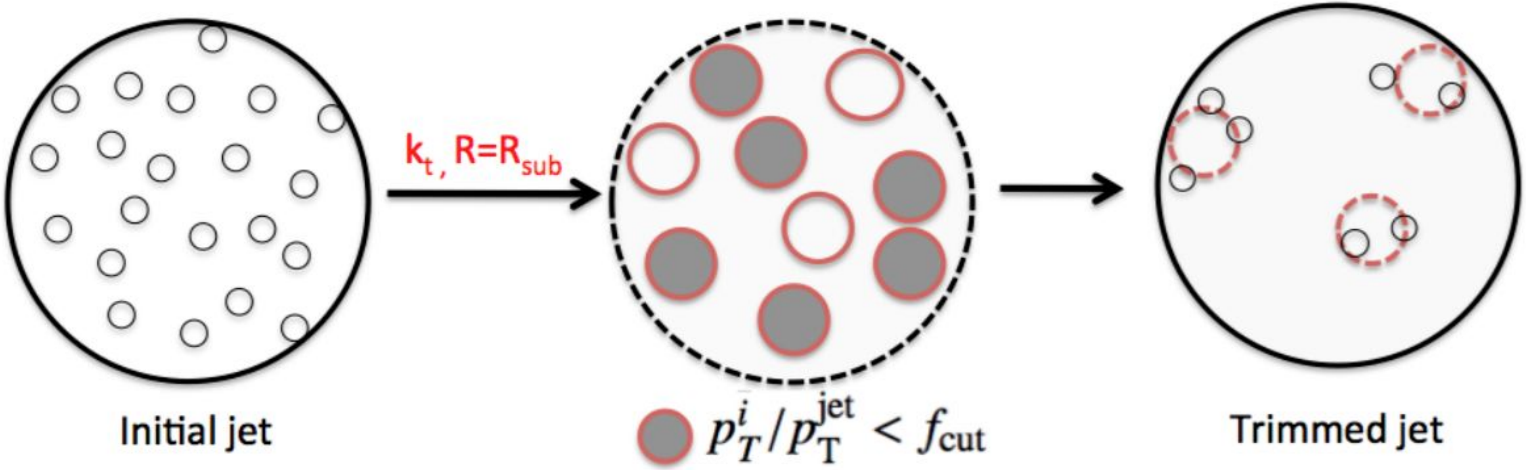

2.5 Monte Carlo simulations

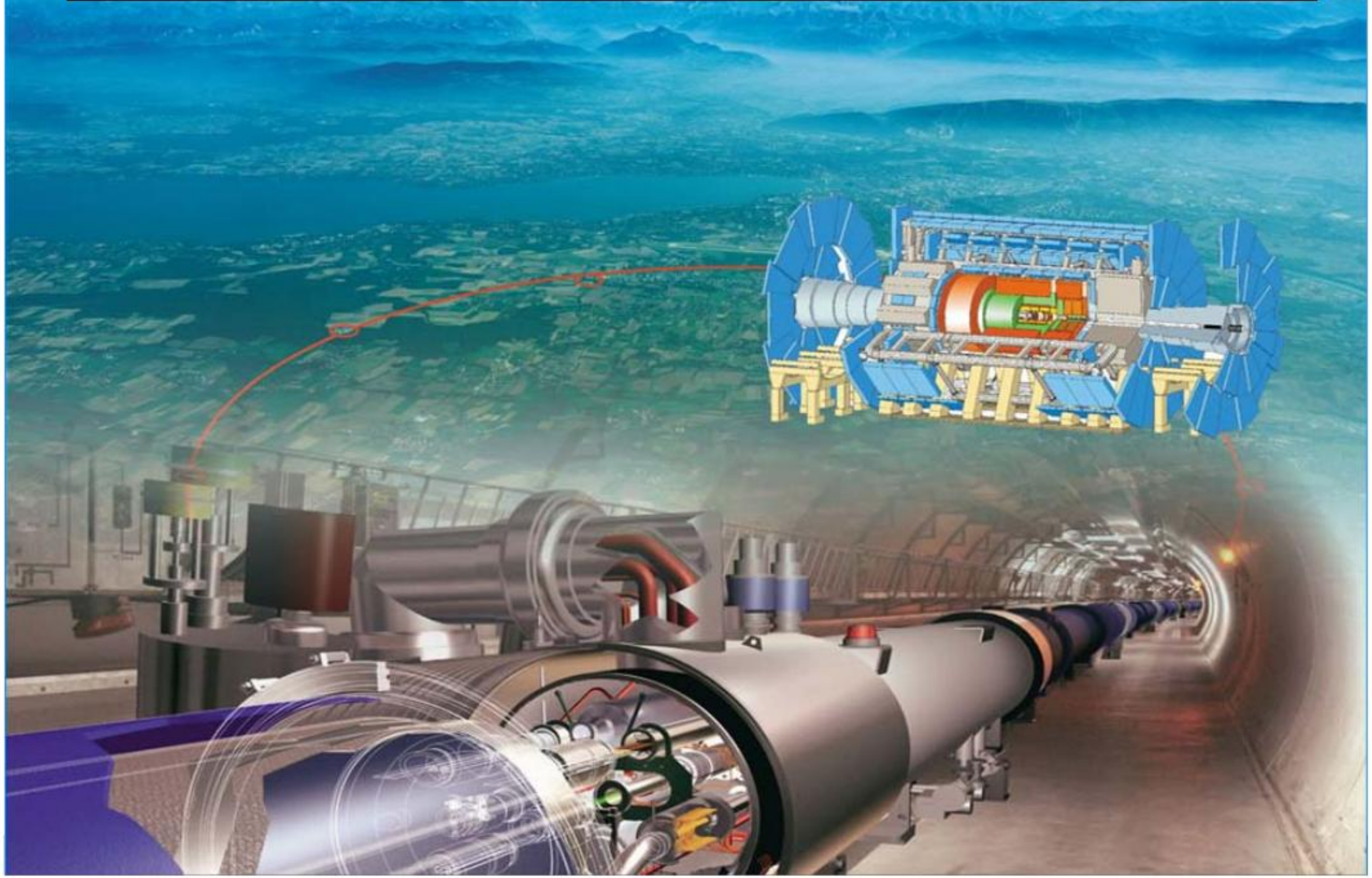

Monte Carlo simulation

- Observations in data are compared to SM predictions (Monte Carlo simulations)
- **Use factorisation approach**:
  - Parton distribution functions (PDF)
  - Hard process (matrix element/scattering amplitude)
  - Parton shower (fragmentation, hadronization, decay of unstable particles)
  - Detector simulation (including overlay with pile-up)

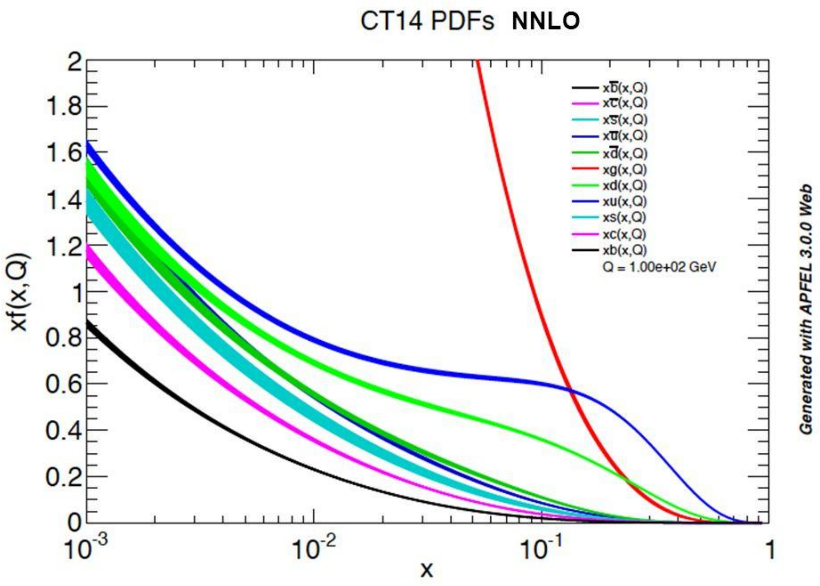

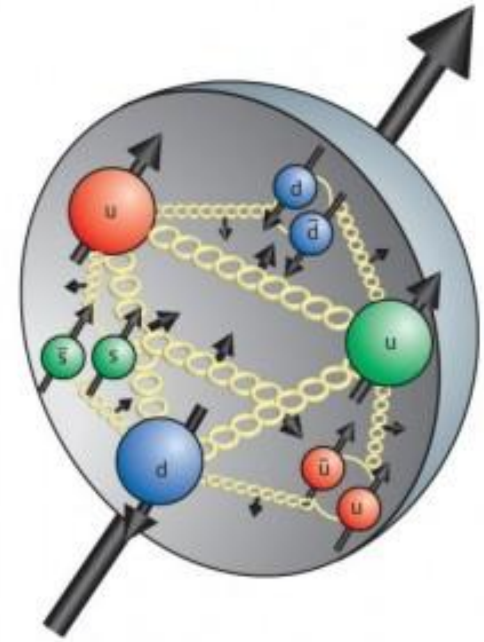

Monte Carlo simulation

- Observations in data are compared to SM predictions (Monte Carlo simulations)
- **Use factorisation approach**:
  - Parton distribution functions (PDF)
  - Hard process (matrix element/scattering amplitude)
  - Parton shower (fragmentation, hadronization, decay of unstable particles)
  - Detector simulation (including overlay with pile-up)

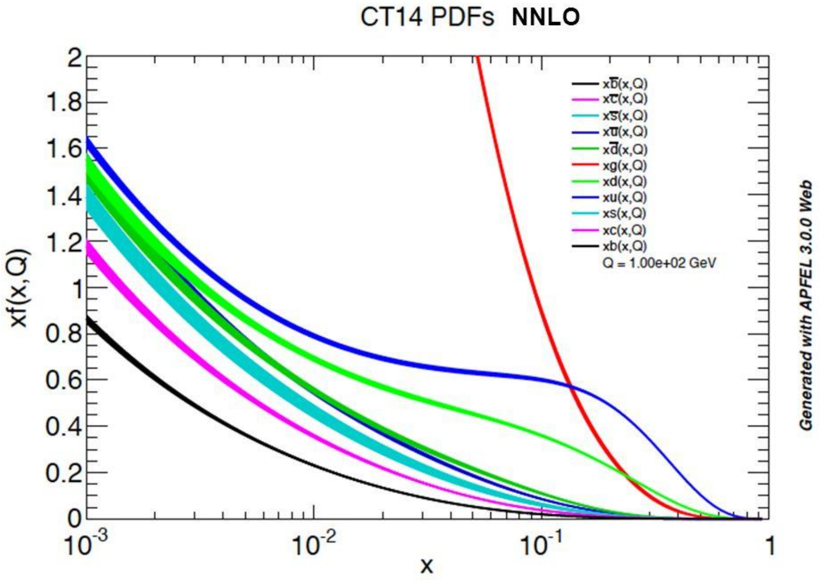

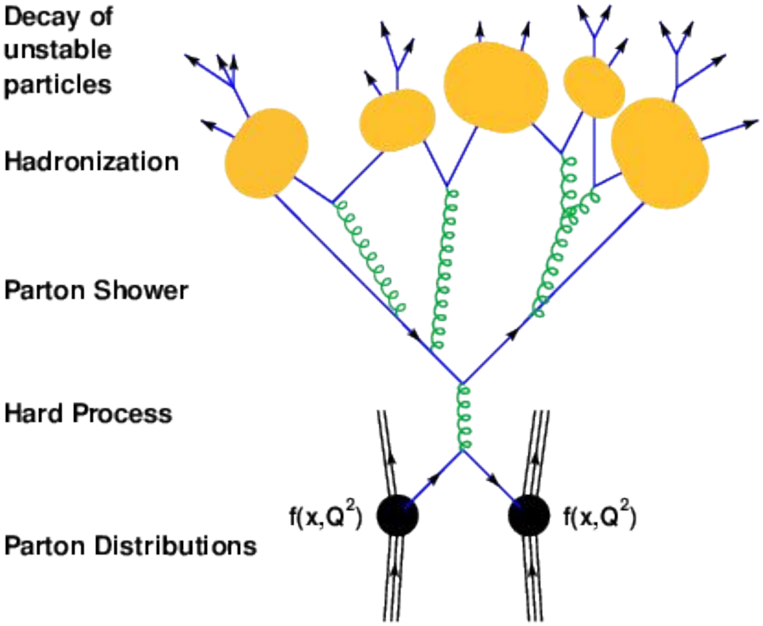

Monte Carlo simulation

$\mu \approx \lambda_{QCD}$ — Decay of unstable particles; Hadronization

$\lambda_{QCD} < \mu < Q$ — Parton Shower

$\lambda_{QCD} \ll \mu \approx Q$ — Hard Process

Parton Distributions

(Multiparton Interaction)

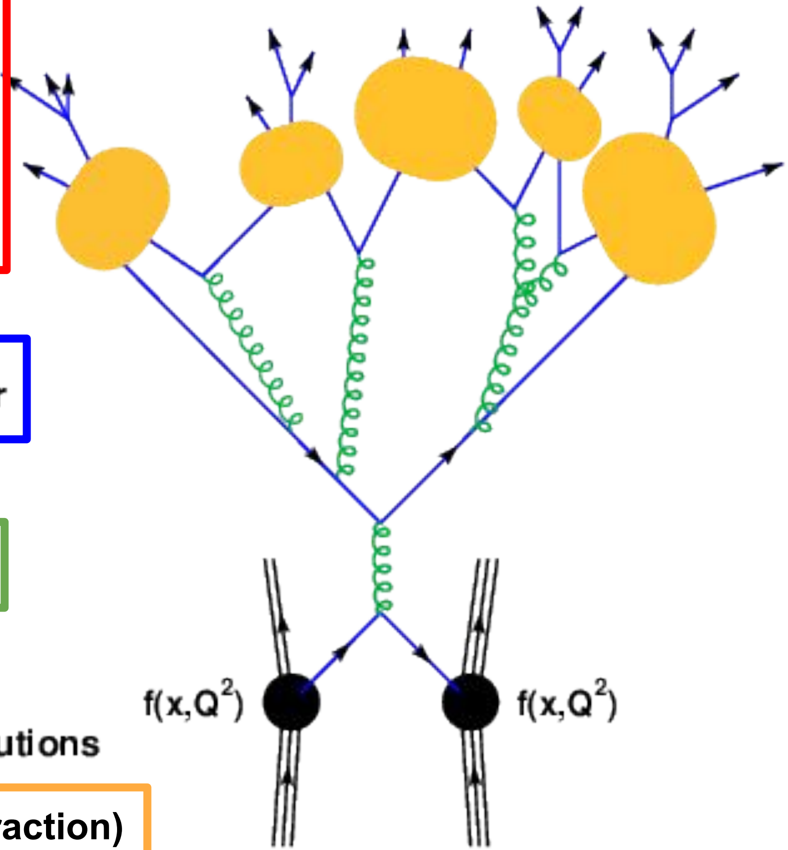

Monte Carlo simulation

Parton distribution functions (PDFs) → **Determined from data (as PDF sets)**

Hard scattering

$\lambda_{QCD} \ll \mu \approx Q$

→ **Hard process computed using fixed order (FO) or mixed order perturbation theory at LO, NLO, NNLO, N3LO,…**

Parton shower

$\lambda_{QCD} < \mu < Q$

→ **Hierarchy of scales appearing as large logarithms in the calculation. Computed using resummation or MC parton showers (PS)**

Hadronization and hadron decay

$\mu \approx \lambda_{QCD}$

Multiparton interaction

→ **Cannot be computed directly: non-perturbative models tuned to e^+e^- data**

Monte Carlo simulation

Parton distribution functions (PDFs) → Determined from data (as PDF sets)

Hard scattering

$\lambda_{QCD} \ll \mu \approx Q$

→ Hard process computed using fixed order (FO) or mixed order perturbation theory at LO, NLO, NNLO, N3LO,…

+ ME and PS matching (different order → different schemes)

Parton shower

$\lambda_{QCD} < \mu < Q$

→ Hierarchy of scales appearing as large logarithms in the calculation. Computed using resummation or MC parton showers (PS)

Hadronization and hadron decay

$\mu \approx \lambda_{QCD}$

Multiparton interaction

→ Cannot be computed directly: non-perturbative models tuned to e^+e^- data

Master formula for hadron collisions

$$\sigma_{h_1+h_2\to X} = \sum_{a,b} \int \underbrace{dx_1 dx_2 d\Phi}_{\text{phase - space integral}} \underbrace{f_a(x_1, \mu_F) f_b(x_2, \mu_F)}_{\text{Parton distribution function}} \underbrace{\hat{\sigma}_{a+b\to X}(\hat{s}, \mu_F, \mu_R)}_{\text{Parton-level cross section}}$$

phase - space integral

Parton distribution function

Parton-level cross section

- The parton-level fixed order cross section can be computed as a series in perturbation theory, using the coupling constant as an expansion parameter

$$\hat{\sigma} = \sigma^{\text{Born}} \left(1 + \frac{\alpha_S}{2\pi}\sigma^{(1)} + \left(\frac{\alpha_S}{2\pi}\right)^2 \sigma^{(2)} + \left(\frac{\alpha_S}{2\pi}\right)^3 \sigma^{(3)} + \ldots\right)$$

Coefficients of the perturbative series

- Including higher corrections improves the predictions and reduces theoretical uncertainties

More information can be found e.g. via: https://arxiv.org/pdf/1207.2389v4.pdf

Particle distribution functions (PDFs)

- Quantify the probability density for finding a parton with a certain flavour and momentum fraction
- Obtained from fits to data
- Crucial source of uncertainties for both searches and measurements

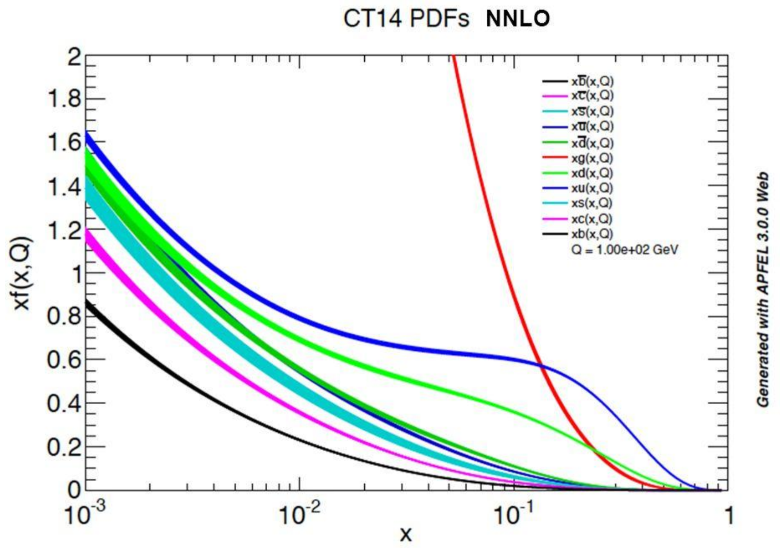

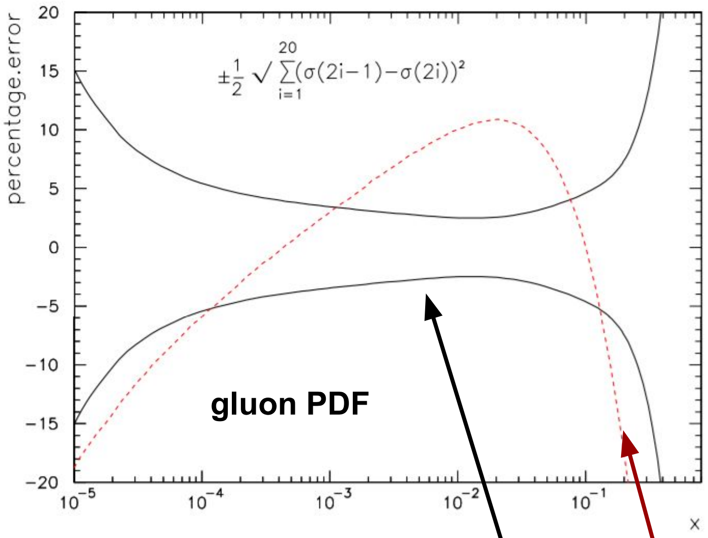

Relative variations of the MSTW set

Variation of CTEQ6 set wrt central values of the MSTW set

Taken from https://arxiv.org/pdf/1207.2389v4.pdf

Particle distribution functions (PDFs)

- PDF sets can be downloaded from **LHAPDF** page (https://lhapdf.hepforge.org/pdfsets):

LHAPDF ID	Set name	Number of set members
251	GRVPI0	1
252	GRVPI1	1
270	xFitterPI_NLO_EIG	8
280	xFitterPI_NLO_VAR	6
10000	cteq6	41
10042	cteq6l1	1
10150	cteq61	41
10550	cteq66	45
10770	CT09MCS	1
10771	CT09MC1	1
10772	CT09MC2	1
10800	CT10	53

260000	NNPDF30_nlo_as_0118	101
260200	NNPDF30_nlo_as_0118_nf_3	101
260400	NNPDF30_nlo_as_0118_nf_4	101
260600	NNPDF30_nlo_as_0118_nf_6	101
260800	NNPDF30_nlo_as_0118_mc	101
261000	NNPDF30_nnlo_as_0118	101
261200	NNPDF30_nnlo_as_0118_nf_3	101
261400	NNPDF30_nnlo_as_0118_nf_4	101
261600	NNPDF30_nnlo_as_0118_nf_6	101
261800	NNPDF30_nnlo_as_0118_mc	101

Monte Carlo generators

- **The Monte Carlo Method:**
  - Monte Carlo (MC) techniques are based on a repeated random sampling of numerical estimations of variables following complicated probability density functions
    - **Based on the implementation of (B)SM predictions**

- **Monte Carlo Event Generators** try to give the **best full description** (according our current knowledge) of a collision combining theoretical predictions for the **different stages** of an event and providing a **fully exclusive final state in terms of hadrons and leptons** which is as close as possible to what is measured in a real experiment

- Predictions are usually fed into a detector-simulation software to emulate the reconstruction effects of our real world detectors

See also: https://pdg.lbl.gov/2019/reviews/rpp2018-rev-monte-carlo-techniques.pdf

Some Monte Carlo generators

- MadGraph_aMC@NLO (https://launchpad.net/mg5amcnlo):
  - Tool for calculation of cross sections for SM and BSM processes and event generation (LO or NLO)
- POWHEG (http://powhegbox.mib.infn.it/):
  - MC generator for hard processes at NLO
- Sherpa (https://sherpa-team.gitlab.io/):
  - MC event generator for the simulation of ℓℓ, ℓγ, γγ, ℓh and hh collisions
- Pythia (http://home.thep.lu.se/Pythia/):
  - *Multi-purpose MC generator (for event generation and/or parton shower)*
    - *Supports* Lund string fragmentation model
- ALPGEN (https://arxiv.org/pdf/hep-ph/0206293.pdf):
  - MC generator for hard multiparton processes in hadronic collisions
- HERWIG (https://herwig.hepforge.org/):
  - *Multi-purpose MC generator (for event generation and/or parton shower)*
    - *Supports angular-ordered and dipole showers as well as MPI*
- MCFM (https://mcfm.fnal.gov/):
  - Tool dedicated to calculate cross sections of various processes at NLO (and NNLO) in QCD
    - Can also be used as event generator for some of these processes
- JHU (https://spin.pha.jhu.edu/):
  - Event generator for pp → X → VV, VBF, X+JJ, pp → VX, ee → VX

Next semester

4. Recent experimental Tests on the Standard Model of Particle Physics
   - 4.1 Precision Measurements of the Electroweak Interaction
   - 4.2 An overview of the physics program at the Large Hadron Collider
   - 4.3 The Higgs Boson (Searches and Measurements)
     - 4.3.1 Searches at LEP, Tevatron and the LHC
     - 4.3.2 Measurements of Higgs boson properties
   - 4.4 The Top quark
   - 4.5 B-Hadron Decays and CP Violation
   - 4.6 Neutrino Masses and Oscillation

Next semester

5. Extension of the Standard Model of Particle Physics
    5.1 Open Questions
    5.2 Great Unification
    5.3 Supersymmetry
    5.4 Dark Matter
    5.5 Extended Higgs sector
    5.6 “Exotic” Beyond the Standard Model theories
    5.7 Ongoing Searches for Beyond the Standard Model Physics
6. Machine Learning in High Energy Physics